Huh7 Hepatocyte Cells Cultured in Human Serum are an Improved *In Vitro* Model for the Study of Two Populations of Hepatitis A Virus

by

Tiing Tiing Chua

A thesis submitted in partial fulfillment of the requirements for the degree of

Master of Science

in
Virology

Department of Medical Microbiology and Immunology
University of Alberta

ABSTRACT

Hepatitis A Virus (HAV) belongs to the family of *Picornaviridae*, a group of viruses that are non-enveloped, single stranded, positive sense RNA viruses. In 2013, studies found not only the standard non-enveloped HAV, but also a novel HAV population, quasi-enveloped HAV (quasi-eHAV), in the samples from HAV-infected chimpanzees and humans. Quasi-eHAV has a lower density (1.06-1.10g/cm^3) and is found only in serum. HAV has a higher density (1.22-1.28g/cm^3) and is found exclusively in feces. The secretion pathway of these two HAV populations is yet to be elucidated.

To clarify this question *in vitro*, a cell culture system representative of hepatocytes which can secrete the two HAV populations is required. This study focuses on the development of an *in vitro* system mimicking the polarized hepatocyte able to secrete two HAV populations. Huh7 (a human hepatocarcinoma cell line) was cultured in a dual-chamber system with DMEM supplemented with 2% human serum (HS cultured cells) instead of the typical 10% fetal bovine serum (FBS cultured cells). HS cultured Huh7 cells undergo growth arrest and become more differentiated. The proper polarization of Huh7 cells in HS media cultured in the dual-chamber system was confirmed by dextran diffusion studies.

In HAV infection studies, we compared the density profiles of the samples collected from HAV-infected HS cells that grown either monolayer or in the dual-chamber system. By using isopycnic gradient ultracentrifugation, we identified HAV populations based on their buoyant density. We used TCID50 assays and neutralization assays to further characterize the HAV populations released from both sides of HS cells in the dual-chamber system. Our results showed that HAV-infected Huh7 cells in HS media that were grown as a monolayer secreted one HAV population, but HAV-

infected Huh7 cells in HS media that were grown in the dual-chamber system secreted two HAV populations. HAV populations were secreted preferentially, either into the upper (apical) or lower (basolateral) compartment of the dual-chamber system. The two *in vitro* HAV populations shared similar characteristics to the two HAV populations found *in vivo*, with respect to their infectivity level and their ability to be neutralized by HAV specific antibodies.

In short, Huh7 cells in HS media grown in the dual-chamber system were shown to be a suitable cell culture model capable of secreting two HAV populations, such a system can be used to study aspects of HAV biology inaccessible by standard tissue culture methods.

Acknowledgement

This work would not be possible without the support and guidance of my supervisor, Dr. D. Lorne J. Tyrrell. Hence, I would like to acknowledge Dr. Tyrrell with the deepest gratitude for giving me the opportunity to work in his lab. Although Dr. Tyrrell has a busy schedule, he always makes time for his students, ensuring their care. He has inspired and motivated me to keep pursuing my passions in the Health Science field.

I would like to express my appreciation to all those with whom I have worked in pursuit of my Master degree. I would like to thank my committee members, Dr. Jim Smiley and Dr. David Marchant for the time and their suggestions. I especially thank my mentor, Dr. Rineke Steenbergen for her guidance and advice in my Masters project. She was always supportive and encouraging, especially during the early difficult phase of project.

I am thankful to all the colleagues who shared their opinions to help my project, especially Karl Fischer and Dr. Aviad Levin for their advice and guidance in experimental design. I am also grateful to Bonnie Bock for taking care of all the administrative work; Dr. Michael Joyce for his advice; Dr. Bill Addison, Justin Shields, Karyn Berry-Wynne, and Gerald Lachance for their technical help; and Darci Loewen-Dobler for taking care of the lab supplies.

In addition, I would like to thank Dr. Judy Gnarpe, Dr. Kimberly Ellison and Dr. Jim Smiley for giving me the opportunity to work as a teaching assistant in the courses. These opportunities not only allowed me to gain more knowledge, but also enhanced my communication skills. I am thankful to the administrative personnel in the Department of Medical Microbiology and Immunology office, especially Tabitha Vasquez and Anne Giles (retired), who helped me a lot when I first arrived and even before I arrived in Edmonton in December 2013.

Tyrrell's laboratory was not only a place for me to pursue my dream, but also a "family". I am grateful for supportive colleagues, especially Darci Loewen-Dobler, Dr. Aviad Levin, and Wilson Tat for being good listeners, and to Karyn Berry-Wynne who motivated me in rock climbing.

Finally, I am grateful to my family members and my friends for being caring and supportive. I would especially like to thank my parents for their open minds, supporting me as I pursued my degree in a country thousands mile from home. I would like to thank my friends for being there when needed. I persisted with their support.

TABLE of CONTENTS

LIST of TABLES

LIST of FIGURES

CHAPTER THREE: RESULTS

Part 2: The behaviour of two HAV populations produced by Huh7 cells in HS media when grown in a dual-chamber system

CHAPTER FOUR: DISCUSSION

Part 1: HAV infection studies on monolayer-infected cells cultured under different media conditions

SUPPLEMENTARY

LIST of ABBREVIATIONS

ΔCt	delta Ct
ΔΔCt	delta-delta Ct
$3C^{pro}$	3C protease
$3D^{pol}$	3D polymerase (RNA-dependent RNA polymerase)
ALIX	apoptosis-linked gene 2-interacting protein X
ALT	serum aminotransferase
ANOVA	analysis of variance
ASGPR	asialoglycoprotein receptor
BSA	bovine serum albumin
CA	cholic acid
Caco-2 cells	human colon carcinoma cell line
cDNA	complementary DNA
Ct	threshold cycle
CDCA	chenodeoxycholic acid
CPE	cytopathic effect
CTLs	cytotoxic T cells
CYP7A1	cholesterol 7α-hydroxylase
DAB	3,3'-diaminobenzidine tetrahydrochloride
DC	detergent-compatible
DDT	dithiothreitol
DMEM	Dulbecco's Modified Eagle Medium
DMSO	dimethyl-sulfoxide
DNA	deoxyribonucleic acid
dNTP	deoxynucleotide

dpi	day post infection
dsRNA	double stranded ribonucleic acid
ELISA	enzyme-linked immunosorbent assay
EM	electron microscopy
ESCRT	endosomal sorting complex required for transport
FAM	6-carboxyfluorescein reporter dye
FBS	fetal bovine serum
FGF19	fibroblast growth factor 19
FGFR4	fibroblast growth factor receptor 4
FRET	Förster-type energy transfer
FRhK6	fetal rhesus kidney cell line
FXR	farnesoid X receptor
GE	genome equivalents
GW4064	FXR agonist drug
H_2O_2	hydrogen peroxide
HAV	Hepatitis A Virus
HAVcr-1	hepatitis A virus cellular receptor 1
HBV	Hepatitis B Virus
HCV	Hepatitis C Virus
HM175/p16 (p16)	cell-culture adapted HAV strain
HRP	horseradish peroxidase
hr(s)	hour(s)
HS	human serum
huHPRT	human hypoxanthine-guanine phosphoribosyltransferase
Huh7 cells	human hepatocarcinoma cell line

Huh7.5 cells	human hepatocarcinoma cell line
IFN-α	Interferon alpha
IFN-β	Interferon beta
IFN-γ	Interferon gamma
Ig	Immunoglobulin
IgA	immunoglobulin A
IgG	immunoglobulin G
IgG(-) HS	immunoglobulin G depleted human serum
IgG(+) HS	immunoglobulin G non-depleted human serum
IgM	immunoglobulin M
IL	Interlukin
IRES	internal ribosome entry site
IRF	IFN regulatory factor 3
kb	kilobase
K24F2	anti-capsid HAV antibody
LRH-1	liver receptor homolog 1
M-MLV RT	Moloney Murine Leukemia Virus Reverse Transcriptase
mAB	monoclonal antibody
MEM	Opti-MEM® I Reduced-Serum Medium
min	minute
MGB™ dye	minor groove binder quencher dye
MOI	multiplicity of infection
MVBs	multivesicular bodies
NCR	noncoding region
NHP	non-human primate

NK	natural killer cells
NTC	non-template control
ORF	open reading frame
PBS	phosphate buffer saline
PBS-T	phosphate buffer saline with 0.1% Tween-20
PCR	polymerase chain reaction
PFA	Paraformaldehyde
PHAC	Public Health Agency of Canada
PLL	poly-L-lysine
PKB/Akt	Protein Kinase B
quasi-eHAV	quasi enveloped Hepatitis A Virus
RT-qPCR	real time quantitative polymerase chain reaction
RIPA	radioimmunoprecipitation assay
RNA	ribonucleic acid
SDS	sodium dodecyl sulfate
SHP-1	small heterodimer partner 1
SSIII	SuperScript^{TM} III Reverse Transcriptase
TAMRA	tetramethylrhodamine quencher dye
TBS	tris-buffered saline
TBS-T	tris-buffered saline with 0.1% Tween-20
TCA	taurocholic acid
$TCID_{50}$	50% tissue culture infective dose
TCR	T-cell receptor
TGF-β	transforming growth factor-beta
Th cells	T-helper cells

TIM	T cell immunoglobulin and mucin domain
Tregs	regulatory T cells
VLDL	very-low-density-lipoprotein
VPg	viral protein genome-linked
VPS4B	vacuolar protein sorting-associated protein 4B
WHO	World Health Organization
wt	wild-type

CHAPTER ONE: INTRODUCTION

1.1 HAV Epidemiology

Hepatitis A Virus (HAV) infections remain a serious cause of public health problems. A recent example is the outbreak of HAV in San Diego County, California over the summer of 2017 which has sickened over 500 people, with 19 deaths and 351 hospitalizations previously in homeless adult patients. This viral infection can cause acute liver infection and is acquired primarily through the fecal-oral route (20), by either close contact with an infected person or consumption of contaminated food or water (9,36). HAV infection has a tendency of cyclic recurrences and about 1.4 million clinical cases of HAV infection are reported worldwide annually. The actual incidence is likely higher because HAV infection is usually asymptomatic and thus, the disease is under-diagnosed (97).

The incidence of HAV infection is highly associated with socioeconomic indicators and access to safe food and drinking water (41,58,132). Based on a systematic review on the global prevalence of HAV infection that was released by World Health Organization (WHO) in 2010, less developed countries with poor sanitary conditions (for example sub-Saharan Africa and parts of South Asia) have higher endemic HAV transmission compared to the developing countries or some regions of developed countries (for examples Western Europe, Australia, New Zealand, Canada, the United States, Japan, Republic of Korea and Singapore) (58,132). Less developed countries have higher estimated child immunity rates against HAV (Fig 1.1A, darker red shade) and lower adult susceptibility rates (Fig 1.1B, lighter blue shade). This indicates that most individuals in less developed countries are infected with HAV in early childhood when disease symptoms are usually not recognized. This leads to a low reported rate of HAV disease and rare disease outbreaks in less developed

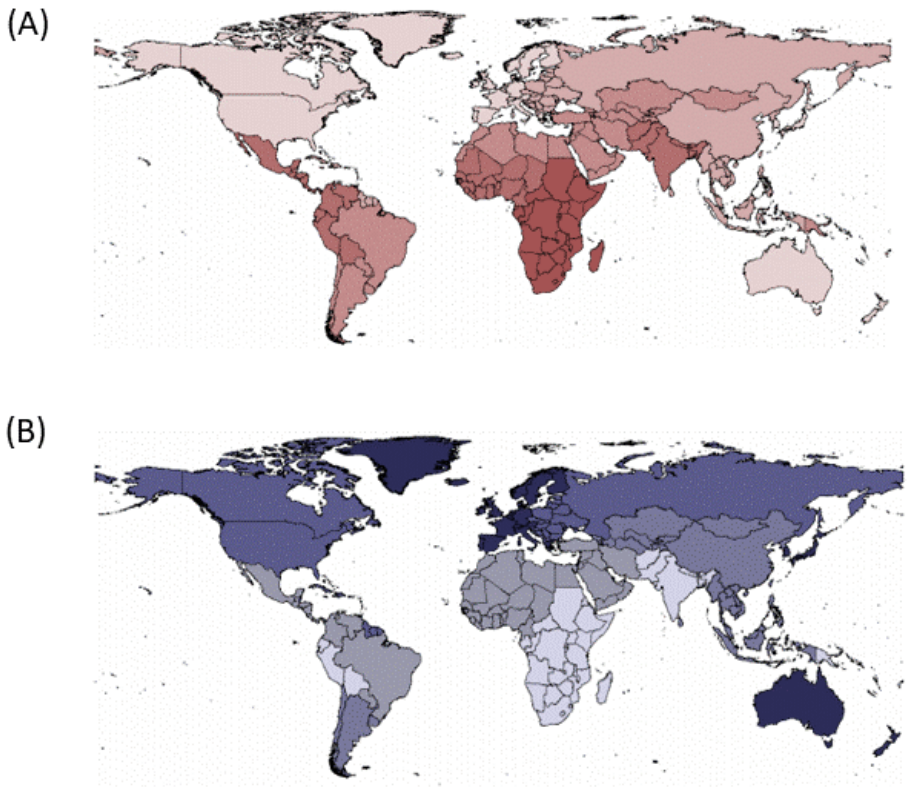

Figure 1.1: Regional age-seroprevalance of Hepatitis A Virus (HAV) in human populations (adapted from WHO, 2010).
HAV seroprevalence data was pooled from more than 500 published articles to fit estimate age-seroprevalance curves from 1980 through 2008 for each of 21 world regions. (A) Estimated child immunity rate where darker shades indicate a high exposure rate. The child immunity rate is based on the estimated proportion of children ages 10 to 14 who are immune. A high child immunity rate indicates a high HAV exposure rate, and vise versa. (B) Estimated adult susceptibility rate where darker shades indicate a greater proportion of at-risk adults. The adult susceptibility rate is based on the estimated proportion of adults age 35 to 44 who are at risk. A high adult susceptibility rate correlated with an elevated risk of disease outbreaks.

countries. This contrasts with the phenomenon observed in higher-income countries where the adult population are more susceptible to HAV (Fig. 1.1B, darker blue shade).This is because there is a lower incidence of HAV infection in higher income countries and the majority of the population is not infected with HAV in early childhood (132). This leads to a higher disease burden in these higher income countries because the disease severity and the risk of death associated with HAV infection increases with age (58,132), as shown by HAV outbreaks in San Diego County.

1.2 HAV Clinical Course

HAV infection usually results in a self-limited disease and rarely causes a fatal outcome. The clinical course of HAV infection is age-dependent (20,41,60,65,70). More than 70% of infected young children are asymptomatic, whereas about 80% of infected adults develop symptom of hepatitis varying from mild to severe symptoms (60,77). The mortality rate associated with HAV infection ranges from 0.1% in patients ≤15 years to 1.8% in patients ≥50 years (63,98). Because there are no antiviral drugs for treatment of HAV, supportive care, including adequate hydration, nutritional support, application of antiemetics (drugs against vomiting and nausea) and antipyretics (drugs against fever) (60) are used when the HAV-infected individuals are in severe condition.

Acute HAV infection is divided into four clinical phases (63,98). HAV infection starts with an *incubation (preclinical)* period ranging from 10 to 50 days (average of 28 to 30 days) (10,36,63,98). During the incubation period, HAV replicates actively in the liver of the infected individuals but the patients remain asymptomatic (98). In this phase, HAV is shed into feces extensively, and to a lesser extent, secreted into the blood (Fig. 1.2) (9,63,83,98). The incubation phase is the period of greatest viral production occurs and transmissibility. The second phase is a short *prodromal or pre-icteric* (the period prior to the appearance of jaundice) stage that usually lasts days to weeks.

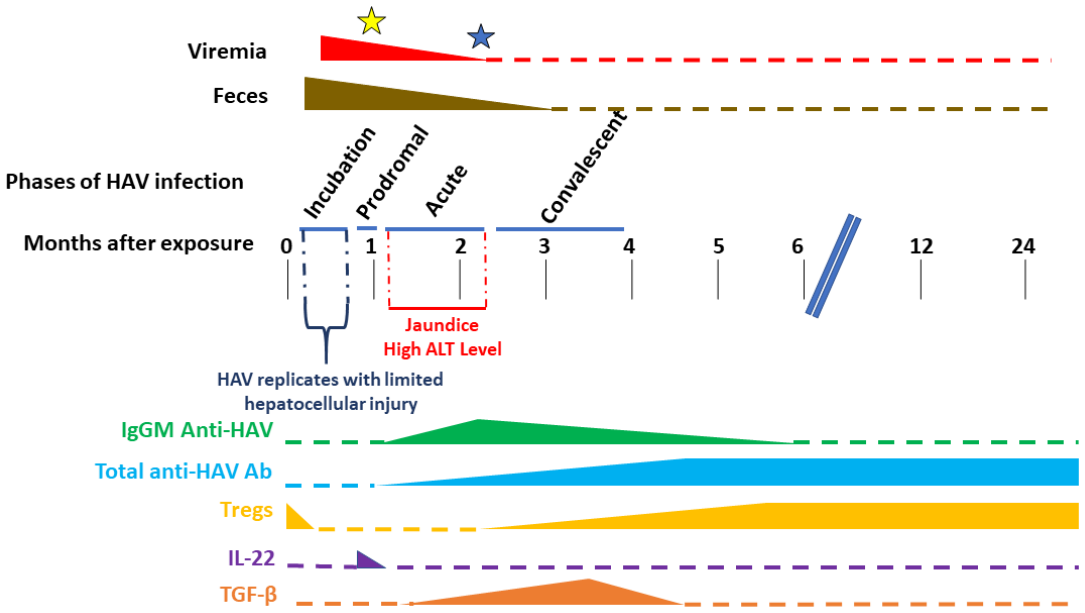

Figure 1.2: The natural history of HAV infection (adapted from Pintó et al., 2014) A schematic representation of the normal clinical course of HAV infection as indicated by different biomarkers at different phases of the infection. The detection of different biomarkers is shown over the time course of HAV infection. Acute HAV infection is divided into four clinical phases: incubation, prodromal, acute and convalescent periods. During the incubation and prodromal periods HAV reaches peak viremia and is shed into stools. The functions of Tregs is blocked by HAV and transiently impaired in early HAV infection period (yellow dotted line). The activation of the bystander CTL response (yellow star) and HAV-specific CTL response (blue star) occurs at different times post-infection. Elevated alanine aminotransferase (ALT) levels occur during the acute infection period (peak at approximately one month after infection) indicates hepatocellular injury. The secretion of interleukins (IL)-22 (purple) and transforming growth factor-beta (TGF-β) (orange) occurs at different times post-infection. Anti-HAV IgM and IgG antibodies are detected in blood. Anti-HAV IgM (green) is typically short-lived and acts as the marker of acute HAV infection. Anti-HAV IgG (blue) usually provides long term protection against HAV.

Patients develop moderate clinical symptoms (including anorexia [loss of appetite], fatigue, malaise, abdominal pain, nausea and vomiting, fever, diarrhea, dark urine and pale stools). After the prodromal stage patients enter an *icteric acute* (indication of jaundice) phase that usually lasts two to four weeks. This phase is characterized by the development of jaundice (appearance of yellow skin and eyes) and the elevation of both bilirubin and ALT levels. The ALT levels of patients are typically more than ten times the upper normal limit. In the acute phase, there is a transient elevation of immunoglobulin M (IgM) against HAV (Fig. 1.2). Anti-HAV IgM response is triggered two to three weeks after HAV infection and remains detectable for up to six months. This explains the termination of viremia shortly after the development of hepatitis. Feces from the infected individuals remain infectious for another one to two weeks. The appearance of anti-HAV IgM response is followed by the presence of persisting anti-HAV IgG (immunoglobulin G), resulting in a rapid decline in the level of virus in both feces and blood (Fig 1.2) and lifelong protection against hepatitis A (9). The final clinical phase of acute hepatitis A infection is the *convalescent* period when the virus is cleared and the patients recover. Cellular immunity plays a role in final clearance of virus with the peak of cytolytic activity detected in the early convalescent period (Fig. 1.2, blue star) (63,125).

1.3 HAV Pathogenesis Mechanism

HAV can replicate escaping the surveillance of the immune system, for several weeks without causing hepatocellular injury. Besides, HAV production reaches a peak in shedding and viremia before infection is detected by the immune system (63,98). Studies show that HAV infection prevents IFN-β induction(12,35) through the action of 2B protein (91), 3ABC intermediate (136) and 3CD intermediate (103) of HAV by interfering the activation of IFN regulatory factor 3 (IRF3). However, the mechanism

utilized by HAV to evade other innate immunity currently remains unknown (98). To clear HAV infection, B cells and CD4+ T helper cells predominantly infiltrates the liver during acute HAV phase (48,69,112,139). However, using HAV-infected chimpanzee model, there is no temporal association between CD8+ T cells effector function and viral control in acute phase until after viremia (139). Besides, CD8+ T cells contract rapidly before HAV clearance but CD4+ T cells contract slowly over times after HAV is cleared from the infected cells, suggesting a dominant role of CD4+ T cells in HAV clearance (139).

Although mechanism for HAV to evade innate and adaptive immune system remains to be studied, a model involving the transient impairment of regulatory T cells (Tregs) ($CD4^+/CD25^+/Foxp3^+$ cells) is used to describe HAV pathogenesis (Fig. 1.3) (19,63,81,94). During early HAV infection stage, HAV infects and replicates in the liver (Fig. 1.3a). HAV replication blocks the production of interferon beta (IFN-β) and other antiviral effectors that are triggered by double-stranded RNA (dsRNA) (12,35,92). Virions are either shed in feces or enter the blood causing viremia (Fig. 1.3b). At this stage, Tregs activities are blocked where the two possible mechanisms are proposed to shut-off Treg function. First, when HAV circulates within the blood system the virus binds to its entry receptor, hepatitis A virus cellular receptor 1 (HAVcr-1), expressed on Tregs (Fig. 1.3c) (81). HAVcr-1 (also known as TIM1) is a member of the T cell immunoglobulin and mucin domain (TIM) gene family (30). HAVcr-1 is expressed on activated CD4+ T cells and acts as a costimulatory molecule for T cell activation and regulation of tolerance development (25,124). The interaction between HAV and HAVcr-1 inhibits the activation of Protein Kinase B (PKB/Akt) and T-cell receptor (TCR) and thus, temporarily shuts off the functions of Tregs. The frequency of Tregs is comparable between acutely infected individuals and healthy controls (81,94). This

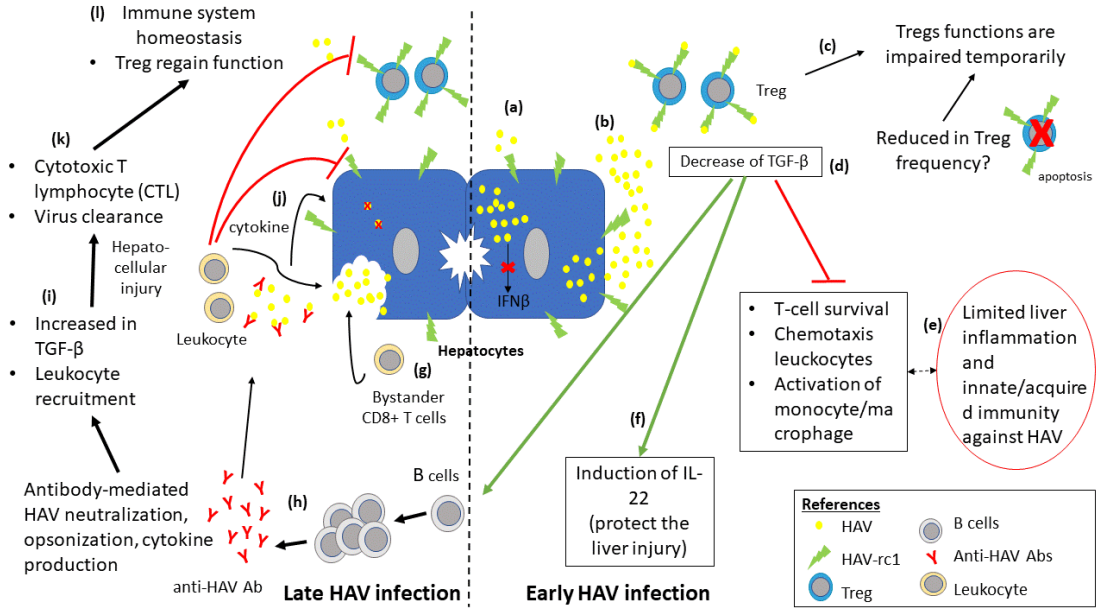

Figure 1.3: The Pathogenesis Mechanism of HAV (adapted from Kaplan et al., 2013) A schematic representation of the cycle of immune events leading to a typical clinical course of HAV infection. (a) When HAV infects and replicates in liver, IFN-β production is blocked. (b) Viruses either are shed into feces or enter blood circulation to cause viremia. (c) The activities of regulatory T cells (Tregs) are reduced transiently by two possible mechanisms. First, HAV interacts with its entry receptor, hepatitis a virus cellular receptor 1(HAVcr-1) expressed on Tregs to temporarily shut-off Treg function. Second, the frequency of Tregs is reduced through Fas-mediated apoptosis that is triggered by strong TCR/costimulatory signals or secreted cytokines during acute HAV infection, subsequently reduces Treg activities. (d) The reduction of Treg activities blocks the secretion of TGF-β (one of the cytokines produced by activated Tregs) and prevents its downstream pathways. This lead to (e) limited liver inflammation and limited innate/acquired immunity against HAV and (f) an increase in interlukin-22 (IL-22) during early HAV infection stages (incubation, prodromal, early acute phases). Low level of TGF-β and the secretion of IL-22 allow HAV replication in liver with limited inflammation and limited hepatocellular injury during early stages. (g) Limited Treg activities during the acute infection activate bystander CD8+ T cells that mediates hepatocellular damages. (h) The low levels of TGF-β also trigger a strong anti-HAV antibody response. (i) Both gradual restoration of Treg functions and production of TGF-β promote the recruitment of leukocytes to liver. This leads to the inflammatory process in late acute and convalescent stages, inducing hepatocellular injury. (j) In the convalescent phase, cytokines produced by infiltrating leukocytes promote viral clearance through cytolytic and non-cytolytic mechanisms. (k) The activation of HAV-specific cytotoxic T cells (CTLs) and a strong humoral response to neutralize virus contribute to the non-cytolytic viral clearance. This stage likely completes HAV clearance. (l) The immune system returns to homeostasis with contraction of the T-cell response and the restoration of Treg function.

contradicts mechanism of Treg impairment proposed by Choi et al. (2015). They proposed that during acute HAV infection, strong TCR/costimulatory signals or cytokines secretion, rather than HAV particles, induce overexpression of Fas on Tregs leading to their apoptosis and a reduction in their frequency (19). Although there is the contradiction between the two mechanisms, both agree that the transient Treg impairment is crucial in HAV pathogenesis mechanism.

The transient impairment of Treg functions blocks secretion of transforming growth factor-beta (TGF-β), one of the cytokines produced by activated Tregs (Fig. 1.3d) (81). Inhibition of TGF-β production can prevent T-cell survival, leukocyte chemotaxis to the site of infection, and monocyte activation. This leads to limited liver inflammation and limited innate or acquired immune response against HAV (Fig. 1.3e). During the viremia phase, there is an increase in the production of interlukin-22 (IL-22), a cytokine produced primarily by T-helper (Th)17, Th22, and natural killer (NK) cells (Fig. 1.3f) (81,89). IL-22 plays a role in protecting the liver from injury (16,89,107,135). The elevation of IL-22 is suggested to compensate for Treg functions transiently impaired early in HAV infection. As shown in Fig. 1.2, low TGF-β production level and the secretion of IL-22 allow HAV to replicate in the liver with limited inflammation and limited hepatocellular injury early in HAV infection.

Limited Treg activity during the acute phase favours the activation of bystander CD8+ T cells that cause hepatocellular damage (Fig. 1.2, yellow star; Fig. 1.3g) (114). The low levels of TGF-β also trigger a strong anti-HAV antibody response to reduce viremia and to prevent the interaction between HAV and its entry receptor, HAVcr-1 (Fig. 1.3h). A gradual restoration of Treg function and the production of TGF-β promote the recruitment of leukocytes to the liver (40,111,127) where the immune regulation involving TGF-β and Treg is reviewed herein (128) . This leads to the liver

inflammation and injury in the late acute and convalescent stages of infection (Fig. 1.3i) (40). In the convalescent phase, the cytokines produced by infiltrating leukocytes promote viral clearance through cytolytic and non-cytolytic mechanisms (Fig. 1.3j). The activation of HAV-specific cytotoxic T cells (CTLs) peaks at three to four weeks after jaundice in the convalescent phase (125,127). A strong humoral response to neutralize the virus contributes to non-cytolytic clearance of the virus from infected cells (Fig. 1.3k). After clearance of HAV, the immune system returns to homeostasis with contraction of T-cell response and the restoration of Treg function (Fig. 1.3l).

1.4 HAV Transmission Routes, Preventions and Treatments

HAV is a global health burden despite the fact that HAV induces a self-limited disease. Symptomatic HAV infection reduces an individual's work performance and productivity. The economic impact of HAV outbreaks can be substantial. This has been reviewed in a global analysis of 13 reported HAV outbreaks and summarized by Luyten et al. (76). Thus, it is important to prevent HAV outbreaks in the populations.

HAV infection is transmittable through foodborne (acquired primarily through the fecal-oral route) and waterborne (highly transmittable through sewage-contaminated water) routes. HAV outbreak occurs when virus contaminated water used for agriculture practices and food processing contaminates food. Food that often cause disease outbreaks include semi-dried tomatoes (15,28,42,95), frozen fruits (22,37,113) and seafood harvested from the polluted water (9,23,27,50,73,78,108). Current water treatments do not assure the complete removal of HAV in human sewage (8). It is also challenging to prevent hepatitis A outbreaks when the virus is circulating among the population (98). Reduction of HAV spread was reported when there were adequate safe drinking water supplies, proper disposal of sewage and personal hygiene practice (41).

HAV-infected food handlers are a leading cause of HAV foodborne outbreaks

(36,106,109). HAV infection is often asymptomatic. Such asymptomatic infected individuals working in the food industry may contaminate food and lead to a HAV outbreak. To prevent foodborne hepatitis A outbreaks in food industries, good production practice is required. First, hand hygiene in the processing industry is a crucial control point in preventing viral contamination of food. Second, personnel in food industries with suspected HAV infection must be strictly banned from workplaces until they recover completely from hepatitis A disease.

There is no specific antiviral drug targeting HAV, but HAV infection is completely preventable by two dose hepatitis A vaccination. The vaccine was approved and licenced since the early 1990's and introduced in Canada in 1996. According to the report of Public Health Agency of Canada (PHAC), the incidence of hepatitis A in Canada dropped after hepatitis A vaccine was introduced (97).

The history of the hepatitis A vaccine development was discussed by Hillemen (1993) (51). The production of a prototype killed HAV vaccine used HAV produced in infected marmosets (100). This was followed by the production of a live attenuated HAV vaccine using HAV propagated fetal rhesus kidney cells, FhrK6 cells (101). In 1986 an inactivated (killed) HAV vaccine was produced using virus produced in rhesus monkey kidney epithelial cells, LLC-MK2. This vaccine was prepared by inactivating the viral particles with formalin and adsorbing the viral particles on an aluminium hydroxide adjuvant (102). Inactivated HAV vaccine was shown to be highly potent, safe, and provides lifelong protection (57,64). The protection mechanism of inactivated HAV vaccines is proposed to be antibody-based (72,83). The vaccines are effective against all human strains, consistent with the existence of a single serotype of HAV. This probably explains statistical studies showing that pre-exposure to HAV is 90-97% effective in preventing clinical illness (97,130,131).

Hepatitis A vaccine is recommended for high risk populations: travellers to or immigrants from hepatitis A endemic areas, persons with chronic liver disease, homosexuals, drug abuses, persons with clotting factor disorders, the military, and persons handling non-human primates (41,97). For those whom hepatitis A vaccine is contraindicated: infants below one year of age or immunocompromised individuals, human immune globulin (Ig) can be used as a passive immunizing agent (97).

1.5 HAV Genome Structure and Replication Cycle

HAV is a single stranded positive-sense ribonucleic acid (RNA) virus and stands alone in the genus *Hepatovirus* within the family *Picornaviridae* (26,83,87,98). HAV has a genome of approximately 7.5 kilobase (kb). The viral RNA genome is surrounded by an icosahedral protein capsid composed of three major structural proteins, VP1, VP2 and VP3, with 60 copies of each protein (83). HAV is subdivided into six genotypes (1-VI), but is of a single serotype. The first three genotypes (I-III) are of human origin whereas the other three genotypes (IV to VI) are of simian origin (26). The main replication site of HAV is hepatocytes, though other cells types, for example spleen, lymph node and kidney have been reported to contain HAV antigens (84,98,110).

Two cell entry mechanisms have been proposed to initiate HAV infection (Fig. 1.4a). The first entry mechanism is the binding of HAV to the cell surface receptor HAVcr-1 (26,62). The second mechanism is the formation of a complex between HAV and immunoglobulin A (IgA) molecules. This complex binds to and is internalized by asialoglycoprotein receptors (ASGPR), carbohydrate-specific receptors expressed on the surface of hepatocytes (4,5,26,29). Once the virus is internalized, the uncoating process is initiated to release the messenger-sense RNA into the host cell cytoplasm (Fig. 1.4b). The presence of heterogeneous mixture of infectious HAV particles (virions and provirions [immature virions]) results in a slow and asynchronous

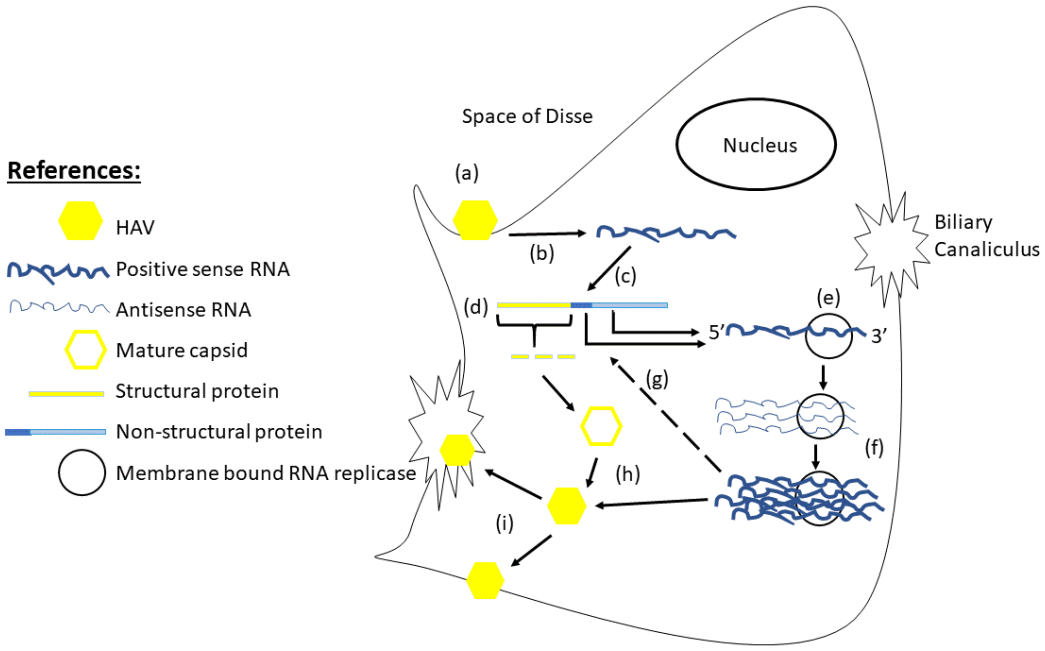

Figure 1.4: HAV life cycle (adapted from Martin *et al.*, 2006).
The figure showed the enterohepatic cycle of HAV. (a) HAV (yellow) infects the hepatocytes by interacting with a cellular receptor. (b) This is followed by the uncoating process to release RNA genome into the host cytoplasm. (c) The virus employs an internal ribosome entry site located within the 5' non coding region of the genome to direct the cap-independent translation of the viral polyprotein. (d) The polyprotein will undergo co- and post-translational proteolytic cleavage directed by the viral protein, $3C^{pro}$. (e) Non-structural viral proteins assemble into a membrane-bound RNA replicase (not drawn to scale), bind the 3' end of the genomic RNA to synthesize the antisense RNA. (f) The antisense RNA is used as the template to synthesize new copies of genomic messenger RNA. (g) Some of the newly synthesized positive-sense RNA is recycled for further RNA synthesis or translation of new protein. (h) Other viral RNA molecules are packaged into new viral particles formed by assembly of the structural proteins, followed the cleavage of the VP1-2A precursors as well as VP4/VP2 junction (yellow empty hexagon). (i) Newly assembled virion particles are released across the apical membrane of the hepatocyte into the biliary canaliculus and secreted in feces via bile. Alternatively, they are secreted from basolateral membrane of the hepatocyte to circulate in the blood.

uncoating process with a reported duration of four to ten hours (6,26).

HAV genome is composed of a 5' noncoding regions (5' NCR) followed by a single large open-reading frame (ORF) encoding a polyprotein and a 3' NCR with a short poly(A) tail. (Fig. 1.5) (26,83,98). The polyprotein can be divided into structural proteins (P1-2A segment) composing of major capsid proteins (VP1, VP2, VP3) and non-structural proteins (2BC and P3 segments) that are required for HAV RNA replication (2B, 2C, 3A, 3B, $3C^{pro}$ and $3D^{pol}$) (Fig. 1.5) (98).

After uncoating and delivery of genomic RNA to the cytoplasm, the messenger-sense genomic RNA is translated directly into the viral proteins (Fig. 1.4c) (83). HAV uses an internal ribosome entry site (IRES) located within 5' NCR RNA genome segment to direct 5'cap-independent translation of the polyprotein (14,83,83,98). The polyprotein undergoes co- and post-translation processing by a series of proteolytic cleavages to release mature structural and non-structural proteins (Fig. 1.4d) (26,83,98). The initial cleavage takes place at 2A/2B junction (Fig. 1.5, red star). Major proteolytic cleavage events within the polyprotein (Fig. 1.5, star) are mediated by viral cysteine protease $3C^{pro}$ (Fig. 1.5, gray box) (26,45,82,83,98).

RNA synthesis takes place in the replicase complex (Fig. 1.4e, round icon) consisting of the non-structural viral proteins spanning 2B-$3D^{pol}$ segment of the polyprotein (83). The uridylylated 3B protein (also known as viral protein genome-linked, VPg) is covalently linked to 5' end of the genomic RNA and likely serves as the protein primer to initiate RNA replication (26,83,98). During replication, transmembrane protein 3A tethers the growing viral RNA strand and associated proteins to the membranes of the replication complex (19,26).

Non-structural viral proteins assemble into a membrane-bound replication complex to promote viral genome replication (Fig. 1.4e). The replicase together with

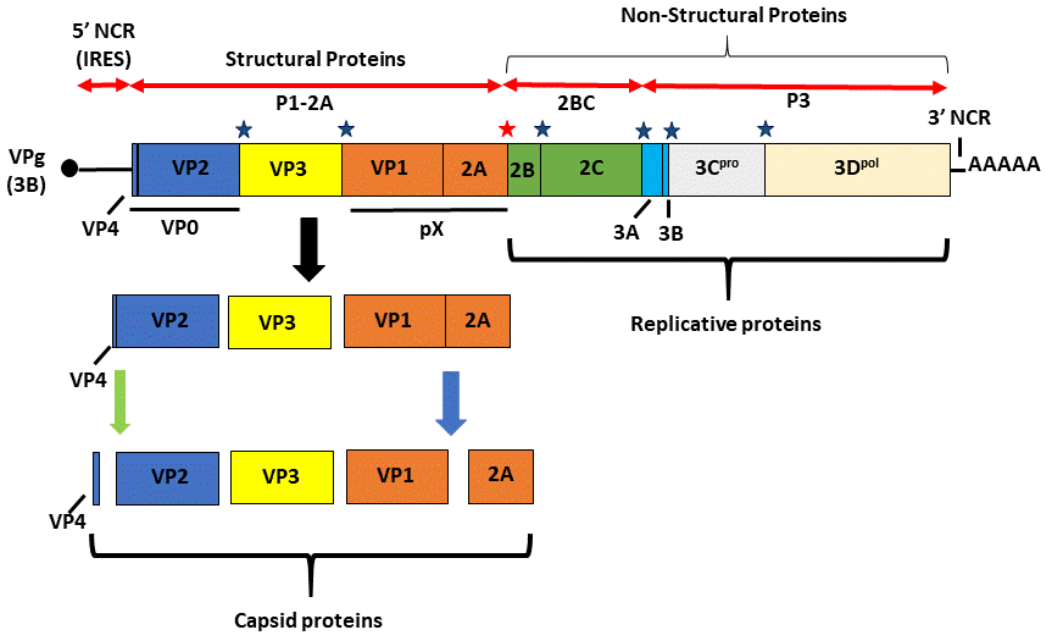

Figure 1.5: HAV genome organization and viral protein expression (adapted from Debing et al., 2014).

HAV has a single strand positive RNA genome of 7.5kb in length. Its genome contains 5' noncoding region (NCR), a single open reading frame (ORF) encoding a polyprotein, followed by 3' NCR with a short poly(A) tail. The polyprotein can be divided into structural proteins (P1-2A segment) and non structural proteins (2BC and P3 segments). The polyprotein will undergo a series of proteolytic cleavage to release precursor and mature proteins. The primary post-translation cleavage is carried out by viral protease $3C^{pro}$ (gray box) at the junction between P1-2A and 2B (indicated by red star). The following proteolytic cleavage sites that are carried out by the viral protease $3C^{pro}$ are indicated by blue star. VP1-2A precursor cleavage is carried out by an unknown cellular protease (blue arrow) and the proteolytic activity at VP4/VP2 junction remains unknown (green arrow). $3D^{pol}$ viral RNA-dependent, RNA polymerase; AAAAA poly A tail, *IRES* internal ribosome entry site, pX domain VP1+2A; VP0 domain VP4+VP2; *VPg* small viral protein 3B linked to the 5' end of the viral genome.

newly generated RNA-dependent RNA polymerase ($3D^{pol}$) binds 3' end of the genome RNA to initiate the synthesis of antisense RNA (26,83,98). This negative-strand RNA serves as template for new viral genome production (Fig. 1.4f) (98). Some newly synthesized viral genomes are recycled for further RNA synthesis or translation of new proteins (Fig. 1.4g) (98). Other newly synthesized RNA molecules are packaged into the viral capsid for secretion (Fig. 1.4h) (26,83,98).

The maturation of viral capsid is promoted by a series of cleavage events (Fig. 1.5). After the cleavage event at 2A/2B junction, the resulting P1-2A protein is further processed by viral protease $3C^{pro}$ and its stable precursor $3ABC^{pro}$. This cleavage event leads to the production of VP0 (composed of VP4 and VP2), pX precursor (composed of VP1 and 2A), and mature VP3 protein. These building blocks assemble into pentameric capsid particles followed by packaging of viral RNA to form preprovirions. Lastly, VP0 is cleaved by an unknown protease to form VP4 and VP2 (Fig. 1.5, green arrow) (99) and precursor pX is cleaved by an unknown host protease into VP1 and 2A (Fig. 1.5, blue arrow) (49,82) to generate mature virus particles with VP1, VP2 and VP3 proteins (Fig. 1.4h, yellow empty hexagon) (2,99). The newly synthesized virions are released from either apical or basolateral membranes of the hepatocytes (Fig. 1.4i). The viruses released across the apical membrane of the hepatocyte into the biliary canaliculus are excreted into the feces. Alternatively, the viruses secreted from the basolateral membrane enter the bloodstream for circulation.

Studies to understand enterohepatic cycle of HAV became challenging when two HAV populations, enveloped (in blood) and non-enveloped HAV (in feces), were reported (see Sec. 1.6 for the details of two HAV populations). HAV circulating in the bloodstream was shown to be fully cloaked in a lipid membrane (enveloped populations). HAV in the feces was not enveloped.

1.6 Two HAV Populations

In 2013, Feng et al. reported two HAV populations *in vivo*: quasi-enveloped (quasi-eHAV) and non-enveloped (standard form) (32) distinguishable by several criteria. First, the two HAV populations have different densities. Quasi-eHAV is less dense (1.06-1.10 g/cm^3) than non-enveloped HAV (1.22-1.28 g/cm^3). Second, quasi-eHAV is found exclusively in blood while non-enveloped HAV is found in feces. Third, quasi-eHAV is seem as membrane-wrapped particles by electron microscopy (EM). The diameter of quasi-eHAV is between 50-110 nm, whereas standard non-enveloped HAV has a diameter of ~27 nm. Fourth, the capsid of quasi-eHAV, unlike non-enveloped HAV, is not detected in capsid antigen enzyme-linked immunosorbent assay (ELISA). This is consistent with the capsid of quasi-eHAV being membrane coated. After treatment with the non-ionic detergent (1% NP40), the capsid of quasi-eHAV becomes detectable by ELISA and the viral density shifts to intermediate density (1.15-1.17 g/cm^3). Fifth, both HAV populations have equivalent infectivity levels. However, chloroform treatment reduces the infectivity levels of quasi-eHAV.

The pX domain, an carboxy-terminal extension on VP1 domain, plays a role in virion assembly. It is cleaved by unknown host protease late in virion maturation to produce fully processed VP1. By performing immunoblotting, gradient-purified quasi-eHAV has the unprocessed VP1-pX domain (~37 kDa) where the pX domain is not cleaved from VP1-pX domain while chloroform-treated HAV (non-enveloped HAV) has a mature VP1 domain (~30 kDa). Besides, the treatment of quasi-eHAV with 1% NP40 renders its pX domain susceptible to the digestion of Proteinase K, suggesting that VP1-pX domain is fully enclosed within the membrane of quasi-eHAV.

To acquire the envelope, HAV is proposed to utilize a cellular membrane hijacking mechanism (32). The formation of quasi-eHAV is mediated by the interaction

of capsid with ALIX (apoptosis-linked gene 2-interacting protein X, a protein involved in exosome biogenesis) and the ESCRT system. Quasi-eHAV then buds into multivesicular bodies (MVBs). Feng et al. (2013) reported that knock down of either ESCRT-III associated proteins, VPS4B (vacuolar protein sorting-associated protein 4B) an ATPase catalysing disassembly of ESCRT-III complexes during membrane fission, or ALIX decreases the amount of quasi-eHAV released from the infected cells (32).

Several egress pathways for the two HAV populations have been proposed (Fig. 1.6) (34). The first mechanism is that the two HAV populations are secreted from hepatocytes by a bipolar mechanism (Fig. 1.6A). HAV is produced as both quasi-enveloped (yellow hexagon within the circle) and non-enveloped (yellow hexagon) viral species and they egress from the polarized hepatocytes in different directions. Non-enveloped HAV are secreted from the apical surface into bile canaliculus whereas quasi-eHAV are secreted from the basolateral surface of the hepatocytes.

The second proposal is that HAV uses a carrier-mediated transcytosis mechanism (Fig. 1.6B). Both quasi-eHAV and non-enveloped HAV are secreted basolaterally into the space of Disse. There, non-enveloped HAV forms a complex with HAV specific-immunoglobulin A (IgA) and re-enters the hepatocyte, transits to the apical membrane and is released into the biliary tract. The secretory pathway of IgA is in the basolateral to apical membranes direction in epithelial cells, and thus, IgA is proposed as a candidate carrier. Counihan et al. (2016) reported that HAV complexed with IgA enhanced HAV transcytosis and excretion *in vitro* and *in vivo* (24).

The third mechanism is that bile acids act as a detergent to strip off the membrane of quasi-eHAV (Fig. 1.6C). After acquiring the membrane, quasi-eHAV are secreted from the basolateral surface of hepatocyte resulting in systemic circulation of the enveloped viral population. Bile acid concentration is thought to being highest at

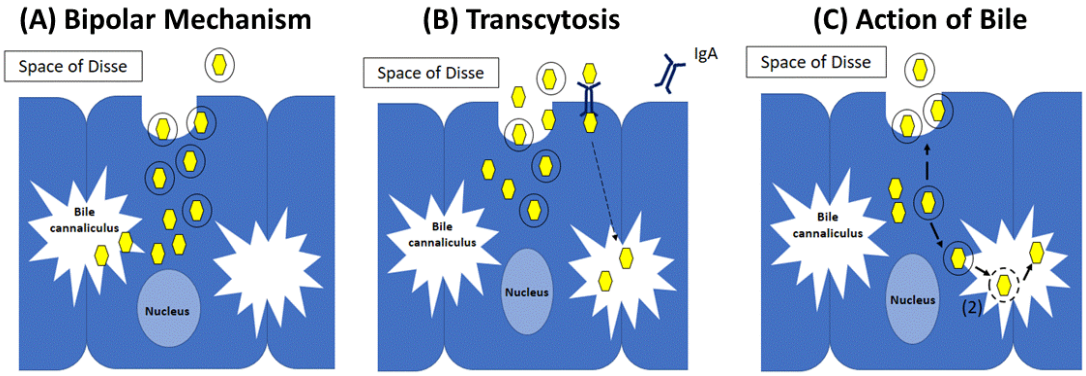

Figure 1.6: Proposed egress mechanisms of the two HAV populations (adapted from Hirai et al., 2016)

A simplistic diagram to depict three different egress mechanisms of the two HAV populations *in vivo*. (A) The first possibility is that quasi-eHAV and non-eneveloped HAV use a bipolar mechanism to exit the hepatocyte. Quasi-eHAV are released across the basolateral membrane into the space of Disse while non-enveloped HAV are secreted into the bile canaliculus. (B) The second possibility is that both quasi-eHAV and non-enveloped HAV are released into the space of Disse. Non-enveloped HAV will undergo transcytosis by forming a complex with immunoglobulin A (IgA) to re-enter the hepatocyte and be secreted into the bile canaliculus from the apical membrane. (C) The third possibility is that quasi-eHAV enters the bile canaliculus where bile acid act as a detergent to strip off the membrane of quasi-eHAV to form the non-enveloped HAV population secreted into the feces. Yellow hexagon: non-enveloped HAV; yellow hexagon in circle: quasi-eHAV

the luminal surface of the canalicular membrane. Thus, if quasi-eHAV are secreted into bile canaliculus at the apical surface, quasi-eHAV is stripped of its membrane by bile. This results in the secretion of standard non-enveloped HAV in the stool of infected individuals. Hirai-Yuki et al. (2016) reported human bile acid components, chenodeoxycholic acid (CDCA) and taurocholic acid (TCA), stripped off the membrane of quasi-eHAV *in vitro* (53). The concentration of the bile used to treat the quasi-eHAV shifted the density of quasi-eHAV to different ranges. Treatment with either 24 mM CDCA or 93 mM TCA partially increased the density of quasi-eHAV, but the treatment with 930 mM TCA completely shifted the density of quasi-eHAV to that of non-enveloped eHAV (53). The authors proposed that the bile acid components required to strip off the membrane of quasi-eHAV is species-dependent (75). This might explain why concentrated porcine bile failed to strip off the membrane of quasi-eHAV (32).

1.7 *In vitro* models for HAV studies

Culturing wild-type (wt) HAV was once a challenge because the virus replicated inefficiently *in vitro* (26,83). HAV was first observed under immune electron microscopy (immune EM) by Stephen M. Feinstone in 1973 (31). It took six years after this discovery to develop the first cell culture model system. HAV was initially passaged through marmosets was found to replicate in fetal rhesus kidney cell line (FRhK6 cells) (101). In the following years other cell lines, including cells of non-hepatic or hepatic, primate or non-primate origin, were developed to support propagation of cell-culture adapted HAV strains (38,39,44,126). Adaptation was achieved by serially passaging HAV *in vitro* to undergo adaptive mutation (9,83). Mutations in the P2 region (especially in 2B and 2C) and the 5' NCR of HAV are thought to be important in the efficient growth of the virus *in vitro* (9). These mutants

are genetically unstable and tend to acquire additional mutation in cell cultures. In 2006, Konduru et al. established the first cell line, Huh7-A-I (a selection of Huh7 cells) that permitted the genetically stable growth of human wild-type (wt) HAV *in vitro* (66).

While *in vitro* models are available for HAV studies, some aspects of the molecular biology of HAV are not fully understood. The enterohepatic cycle of HAV, especially the viral release mechanisms, remains unsolved (9). Several studies of HAV release mechanisms have been reported. Debing et al. (2014) has reviewed the cell types used to study HAV exit mechanisms (26). In polarized human intestinal epithelial Caco-2 cells Blank et al. (2000) showed that HAV exit was largely restricted to the apical membrane (7). On the other hand, in polarized human hepatocytes cultured in media supplemented with 1% of dimethyl-sulfoxide (DMSO) Snooks et al. (2008) demonstrated that the release of HAV occurred most efficiently through the basolateral surface (117). Studies to understand the enterohepatic cycle of HAV *in vitro* become more challenging when both enveloped and non-enveloped HAV were discovered (see Sec. 1.6).

1.8 Human Serum (HS) Cells

In 2013 Steenbergen et al. reported remarkable changes in the properties of Huh7.5 cells (a hepatoma cell line) grown in culture media supplemented with 2% of human serum (HS) (120) compared to the properties of cells grown in standard culture media supplemented with 10% of fetal bovine serum (FBS). Cells cultured in HS-containing media and FBS-containing media are referred to as “HS cultured cells” and “FBS cultured cells” respectively.

HS cultured cells exhibited properties more typical of human hepatocyte (120). Unlike FBS cultured cells, HS cultured cells are growth arrested after a week in HS-containing media (120). HS cultured cells also develop a pavement-like organization

(hepatocyte-like morphology), whereas FBS cultured cells have a fibroblast like morphology (120). When compared to FBS cultured cells, HS cultured cells had increased albumin mRNA and elevated albumin secretion levels, a functional marker of differentiation. There was an increase in cell-cell contact components including claudin-1, occludin and E-cadherin (120). Very-low-density-lipoprotein (VLDL) secretion was restored in HS cultured cells, a hepatocyte function absents in FBS cultured cells (120).

1.9 Hypothesis and Objective

The biological relevance of the two HAV populations reported by Feng et al. (2013) (32) remains unknown. To study these two HAV populations *in vitro* a good cell culture system representative of hepatocytes and able to secrete the two HAV populations is required.

The objective of this study is to develop an *in vitro* model, mimicking the polarized hepatocyte, capable of secreting the two HAV populations as defined by their density. We hypothesize that the polarized and differentiated hepatoma cell line cultured in a dual-chamber system with HS media (HS cultured cells) is a cell culture model that is able to secrete the two HAV populations *in vitro*. We will compare the ability of this system to support production of the two HAV populations with that of the standard cell culture system which uses 10% FBS as a serum supplement.

We will also compare HAV populations secreted by the infected cells cultured as a monolayer on either standard plates/culture flasks or in dual-chamber systems with HS media. We will show the proper formation of tight junction by HS cultured cells in the dual-chamber system using dextran diffusion studies. With the well-differentiated HS cells in the dual-chamber system we will attempt to identify the populations of HAV secreted from the apical (upper chamber) and basolateral (lower chamber)

surfaces by performing isopycnic gradient ultracentrifugation to determine the virion density. We will compare the proportion of non-enveloped HAV (the higher density) and quasi-eHAV (the lower density) that are secreted into the upper (apical) and lower (basolateral) compartments of the dual-chamber system. This is to study whether the secretion of the each HAV population at apical and basolateral surfaces is either exclusive, preferential or random.

We will attempt to study the properties of the two HAV populations secreted *in vitro*. Are the virus populations secreted *in vitro* similar to those secreted *in vivo* as reported by Feng et al. (2013)? We will investigate the specific infectivity of the HAV populations by performing endpoint dilution assays (or 50 tissue culture infective dose, $TCID_{50}$ assays). We will also perform neutralization assays to determine the ability of different HAV populations to be neutralized by immunoglobulin G (IgG) specific to HAV.

CHAPTER TWO: METHODS AND MATERIALS

2.1 Human Samples and Clinical Information

The ethics of human blood sample collection as outlined in "Immunologic and Virologic Features of Hepatitis A, Hepatitis B, and Hepatitis C: Biobank for Comprehensive Analysis", were followed. Blood samples were collected from volunteers who were either vaccinated against HAV or not. Blood samples were centrifuged (3,000 x *g*) at room temperature (20-23°C) for 20 min. The sera were collected, aliquoted and stored at -80°C until needed.

2.2 Standard Cell Culture Conditions (referred as to FBS cultured cells)

Huh7 cells (human hepatocarcinoma cell line) were maintained in Dulbecco's Modified Eagle's medium (DMEM, D5796 Sigma-Aldrich, St. Louis, MO) supplemented with 10% fetal bovine serum (FBS) (F1051 Sigma-Aldrich, St. Louis, MO), 10.0 µg/mL streptomycin sulfate (#11860-038 Thermo Fisher Scientific, Massachusetts, United States) and 50.0 U/mL penicillin G (P3032 Sigma-Aldrich, St. Louis, MO). The cells were grown to confluency in T75 Corning^{TM} cell culture flasks (75 cm^2, canted neck, vented cap) and were passaged on a three days cycle seeded at a density of approximately 25% confluency. The media was aspirated, and the confluent cells were washed with 1X phosphate buffer saline (PBS) (137.0 mM NaCl, 2.7 mM KCl, 6.48 mM Na_2HPO_4, 1.45 mM KH_2PO_4, pH 7.15-7.4) and aspirated. Two millilitre (mL) of Trypsin/EDTA solution (8.0 g/L KCl, 0.4 g/L NaCl, 1.0 g/L $NaHCO_3$, 0.58 g/L dextrose, 0.5 g/L 1:250 trypsin, 0.2 g/L disodium EDTA, pH 7.4-7.5) was added to the cells and incubated at 5% CO_2 incubator (37°C) for three to five minutes. A volume of two mL DMEM/ 10% FBS/ penicillin-streptomycin was added to trypsinized cells at 1:1 ratio to inactivate trypsinization. Then, one mL of the resuspended cells was transferred to a new T75 Corning^{TM} cell culture flask containing 10.0 mL of fresh

DMEM/ 10% FBS/ penicillin-streptomycin. Cells were incubated in 5% CO_2 at 37°C. The cells were passaged following this protocol up to 35 times. All solutions were sterilized by Stericup-GP sterile vacuum filtration through 0.22 µm membranes (SCGPU05RE EMD Millipore, Darmstadt, Germany) and stored at 4°C.

2.3 Maintenance of Cells in HS (referred as to HS cultured cells)

To differentiate Huh7 cells, they were cultured and maintained in media supplemented with human sera (HS) (120). Huh7 cells initially grown in FBS media were washed with 1X PBS, trypsinized and resuspended in DMEM/ 10% FBS/ penicillin-streptomycin to inactivate Trypsin-EDTA solution, as described above (Sec. 2.1). Cell counting was performed by mixing 10.0 µL of cell suspension and 10.0 µL of trypan blue, using a Bright-Line® hemacytometer (Z359629 Sigma-Aldrich, St. Louis, MO). The volume of resuspended cells required to achieve a density of 30%-33% was transferred to a T75 Corning™ cell culture flask containing 10.0 mL DMEM supplemented with 2% HS (HP1022 Valley Biomedical, Virginia, United States), 50.0 IU/mL penicillin and 10.0 µg/mL streptomycin G. The cells were placed in the incubator (5% CO_2, 37°C). The cells grew to confluency in four days in HS media. These confluent HS cultured cells were split and transferred to a new Corning™ T75 flask at the ratio of one to three. Huh7 cells growth slowed in HS media and they differentiated gradually. For this reason, HS cultured cells had their final split by day 11 to form undividing Huh7 cells. At day 11, the cells were split onto either collagen-coated Transwell® Permeable Supports dual-chamber systems (3.0 µm pore size, #3492 Corning Inc., New York, United States) or 12 wells plates (culture plates). The Transwell® dual-chamber systems were pre-incubated with DMEM only for at least an hour at 37°C for better cell attachment according to the manufacturer's protocol. Next, HS media with cells at a density of 30%-33% were transferred to Transwell® insert.

The cells in the dual-chamber system formed a confluent layer of growth arrested cells. HS media were replaced every three days.

2.4 Removal of Immunoglobulin G (IgG) from HS by Prepacked Protein A Column

IgG present in HS was removed by a 1mL HiTrap™ Protein A HP column (#29-0485-76 GE Healthcare, Little Chalfont, United Kingdom) with column dimensions of 0.7 x 2.5 cm, according to the manufacturer's protocol. The binding capacity of the column was ~20.0 mg human IgG.

All reagents used were syringe-filtered (0.22 μm, #SLGP033RS EMD Millipore, Darmstadt, Germany) to prevent clogging the column. HS samples (~10.0 mg IgG/mL) was diluted 1:3 with Opti-MEM® I Reduced-Serum Medium (MEM media) (#11058-021 Gibco by Life Technologies, Thermo Fisher Scientific, Massachusetts, United States). A 10 mL BD Luer-Lok™ tip syringe (#309604 Becton Dickinson, New Jersey, United States) was filled with binding buffer (20.0 mM sodium phosphate (Na_2HPO_4), pH 7.0). The column was connected to the syringe. Using the pump (PHD 2000 Harvard Apparatus, Cambridge, Massachusetts), the column was washed with ten column volumes of MEM media, followed by ten column volumes of binding buffer at a flow rate of 0.5 mL/min. On completion of the binding buffer, six mL diluted HS was pumped onto the column at a flow rate of 0.1 mL/min. The first 0.5 mL of the flow through was discarded. The remaining flow through was collected in centrifuge tubes. Finally, the column was washed with two column volumes of MEM media. The first 0.5 mL of the flow through was collected and the rest was discarded.

The column was regenerated after passage of six mL diluted HS. The column was washed with ten column volumes of binding buffer (20.0 mM sodium phosphate) at the flow rate of 0.5 mL/min. IgG bound onto the column was eluted with five column

volumes of elution buffer (0.1 M citric acid in deionized water, pH 3.3). For column storage, the column was washed with five column volumes of storage solution (20% ethanol in deionized water) to prevent microbial growth. The column was capped in storage solution and stored at 4°C. The column was discarded after eight to ten regenerations.

Human sera collected after removal of IgG (post-column HS) was syringe filter-sterilized (0.22 µm, #SLGP033RS EMD Millipore, Darmstadt, Germany) and stored for future media supplementation. Eluted IgG was neutralized by 100.0 µL 1M Tris-HCl (pH 9.0) per mL fraction. Both the sterilized post-column HS and the eluted IgG were stored at 4°C. Anti-HAV IgG testing of the post-column HS samples was performed by the Provincial Laboratory for Public Health, Edmonton or by Anti-HAV IgG ELISA (enzyme-linked immunosorbent assay) (see. Sec. 2.6). MEM media that was used for HS dilution prior to depletion and FBS were confirmed anti-HAV IgG negative and served as negative controls in our studies. Pre-column HS and the eluted IgG were confirmed positive for IgG and served as positive controls.

2.5 Removal of IgG from HS by Protein A Resin in Affinity Chromatography

For HAV infection studies, larger volumes of IgG depleted HS were required. For large scale depletion, IgG present in HS was removed with ultra-linked rProtein A resin (#10600-P07E-RN SB Sino Biological Inc., Biological Solution Specialist, Massachusetts) according to the manufacturer's protocol. The binding capacity of ultra-linked rProtein A resin is ~30.0 mg human IgG/mL drained medium.

To pack the column, an empty Glass-Econo-Column® chromatography column (2.5 x 20 cm) (#7374252 Bio-Rad) was secured upright in a clamp on a laboratory stand and pre-washed with deionized water. The ultra-linked rProtein A resin was made into a slurry. The slurry was pre-washed with deionized water three times and the washed

slurry was slowly poured into the column. About seven mL of drained resin settled to the bottom of the column. Three column volume of MEM media was used to wash the column. Forty-five mL of diluted HS samples were loaded onto the column to deplete IgG and the flow through was collected. After completion of flow through of HS samples, three column volumes of MEM media were used to wash the column. The first three mL of wash was collected and the rest was discarded.

The column was regenerated following each collection of 45.0 mL of the diluted HS (~35.0 mg of IgG per 45.0 mL diluted human sera). The column was washed with three column volumes of binding buffer (20.0 mM sodium phosphate pH 7.0, 50 mM Tris buffer pH 7.0, 1X PBS). IgG was then eluted with 0.1 M glycine in deionized water pH 3.0. The eluate was collected in 1.0 mL fractions in 1.5 mL centrifuge tubes containing 100.0 µL of 2.0 M Tris, pH 8.8. The protein absorbance at 280 nm of each fraction was read by NanoDrop® 2000 UV-Vis Spectrophotometer (Thermo Fisher Scientific, Massachusetts, United States) to monitor protein content. Peak fractions were pooled as IgG. The column was then washed with three column volumes of elution buffer, followed by three column volumes of binding buffer and three column volumes of storage solution (20% ethanol in 1X PBS). The column was stored at 4°C until needed. The resin was discarded after eight to ten regenerations.

Post-column diluted HS was filter-sterilized and stored for future use as media supplement. Both post-column HS and eluted IgG were stored at 4°C. The presence of anti-HAV IgG was determined by the Provincial Laboratory for Public Health, Edmonton or by using Anti-HAV IgG ELISA (see Sec. 2.6). MEM media used for HS dilution and diluted FBS (1:3 in MEM media) were confirmed to be anti-HAV IgG negative and served as negative controls in our studies. Pre-column diluted HS and eluted IgG confirmed positive for anti-HAV IgG served as positive controls.

2.6 Anti-HAV IgG ELISA

The presence of anti-HAV IgG was detected using a qualitative Anti-HAV IgG ELISA commercial kit, HEPAVASE A-96 (TMB) (#68-4AGE3 ALPCO Diagnostics, New Hampshire, United States), based on a competitive principle. The assay was used according to manufacturer's protocol. All the reagents, including positive and negative controls, were provided in the kit. Specimens and human peroxidase conjugated anti-HAV (mouse monoclonal) solution were mixed and incubated, washed with Washing Solution, incubated with TMB mixture solution and the reaction was stopped by 2N sulfuric acid (H_2SO_4). The absorbance of specimens was read within at 450 nm using Molecular Devices SpectraMax microplate reader. Specimens containing anti-HAV IgG competed over human peroxidase conjugated anti-HAV to bind to HAV Ag-coated wells and thus, no color developed.

2.7 Virus Stocks and Infections

A non-cytopathic cell culture adapted HAV variant HM175/p16 obtained from Dr. Stanley Lemon, University of North Carolina was grown in Huh7 cells maintained in FBS-containing media. When the infected cells were confluent, the supernatant was collected and centrifuged in a Sorvall™ Legend™ Micro 21R Microcentrifuge (#75003424 Thermo Fisher Scientific, Massachusetts, United States) at 21,100 x g, 4°C for 10 min to remove cell debris. The clarified supernatant was collected and stored at -80°C. A volume of 200.0 µL sample of the supernatant was assayed for HAV RNA (see Sec. 2.9 and 2.10). Typical titer was approximately 10^8 genome equivalents per mL (GE/mL).

2.7.1 Infection Studies

A five microliter (1E+08 GE/mL) inoculum was applied to 5E+05 Huh7 cells per well of Corning® Costar® 12-wells-plates (CLS3515 Sigma-Aldrich, St. Louis, MO)

(1 GE per cell) and incubated overnight at 37°C. The inoculum was aspirated and the infected cells were washed four times with DMEM. The last wash was collected to determine background viral titer at day zero of time course studies. Viral supernatant was collected from infected cells cultured in four different media was designated as follows:

1. DMEM/ 10% FBS/ penicillin-streptomycin (the virus referred to as "**FBS HAV**")
2. DMEM/ 2% volunteer human sera lacking anti-HAV IgG/ penicillin-streptomycin
3. DMEM/ 2% commercial HS/ penicillin-streptomycin with IgG present (the virus referred to as "**HS HAV**")
4. DMEM/ 2% commercial HS/ penicillin-streptomycin with depleted IgG (the virus referred to as "**IgG(-) HS HAV**")

Infected cells cultured in media containing HS lacking anti-HAV IgG (both IgG depleted commercial HS and volunteer sera lacking anti-HAV IgG) were maintained as described in Sec. 2.6.1.1. Uninfected cells were included as control. In time course experiments, supernatant was collected every three days. The supernatant was clarified to remove cell debris (21,100 x g, 10 min, 4°C) and stored at -80°C until needed. A volume of 200.0 µL sample of the supernatant was aliquoted for HAV RNA quantification assay.

2.7.1.1 HS without anti-HAV IgG

IgG depleted HS (IgG(-) HS) (see Sec. 2.4 and 2.5) and volunteer sera collected from an individual negative for anti-HAV IgG were used to culture HAV-infected cells.

Prior to infection, cells were cultured in HS media that had anti-HAV IgG. These cells cultured in 12-wells-plates grew to confluency and became well-differentiated over three weeks. They were then washed with DMEM three times and maintained in IgG(-) HS media for three days before infection. HAV infection studies were performed as described previously (see Sec. 2.7.1).

2.7.2 Infection Studies in the Dual-Chamber System

Huh7 cells cultured in the Transwell® dual-chamber system with pre-column HS media were grown to confluency and full differentiation (see Sec. 2.7). The cells were washed with DMEM three times and maintained in IgG(-) HS media for three days prior to HAV infection studies. Inocula containing HAV were applied to Huh7 cells basolaterally at one GE virus per cell and incubated overnight at 37°C. Inocula were aspirated from both compartments and washed four times with DMEM. The last washes from both upper and lower compartments were collected to determine background viral titer. IgG(-) HS media was added to each well and HAV-infected cells were incubated until the next collection time point was reached (every three days). Supernatants of uninfected cells collected from both upper and lower compartments were used as a negative control. Supernatants were clarified (21,100 x g, 10 min, 4°C) and stored at -80°C until needed. A volume of 200.0 µL sample was assayed for HAV RNA (see Sec. 2.9 and 2.10). A log scale graph of HAV RNA titer (GE/mL) versus time point (day post infection, dpi) was plotted.

2.8 Dextran Diffusion Studies

As a measure of differentiation prior to HAV infection studies, the time needed for Huh7 cells grown in HS media to form tight junctions was determined by dextran diffusion (53,86).

Huh7 cells in HS media that were cultured in the Transwell® dual-chamber

system (see Sec. 2.3). Cells were washed once and placed in MEM media: 1.5 mL in the upper compartment and 2.5 mL in the lower compartment. Huh7 cells in FBS media grown to confluency in the dual-chamber system were used as the control in the dextran diffusion studies. The confluency of Huh7 cells in FBS media that were grown in the dual-chamber systems was based on their growth rate. Their proliferation rate was determined based on their progression to confluency in Corning™ T75 flasks. Huh7 cells in FBS media took about three days to grown to confluency (~1E+07 cells) in Corning™ T75 flasks after splitting 1:4. Cell counting was performed to determine the plating density for Huh7 cells in FBS media to be grown on the dual-chamber system for the dextran diffusion studies. A dual-chamber system without cells (blank) was included to determine the maximum dextran diffusion level.

To perform dextran diffusion studies, three µL of 0.5 mg/mL Oregon Green® 488 labelled 70.0 kDa dextran conjugate (D1826 Molecular Probes™ Invitrogen Detection Technologies) was added to the upper compartment (1.5 mL MEM) to a concentration of 1.0 µg/mL. Samples with a volume of 100.0 µL were taken from the lower compartment to determine dextran diffusion rates every 30 min for two hrs. The samples were placed in the wells of Corning™ 96-well white polystyrene microplate (#3912 Corning Inc., New York, United States). The plate was read after two hours after sample collection was completed. The plate was covered by a piece of aluminum foil to protect Oregon Green fluorescence from being exposed to the light during this period.

Oregon Green fluorescence was measured using an EnSpire Multimode Plate Reader (#2300 Perkin Elmer). To measure background, the fluorescent of 100.0 µL of MEM was measured on each plate. The true fluorescence value of the samples (true fluorescence reading) was:

$$True\ fluorescence\ reading = Sample\ fluorescence\ reading - MEM\ fluorescene\ reading$$

The value of a control reading was included by adding 100.0 µL of MEM with three µL of 0.5 mg/mL of Oregon Green fluorescence directly to the plate. The maximum diffusion rate of Oregon Green from upper chamber to lower chamber of Transwell® dual-chamber system was estimated by measuring the fluorescence of 100.0 µL MEM containing 1.5 µg of Oregon Green dextran.

The value of maximum diffusion value of Oregon Green fluorescence from upper to lower chamber was used to compare the diffusion level of Oregon green fluorescence of the samples by calculating the percentage (%) of dextran diffusion.

$$\%\ of\ maximum\ dextran\ diffusion = \frac{true\ fluorescence\ reading}{Maxiumum\ value} \times 100\%$$

All dextran diffusion experiments were done in duplicate and averaged for each time point (t (min)= 0, 30, 60, 90, 120). Huh7 cells cultured in FBS media do not form tight junctions (120) and Oregon Green fluorescence can diffuse easily from the upper to the lower compartments of the dual-chamber system. For this reason, the diffusion values of Huh7 cells in FBS media were used as a baseline of 100%. The fluorescence readings of Huh7 cells in HS media or the control (dual-chamber system without cells) were normalized to this baseline for analysis.

The true fluorescence readings of both HS cultured cells and the empty wells of the systems were normalized to the value of FBS cultured cells for each time point.

$$Samples = HS\ cultured\ cells\ \boldsymbol{OR}\ dual-chamber\ system\ without\ cells$$

$$Normalized\ value = \frac{True\ fluorescence\ value\ of\ samples}{True\ fluorescence\ value\ of\ FBS\ cultured\ cells} \times 100\%$$

For the analysis of dextran diffusion studies, normalized fluorescence values of all time point were averaged to obtain a value of relative dextran diffusion. A bar graph of relative dextran diffusion (normalized to FBS cultured cells) over time courses was plotted in Fig. 3.2.1.

The same protocol was used with infected cells grown in the Transwell® dual-chamber system at the final sample collection time point (dpi of 15). This was to test whether HAV infection disrupted the tight junctions formed by HS cultured cells grown in the dual-chamber systems. Because the samples were collected from the infected cells, we added one µL Micro-Chem Plus (detergent) (#0255 National Chemical Laboratories, Inc, Philadelphia, USA) to the samples to inactivate the viruses before measurement. The blank (MEM) and control (MEM + Oregon Green dextran) samples were treated similarly to control for any fluorescence due to Micro-Chem Plus. The same analysis method described above was applied, except that the readings of the relative dextran diffusion were normalized to the empty wells of the dual-chamber system (blank insert).

2.9 Viral RNA Isolation

Viral RNA was extracted from the culture supernatants and the gradient fractions using High Pure Viral Nucleic Acid Kit (#11 858 874 001 Roche Diagnostics, Indianapolis, IN), according to the manufacturer's instructions. All buffers solutions and reagents used for viral RNA isolation were supplied in the kit. This extraction kit is of proven extraction efficiency (104). Nuclease are rapidly inactivated by guanidine hydrochloride and Proteinase K (52,93,133,134) and nucleic acids purified by selective binding to silica. Isolated RNA was eluted in 50.0 µL of elution buffer (water, PCR grade) (8,000 x g, 1 min). Eluted viral RNA was either processed directly for first strand complimentary DNA (cDNA) preparation or stored at -80°C until processed. In each

assay, HAV (cell culture adapted HM175/p16) supernatant that was collected from Huh7 cells grown in FBS media with a known titer served as a positive control. Pooled sera from uninfected individuals extracted using the same procedure served as a negative control.

2.10 HAV RNA Absolute Quantification by Real-Time Quantification-PCR (RT-qPCR)

Extracted HAV RNA was used in a two-step real-time qPCR (RT-qPCR): RNA was first converted to cDNA, followed by subsequent RT-qPCR reaction (18,56). The cDNA synthesis was performed using random primers (3.0 µg/µL in 3.0 mM Tris-HCl, pH 7.0, 0.2 mM EDTA, #48190011 Invitrogen) and SuperScript^{TM} III Reverse Transcriptase (SSIII) [200.0 U/µL] (10,000 U, #18080044 Invitrogen), according to the manufacturer's instructions.

A volume of 11.0 µL of extracted viral RNA used for cDNA reaction incubated with 1.0 µL random primers (300.0 ng), 1.0 µL of 10 mM deoxynucleotide (dNTP) mix (65°C, 5 min), followed by 7.0 µL mixture reagents containing: 4.0 µL 5X first-strand buffer (250.0 mM Tris-HCl, pH 8.3, 375.0 mM KCl, 15 mM $MgCl_2$, #18080044 Invitrogen), 1.0 µL dithiothreitol (DDT) [0.1 M] (#18080044 Invitrogen), 1.0 µL SSIII and 1.0 µL RNaseOut^{TM} recombinant ribonuclease inhibitor (in 20.0 mM Tris-HCl, pH 8.0, 50.0 mM KCl, 0.5 mM EDTA, 8.0 mM DTT, 50% (v/v) glycerol, #10777019 Invitrogen). The cDNA synthesis reaction was performed in a PTC-100 Thermal Cycler (MJ Research Inc., Massachusetts, United States). The reaction conditions were: 25°C for 5 min to extend the primers, 50°C for 1 h to synthesis cDNA (this is the optimal temperature for SSIII) and 70°C for 15 min to inactivate the reaction of SSIII.

The absolute quantification method was used to quantify viral RNA titer. RT-qPCR was performed on each sample in duplicate using an Applied Biosystems Real

Time PCR System, either 7900HT or QuantStudio™ 3, with TaqMan chemistry that exploits the 5' to 3' exonuclease activity of thermostable AmpliTaq Gold® DNA polymerase (3). When the probe is intact, both reporter (higher energy, shorter wavelength) and quencher (lower energy, longer wavelength) dyes are in close proximity. This proximity suppresses the fluorescent emission of the reporter dye by Förster-type energy transfer (or fluorescence resonance energy transfer, FRET). If the target of interest is present in the RT-qPCR reaction, the probe binds to the target between the forward and reverse primer sites (Fig 2.1A). During the extension phase of the PCR reaction the 5'→ 3' exonuclease activity of the polymerase degrades the probe as it advances separating the reporter dye from the quencher (Fig. 2.1B) and increasing fluorescence of the reporter dye (Fig 2.1C). Meanwhile, the polymerization of the strands continues until the complete PCR products are made (blue dotted line, Fig. 2.1D). The quencher blocks the 3' end of the probe to prevent its extension by DNA polymerase during the reaction. This process occurs in every cycle (Fig 2.1).

HAV primer/probe sequences bind between nucleotides 392 and 480 within the 5' untranslated RNA (5'-NCR) segment of the genome. The following primers were used: forward primer: 5'-GGT AGG CTA CGG GTG AAA C-3' and reverse primer: 5'-AAC AAC TCA CCA ATA TCC GC-3' (32,61,69). HAV probe used in the reaction was CTT AGG CTA ATA CTT CTA TGA AGA GAT GC with 5'-FAM 6-carboxyfluorescein (FAM™ dye) as the reporter dye and 3'-tetramethylrhodamine (TAMRA™ dye) as the quencher dye (32,61,69).

Each RT-qPCR reaction of 25.0 µL consisted of 12.5 µL 2X TaqMan Universal PCR Master Mix (#4324018 Applied Biosystem®, Thermo Fisher Scientific, Massachusetts, United States), 2.25 µL forward primer [10.0 µM], 2.25 µL reverse primer [10.0 µM], 2.5 µL probe [2.5 µM], 3.5 µL distilled water and 2.5 µL of cDNA

samples. The standard reaction conditions for RT-qPCR were: 50°C for two min (to optimize UNG enzyme activity), 95°C for 10 min (to activate DNA polymerase in TaqMan Universal PCR Master Mix), followed by 40 cycles of: 95°C for 15 s (to denature) and 60°C for one min (to anneal/extend).

Plasmid DNA of HM175/18f, a cloned HAV genome, (prepared by Daniel Pang, Tyrrell's laboratory) was used to generate a standard curve of known HAV concentrations (from 10^1 to 10^6 GE) (90). The absolute quantification of viral RNA copies from supernatant and gradient fractions was generated by interpolating their Ct values on the standard curve. The threshold was manually set at 0.2 in the middle of the exponential phase of the amplification curve which resulted in the highest precision of replicates. HAV RNA copies were calculated based on the dilutions used and presented as GE/mL. The positive control (HAV supernatant collected from Huh7 cells in FBS media) and the negative control (volunteer sera that was negative for HAV) were assayed by the same viral RNA purification, cDNA synthesis and qPCR protocols for normalization of HAV extraction efficiencies. A no-template control (NTC) was included to ensure that the expression level detected was not due to contamination of qPCR reagents with viral RNA.

2.11 Isopycnic Gradient Ultracentrifugation

To identify viral populations secreted by the infected Huh7 cells cultured in different media conditions, the infected supernatants prepared as discussed previously (see Sec. 2.6) were separated by density using isopycnic gradient ultracentrifugation (32). If the starting titer was lower than 1E+06 GE/mL, the virus was concentrated using a Amicon® Centrifugal Filter Units (30 kDa, EMD Millipore, Darmstadt, Germany) before density gradient centrifugal.

To prepare the iodixanol step gradient, 60% w/v iodixanol in water (Opti-

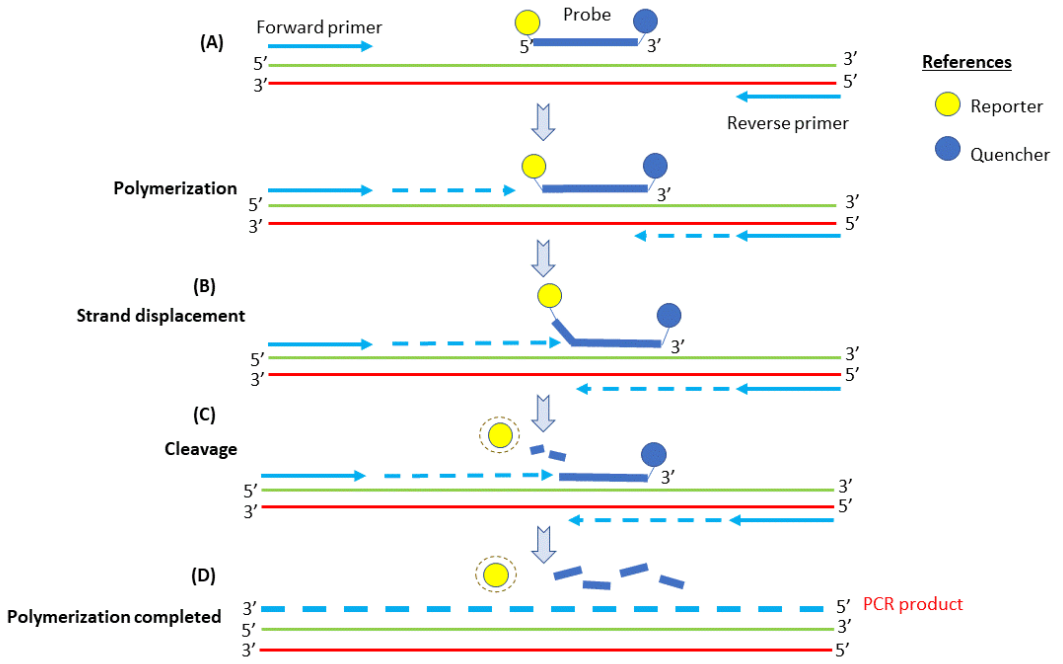

Figure 2.1: TaqMan chemistry as used in real-time quantification PCR (RT-qPCR) of HAV RNA (adapted from TaqMan Universal PCR Master Mix protocol). TaqMan chemistry exploits the 5' to 3' exonuclease activity of AmpliTaq Gold® DNA polymerase. In the HAV RNA quantification assay, the probe uses FAM as the 5'-reporter dye and TAMRA as the 3'-quencher dye. (A) When the probe is intact, reporter and quencher dyes are in proximity which suppresses reporter fluorescence by Förster-type energy transfer (FRET). In the presence of the target of interest in the RT-qPCR reaction, the probe anneals between the forward and reverse primer sites. (B and C) In the polymerization step, the probe is degraded and displaced from the target of interest by DNA polymerase. This relieves the quenching effect to allow detection of fluorescence of the reporter dye. (D) The polymerization of the strands continues until the complete PCR product is made (blue dotted line).

Prep™ #D1556 Sigma-Aldrich, St. Louis, MO) was diluted with DMEM to prepare 40%, 30%, 20% and 8% iodixanol solutions. All reagents were kept on ice. The step gradient was prepared by adding 3.0 mL 40% to a thin wall polypropylene tube (#331372 Beckman Coulter Inc., Brea, CA), followed by 3.0 mL 30%, 3.0 mL 20% and 2.0 mL 8% of iodixanol. A one mL sample was loaded on top of the 8-40% step gradient. The samples were centrifuged in a Beckman Coulter SW40T$_i$ rotor in a Beckman Optima LE-80K ultracentrifuge (141,000 x *g*, 42 hrs, 4°C). For each tube, 20 ± 1 fractions (each ~600.0 µL) were collected from the bottom of the tube. This was done by poking a hole there using a 21 Gauge needle, initially with the top of the tube sealed with two layers of parafilm. Each fraction with a volume of 50.0 µL was processed for density determination by refractometer (HI 96801 Hanna Instruments, Padova, Italy) and for HAV RNA quantification.

OptiPrep™ iodixanol was diluted to generate a standard curve of density from refractive index. First, 60% Opti-Prep™ iodixanol (reported density 1.320 g/mL) was diluted in DMEM (reported density 1.006 g/mL) to prepare 50%, 40%, 30%, 20%, 15%, 10%, 5%, and 2.5% iodixanol standard. The density of each OptiPrep™ iodixanol standard was calculated using the equation:

$$Density = \frac{Volume\ OptiPrep\ x\ 1.320\frac{g}{mL} + Volume\ DMEM\ x\ 1.006\frac{g}{mL}}{Volume\ of\ OptiPrep + Volume\ of\ MEM}$$

The refractive index of each standard was determined by refractometer (HI 96801 Hanna Instruments, Padova, Italy). A standard curve of density (g/mL) versus refractive index was generated every batch of iodixanol. The density of each gradient fraction was generated by interpolating the refraction value on the standard curve. The fractions with the density ranges defining the two HAV populations (either 1.06-1.11

g/cm^3 or 1.21-1.28 g/cm^3) were pooled. The iodixanol was removed (see section 2.12) and the samples were stored at -80°C until needed.

Viral titer of the gradient fractions was calculated in genome equivalent per mL (GE/mL). The viral titer value of all fractions was added to obtain total GE/mL. To normalize the outcome of each experiment, each with a different input viral titer, the titer of each gradient fraction was expressed as a percentage of total HAV RNA (%). A graph of % of total HAV RNA (GE/mL) versus density (g/cm^3) was plotted. For each sample, the percentage of the total virus with the density of either quasi-eHAV or non-enveloped HAV (32) could then be determined.

2.12 Iodixanol Removal from Gradient-Purified Viral Samples

The iodixanol of the gradient-purified viral samples was removed by size exclusion using Amicon® Ultra-15 Centifugal Filter Units (100kDa, #UFC910024 EMD Millipore, Darmstadt, Germany) (53,122). Fractions of the density gradient representing the two HAV populations were pooled (usually three to four fractions per population). The pooled samples were loaded into Amicon® filter tubes pre-washed with sterile MilliQ water in a Beckman Coulter Allegra® X-15R Centrifuge (#41103904) (3,000 x g, 15°C, 5 min). The samples were diluted to 15.0 mL with PBS and loaded into Amicon® filter tubes. The samples were centrifuged (3,000 x g, 15 min, 15°C). The washing step with PBS in a total volume of 15.0 mL was repeated and the samples were collected from the filter in a final volume about 100.0 µL and stored at -80°C until needed.

2.13 Addition of IgG to Low Density HAV Virions

A volume of one mL human sera has approximately 10.0 mg IgG (137). Huh7 cells cultured in 2% HS media are thus exposed to an IgG concentration of only 0.2 mg/mL.

We treated the gradient-purified lower density HAV population with 2.0 mg/mL IgG, 10-fold more than the IgG concentration in the media supplemented with HS. IgG supplement was the eluate collected from the Protein A column used to deplete IgG from HS (see Sec. 2.4). The presence of anti-HAV IgG was confirmed by the Provincial Laboratory for Public Health or by using an ELISA kit that detected the presence of anti-HAV IgG (see Sec. 2.6).

HAV samples were gradient fractions of IgG(-) HS HAV that matched the reported density of quasi-eHAV (32). A volume of two mL HAV were mixed with 0.5 mL anti-HAV IgG (10.0 mg/mL) to a final concentration of 2.0 mg while 2.5 mL of untreated HAV was used as a control. The mixtures were incubated at 37°C for 1.5 hrs and loaded onto isopycnic gradients for ultracentrifugation (141,000 x g, 42 hrs, 4°C). After 42 hrs, twenty fractions were collected for each sample. The refractive index of each was read by refractometer to determine its density (see Sec. 2.11) and 200.0 µL of each fraction was processed for HAV RNA quantification (see Sec. 2.9 and 2.10).

2.14 Immunoprecipitation

To prevent the non-specific binding of HAV to the tubes, which had been shown in pilot experiments, tubes were blocked by adding 1%BSA in PBS and rotating the tubes end-to-end overnight at 4°C. BSA solution was aspirated prior to use in the following experiments.

Gradient-purified HAV samples were divided into two tubes: one with Protein G Sepharose® 4 Fast Flow (10.0 µL settled resin) (#17-0618-01 GE Healthcare Life Science, Little Chalfont, United Kingdom) and one without Protein G Sepharose. This bead has the binding capacity of ~18.0 mg IgG/mL.

Prior to use, Protein G sepharose was washed with 1X Tris-buffered saline (TBS). The samples (100.0 µL) were incubated at 4°C overnight. After incubation, the

samples were centrifuged (21,100 x g, 10 s) and the supernatants were saved. The pelleted beads were washed with 1X TBS/ 0.1% Tween-20 (TBS-T) by rotating the tubes end to end for 30 min at 4°C and centrifuged (21,100 x g, 10 s). The washing step was repeated twice. Both supernatant and bead were assayed for HAV RNA by RT-qPCR (see Sec. 2.9 and 2.10). The sum of total virus for each sample set was determined by adding the viral titer of both supernatant and pellet. A bar graph of the ratio of the virus in pellet to total virus is shown in Figure 3.1.6.

2.15 HAV Infection Assay ($TCID_{50}$ Assay)

To determine the specific infectivity of HAV collected from infected Huh7 cells cultured in different media (FBS versus IgG(+) HS versus IgG(-) HS) as well as the two HAV populations defined by their density, $TCID_{50}$ assays were performed (adapted from Lindenbach et al., 2005) (74).

Corning™ Coster™ flat bottom 96-wells-plates (#3596 Fisher Scientific, Waltham, Massachusetts) were coated with poly-L-lysine (PLL) (P8920 Sigma-Aldrich, St. Louis, MO). The PLL stock solution (0.1% (w/v) in water) was diluted 1:10 in deionized water. A volume of 50.0 µL PLL solution was added per well, incubated for 5 min and aspirated. The plates were dried inside a biological safety cabinet. To sterilize each well, 100.0 µL of 70% ethanol was added and aspirated. The plates were placed under ultraviolet (UV) light inside the biological safety cabinets until dry. The plates were stored until needed.

Huh7 cells in FBS media (9E+03 cells per well, approximately 20% of confluency) were seeded on a PLL-coated-96-wells-plate and the plate was incubated overnight. To perform TCID50 assay, a series of 10-fold serial dilutions of samples containing HAV were made. The media was removed from the wells and 100.0 µL of diluted series were applied to the cells from the most diluted virus to the least diluted

virus. The cells were incubated with inocula overnight (5% CO_2, 37°C). The next day, the inocula were removed from all wells and replaced with 200.0 µL FBS media and incubated at 37°C for 72 hrs post-infection. Uninfected cells were used as a negative control.

After 72 hrs post-infection, the cells were washed twice with cold 1X PBS, followed by a cold acetone: methanol (1:1) solution (100.0 µL per well) and fixed at -20°C for at least 30 min. The fixed cells were then washed twice with PBS, followed by a single wash with PBS-T. To block non-specific antibody binding, the cells were treated with PBS-T/ 1%BSA/ 0.2% skim milk (50.0 µL per well) for at least 30 min at room temperature. This blocking step was followed by treatment with 50.0 µL 3.0% hydrogen peroxide (H_2O_2) (H325-500 Thermo Fisher Scientific, Massachusetts, United States) in PBS for 5 min at room temperature to block endogenous peroxidase activity. The cells were washed twice with PBS followed by a single wash with PBS-T. After the washing steps, the cells were incubated with 50.0 µL/well of monoclonal antibody (mAb) K24F2 against HAV capsid (Commonwealth Serum Laboratories, Victoria, Australia) diluted 1:500 in PBS-T at room temperature for 1.5 to 2 hrs. The cells were washed as described above and incubated with 50.0 µL/well horseradish peroxidase (HRP)-conjugated goat-anti-mouse antibody (#CLCC30007 Cerdalane, Ontario) diluted 1:1000 in PBS-T) at room temperature for 2 hrs. The cells were washed again and incubated with 3,3'-diaminobenzidine tetrahydrochloride (DAB) substrate (50.0 µL per well K3468 DAKO Agilent Pathology Solutions, Santa Clara, CA) for 5 min. The cells were washed twice with PBS and left in 50.0 µL PBS. The wells were observed under a light microscope for the stained cells, indicating the viral infection.

In the presence of peroxidase, DAB yields an insoluble brown product at locations where the peroxidase-conjugated secondary antibody bound viral capsid

recognized by the primary antibody (K24F2). Wells with stained cells were scored as positive. For analysis, the viral stocks used for the assay was quantified (GE/mL). The TCID50/mL value was determined using the Reed and Muench Calculator (68). The specific infectivity of the tested samples was calculated as following:

$$Specific\ infectivity = \frac{Viral\ stock\ \left(\frac{GE}{mL}\right)}{\frac{TCID50}{mL}}$$

The specific infectivity was defined as the ratio of an infectious particle per total viral genome. A bar graph of the specific infectivity of viral samples collected from infected Huh7 cells in different media (FBS versus IgG(-) HS versus IgG(+) HS media) was constructed.

2.16 Neutralization Assay

For neutralization assays, 2.0E+04 cells (~20% confluency) Huh7 cells cultured in FBS media were seeded on the PLL-coated-48-wells-plates (surface area of 1.0 cm^2) and incubated overnight.

Two HAV populations, quasi-eHAV and non-enveloped HAV, were studied in the neutralization experiments (Fig. 2.2). The iodixanol was removed from gradient-purified viruses prior to these studies (See Sec. 2.12). Both quasi-eHAV and non-enveloped HAV were prepared to have a similar number of infectious particles (based on the results of $TCID_{50}$ assay). A volume of 50.0 µL virus samples was mixed with 500.0 µL of human sera, confirmed to be either positive or negative for anti-HAV, and incubated at 37°C for 1.5 hrs. A virus only was similarly treated as the positive control to show that the incubation conditions did not affect viral infectivity. The treated inocula were applied to the Huh7 cells in FBS media. Uninfected cells were included as a negative control. Each treatment was done in duplicate. After overnight incubation,

inocula were aspirated and the infected cells were washed once with PBS. The wash was collected to determine unbound viral titer. The cells were placed in one mL FBS media and incubated at 37°C. At five days-post-infection the supernatant was collected and clarified to remove cell debris (21,100 x g, 10 min, 4°C) and stored at -80°C until processed. A volume of 200.0 µL samples of the supernatant collected at day zero and day five post-infection were assayed for HAV RNA (see Sec. 2.9 and 2.10). The cells were washed once with one mL of PBS and lysed with 100.0 µL of QIAzol Lysis Reagent (1.0 mL per 10.0 cm^2). The cell lysates were stored at -80°C until processed for intracellular HAV RNA (see Sec. 2.17).

2.17 Intracellular Viral RNA Extraction

Intracellular viral RNA was extracted by following the manufacture's protocol, QIAzol Lysis Reagent (105,115). QIAzol Lysis Reagent is a solution containing phenol and thiocyanate compounds. After lysis, the samples were mixed with chloroform and centrifuge for phase separation. The upper RNA in the aqueous phase was precipitated with isopropanol at -20°C, washed with 75% ethanol, air dried and dissolved in 10.0 µL RNase-free water.

2.18 Intracellular HAV RNA Relative Quantification

Total RNA from HAV-infected Huh7 cells was subjected to cDNA synthesis using random primers and Moloney Murine Leukaemia Virus Reverse Transcriptase (M-MLV RT) (#28025013 Invitrogen, 200.0 U/µL, 50.0 mM Tris-HCL, pH 8.3, 40.0 mM KCl, 6.0 mM $MgCl_2$, 1.0 mM DTT, 0.5 mM [^{3}H]dTTP, 0.1 mM poly(A), 0.1 mM oligo$(dT)_{25}$, 0.1 mg/mL BSA), according to the manufacturer's instructions. M-MLV has low RNase H activity and is capable of synthesizing longer cDNA (<7 kb) and achieving a better cDNA yield (46,67).

Briefly, a sample of two µg RNA extracted from infected cells in 9.85 µL

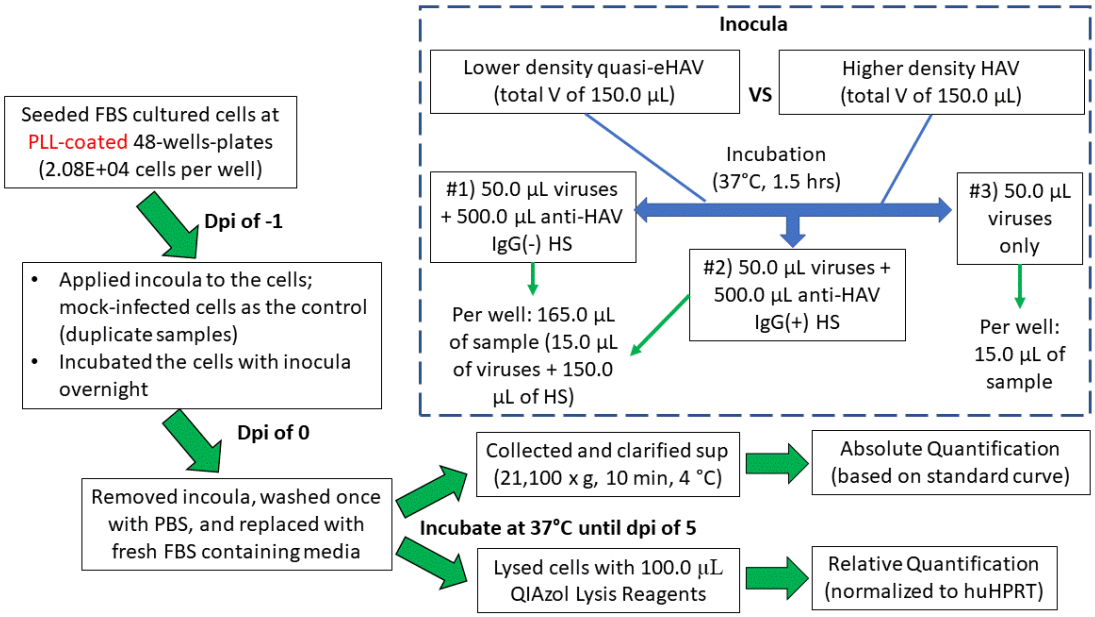

Figure 2.2: The experiment outline of neutralization studies involving quasi-eHAV and non-enveloped HAV.

This is an experimental outline to show the neutralization studies involving quasi-eHAV and non-enveloped HAV. Huh7 cells in FBS media were seeded on PLL-coated-48-wells-plates (2.0E+04 cells per well), and incubated overnight (37°C, 5% CO_2). The next day sub-confluent cells were used for the neutralization studies. The viral samples, containing either quasi-eHVA or non-enveloped HAV, were pre-treated with HS that was either positive or negative for IgG specific against HAV (volume ratio of 1:10, 37°C, 1.5 hrs), as shown in the dashed blue box. Untreated samples (containing viruses only) were included as the control to show that incubation condition did not affect viral infectivity. Then, the inocula were applied to the cells (dashed blue box, green arrow). Uninfected cells were included as a control. The cells were incubated with the inocula overnight (dpi of -1). The next day, the cells were washed once with PBS, replaced with FBS media (dpi 0), and incubated at 37°C. At five days of post-infection the supernatant was collected and clarified (21,100 x g, 10 min, 4°C). The cells were washed once with PBS and lysed with 100.0 µL of QIAzol Lysis Reagent. A volume of 200.0 µL sample of the supernatant collected on dpi 0 and dpi 5 were assayed for HAV RNA using absolute quantification. The cell lysates were assayed for intracellular HAV RNA using relative quantification normalized to a housekeeping gene huHPRT mRNA. dpi= day post-infection.

RNase-free water was then added. For each reaction, we added a master mix reagent containing 4.0 µL 5X first-strand buffer, 0.5 µL of dNTP mix [10.0 mM], 1.5 µL of RNase/DNase free water, 0.2 µL of BSA [10.0 mg/mL], 2.0 µL DDT [0.1 M], 1.0 µL M-MLV RT, 0.8 µL RNaseOut™ recombinant ribonuclease inhibitor and 0.15 µL random primers [3.0 µg/µL]. The cDNA synthesis reaction was performed in a PTC-100 Thermal Cycler in the following setting: 22°C for 5 min to extend primers, 37°C for 60 min to synthesis cDNA (this is the optimal temperature for M-MLV RT), followed by 95°C for 10 min to inactivate the reaction.

The relative quantification was the method used to measure changes in intracellular HAV RNA levels. HAV RNA levels were measured relative to levels of mRNA for human hypoxanthine-guanine phosphoribosyltransferase (huHPRT) a housekeeping gene (endogenous control) to normalize for possible variations in sample preparation. For this reason, we prepared two reaction mixes: one to detect either huHPRT cDNA and one to detect HAV cDNA. To detect huHPRT cDNA, a reaction consisting of 5.0 µL 2X TaqMan master mix, 0.5 µL of 20X primer-probe mix (RefSeq # NM_000194.1, #4326321E Thermo Fisher Scientific, Massachusetts, United States), and 2.0 µL of cDNA sample. huHPRT primer-probe produces a 100 bp amplicon and use VIC® dye as the 5'-fluorescent reporter dye and minor groove binder (MGB™) as the 3'-quencher dye. To detect HAV cDNA, a reaction consisting of 5.0 µL 2X TaqMan master mix, 1.0 µL forward primer [10.0 µM], 1.0 µL reverse primer [10.0 µM], 1.0 µL probe [2.5 µM] and 2.0 µL of cDNA sample (see Sec. 2.10 for HAV primer and probe sequences). The qPCR program was performed on each sample in duplicate using the Applied Biosystems 7900HT or Applied Biosynthesis QuantStudio™ 3 Real Time PCR System TaqMan chemistry (see Sec. 2.10 for the applied theory). The delta-delta Ct (ΔΔCt, threshold cycle) program was used. The standard reaction condition for qRT-

PCR were used (see Sec. 2.10).

The ΔΔCt program of the qPCR instruments provided the averaged ΔCt value between the samples and endogenous control (huHRPT). For analysis, the difference of ΔCt value between the infected samples and the mock-infected samples (control) was calculated to obtain ΔΔCt value:

$$\Delta\Delta Ct = \Delta\Delta Ct \text{ of infected samples} - \Delta\Delta Ct \text{ of control}$$

The calculations were done in logarithm base 2 because the Ct value was decreased by one when the DNA amount was doubled every time. Thus, to get the expression fold change, the following formula was used:

$$Fold\ change = 2^{-\Delta\Delta Ct}$$

A bar graph of fold difference of intracellular HAV RNA versus treatments was plotted.

2.19 GW4064 Treatment

The bile acids synthesis pathway of Huh7.5 cells is upregulated when they are grown in HS media (paper in preparation). To inhibit this pathway, we treated its parental cell line, Huh7 cells cultured in HS media with GW4064 (#G5172 Sigma-Aldrich, St. Louis, MO). GW4064 is a well-known FXR agonist as reported in the literature, increased FXR activity, reduces CYP7A1, the only rate limiting enzyme in the bile acid synthesis (47,88,118). By interfering with bile acid synthesis pathways *in vitro*, we wanted to test the hypothesis that bile acids play an essential role in generating non-enveloped HAV from quasi-eHAV by stripping them of their membrane component.

We dissolved the drug (5.0 mg) in one mL of 100% DMSO to a final concentration of 5.0 mg/mL (solubility 10.0 mg/mL). In these studies, the cells were treated with 1.0 μM GW4064 (EC_{50}= 15 nM).

Huh7 cells in IgG(-) HS media in the dual-chamber system (see Sec. 2.3) were

infected with cell culture adapted strain, p16 HAV (2.0 GE per cell) and incubated overnight. The next day, inocula were aspirated from both compartments, and the infected cells were washed four times with DMEM. IgG(-) HS media was added to each well (1.0 mL to the upper compartment and 2.0 mL to the lower compartment) and every three days. At day six post-infection, infected Huh7 cells were treated as listed below:

1) 1.0 μM GW4064 in IgG(-) HS media
2) 0.01% DMSO in IgG(-) HS media (vehicle control)

Duplicate were done for each experiment. HAV-infected Huh7 cells were treated with 1.0 μM GW4064 or 0.01% DMSO for 72 hrs and samples were collected from HAV-infected Huh7 cells at day nine post-infection. Samples from both upper and lower compartments were collected and clarified (21,100 x g, 4°C, 10 min). The samples collected from the upper chambers were used for isopycnic gradient ultracentrifugation (see Sec. 2.11). HAV RNA in all the fractions was assayed (see. Sec. 2.9 and Sec. 2.10). The proportions of HAV and quasi-HAV in the samples collected from the infected cells treated with either 1.0 μM GW4064 or 0.01% DMSO vehicle control was determined and compared.

2.20 Statistical Analysis

For statistical analysis, the experiments consisted of a minimum of three independent replicates ($n \geq 3$) to calculate the significance of the results. Statistical significance was calculated using either a Student t-test, paired t-test or by ANOVA (analysis of variance) analysis. *P* values of 0.05 or smaller were considered significant.

CHAPTER THREE: RESULTS

Part 1: HAV infection studies on monolayer-infected cells cultured in different media conditions

3.1.1 HAV infection studies of Huh7 cells cultured in HS media

The objective of this study was to determine whether Huh7 cells cultured in HS media develop a persistent HAV infection. HS cultured Huh7 cells were infected with cell culture adapted HAV strain, HM175/p16 (or p16) at 1.0 GE per cell. The cells were incubated with inocula overnight at 37°C. The following day, the infected cells were washed five times with DMEM. The last wash was collected to determine the background titer of HAV. The supernatant was collected every three days until twelve days post-infection. HAV RNA of the samples was extracted and quantified by RT-qPCR as described in the Methods and Materials (Sec. 2.9 and Sec. 2.10).

The infected Huh7 cells cultured in HS media developed a persistent HAV infection. The red dotted line represents the limit of detection level. HAV titer detected in the samples at day zero (4.0E+03 GE/mL) is the baseline of the infection study (Fig. 3.1.1). Compared to this baseline, there were about 230-fold increase in HAV production three days after infection (9.2E+05 GE/mL) by Huh7 cells cultured in HS media (Fig. 3.1.1). HAV production plateaued at 3.7E+06 GE/mL at day six post-infection (Fig.3.1.1). Since p16 HAV strain does not cause a cytopathic effect (CPE), HAV RNA continued to be produced over 12 days post-infection until the infected cells were sacrificed.

3.1.2 The density profiles of HAV secreted by infected cells cultured under different media conditions (FBS vs HS media)

To identify HAV populations secreted by HAV-infected Huh7 cells cultured in either FBS or HS media, we collected the supernatants from the infected cells cultured in

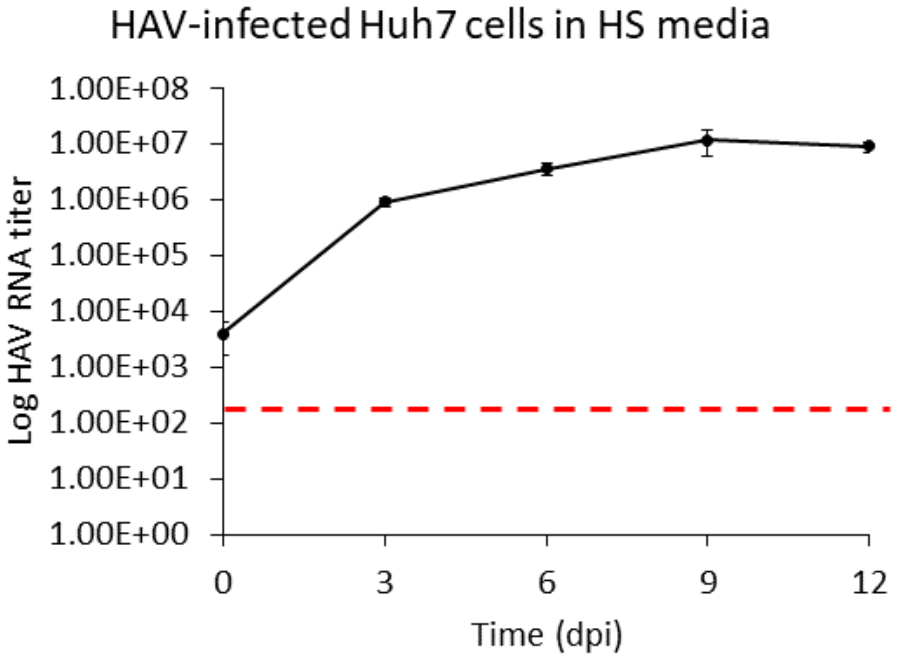

Figure 3.1.1: HAV infection studies of Huh7 cells cultured in HS media
Huh7 cells in HS media were infected with cell culture adapted HAV strain, HM175/p16 (or p16) at 1.0 GE per cell. The cells were incubated with the inocula at 37°C overnight. The following day infected cells were washed five times with DMEM. The last wash was collected to determine the background viral titer. The supernatant was collected every three days and HAV RNA of the samples was extracted and quantified. The red dotted line indicates the limit of detection of the assay. There was a 230-fold increase in HAV titer three days after infection when compared to HAV titer of the baseline. HAV production plateaued after six days post-infection and remained consistent throughout day 6, 9 and 12 post-infection. Infected cells cultured in HS media developed a persistent HAV infection without causing a cytopathic effect (CPE). n=4; HS= human sera; dpi= day of post-infection.

both media conditions and performed isopycnic gradient ultracentrifugation. Twenty fractions were collected for each sample. The refractive index was read to determine the density of the fractions and each fraction was assayed for HAV RNA.

The density profile of HAV produced in Huh7 cells cultured in FBS media showed one major species of virion containing 74% of the total virus in the supernatant (Fig. 3.1.2A). This peak of FBS HAV had a density range of between 1.06 g/cm^3 and 1.11 g/cm^3 with the peak at 1.09 g/cm^3 (referred as to the low density HAV population).

The density profile of the supernatant collected from the infected cells cultured in HS media differs from that of FBS HAV. There were two distinct peaks identified in HS HAV. One of the peaks had a density between 1.06 g/cm^3 and 1.11 g/cm^3 with the peak at 1.08 g/cm^3 (Fig. 3.1.2B), the same as the low density virus shed by cells cultured in FBS media. The second peak had higher density, ranging between 1.17 g/cm^3 and 1.20 g/cm^3 with the peak at 1.18 g/cm^3 (referred as to the high density HAV population) (Fig. 3.1.2B). There were 66% of the total virus in the low density HAV population and 21% in the high density HAV population (Fig. 3.1.2B). The high density HS HAV seen in this experiment was less dense than that reported by Feng et al. (2013) in the feces of HAV-infected humans and chimpanzees, between 1.22 g/cm^3 and 1.28 g/cm^3 (32).

These results showed that different media supplements used for cell culture, FBS versus HS, possibly resulted in different density profiles of HAV secreted by the infected Huh7 cells. However, the high density HAV population of HS HAV did not fall within any previously reported viral density range.

3.1.3 IgG antibodies specific against HAV [anti-HAV IgG(+)] in HS media supplement

IgG is the most abundant antibody in sera (121), including HS media

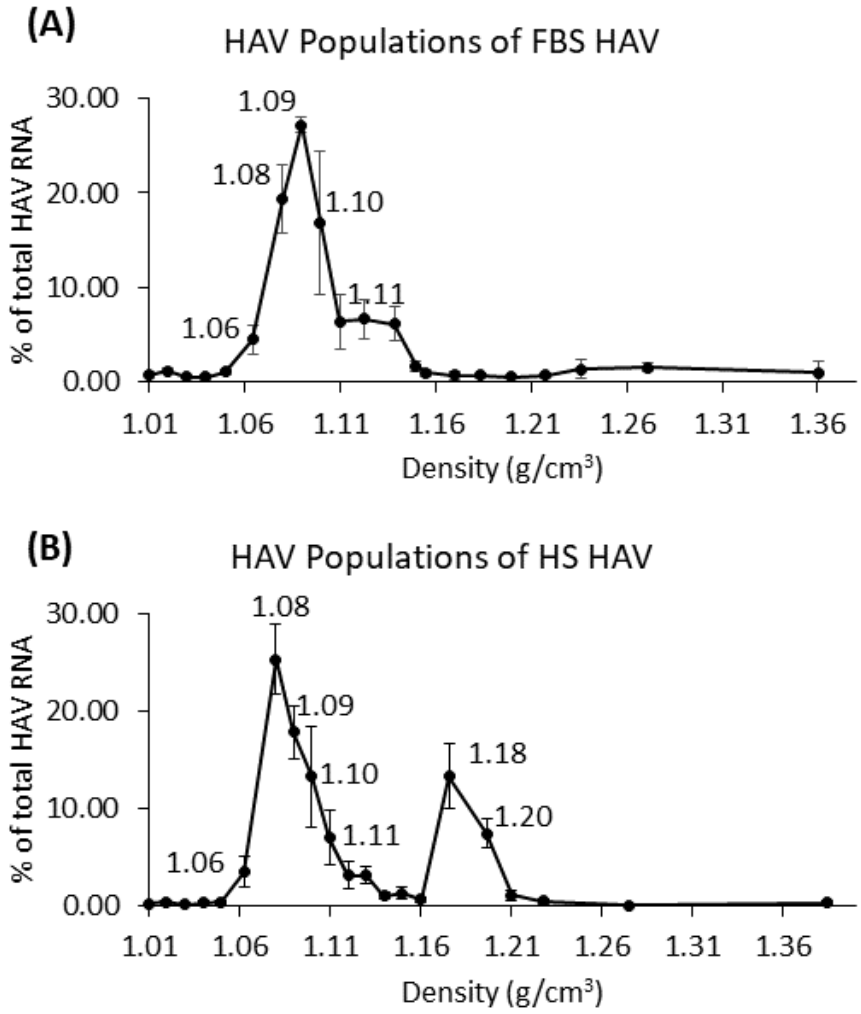

Figure 3.1.2: The density profiles of HAV secreted by HAV-infected Huh7 cells cultured under different media conditions (FBS versus HS media).

The supernatant from the infected cells cultured in either (A) fetal bovine serum (FBS) or (B) human serum (HS) media, was collected and clarified. The clarified samples were loaded onto iodixanol (8%, 20%, 30%, 40%) gradient (141,000 x g, 42 hrs, 4°C). Twenty fractions were collected from the bottom of the tubes. The refractive index of the fractions was read to determine their density. Each fraction was assayed for HAV RNA. (A) There was only one distinct viral RNA peak with the density range between 1.06 g/cm^3 and 1.11 g/cm^3 in supernatant collected from the infected FBS cells. (B) There were two distinct viral RNA peaks with the density ranges of either 1.06-1.11 g/cm^3 or 1.17-1.20 g/cm^3 in the samples collected from the infected HS cells. n=6.

supplements. The HS used to supplement the media was not tested for the specific antibody for HAV (anti-HAV IgG) by the provider. Thus, we thought that anti-HAV IgG might be present in HS, complexed with virions, was responsible for the generation of the second high density viral population produced by HAV-infected Huh7 cells grown in HS media. To test this hypothesis, HS used for cell culture media was tested for the presence of anti-HAV IgG. FBS samples used for media supplement in the standard cell culture protocol was included as the negative control since HAV is a human pathogen and no HAV infection has been reported in cattle.

Anti-HAV IgG was detected in HS sample by a qualitative ELISA assay but not in FBS sample. This suggested that HS was pooled from donors, some of whom had an immune response against HAV either through infection with HAV or vaccination against HAV. As reported by Feng et al. (2013), non-enveloped HAV population is neutralized by a monoclonal antibody specific against HAV capsid (mAB K24F2). Thus, the presence of anti-HAV IgG in the serum supplement could reduce the infectivity of this viral population. For this reason, we depleted IgG from HS to remove antibodies specific against HAV in HS. This yielded anti-HAV IgG free HS for use as a media supplement to culture Huh7 cells, especially for HAV infection studies using Huh7 cells grown in HS media.

3.1.4 IgG antibodies specific against HAV in HS media supplement after IgG depletion

To remove IgG antibodies specific against HAV from HS, we depleted IgG from HS by passing it through a Protein A column. Before loading the column, HS was diluted in Opti-MEM® I Reduced-Serum Medium (MEM media) at the ratio of 1:3 to prevent the blockage of the column by undiluted HS. HS flow-through collected from the Protein A column (post-column HS) were tested for the presence of anti-HAV IgG by

a qualitative ELISA assay.

Several samples were tested. FBS sample was confirmed to be negative for anti-HAV antibodies. The pre-column HS samples and the eluted IgG fractions collected from Protein A column were both positive for anti-HAV IgG. The column efficiently removed anti-HAV IgG from the HS rendering them undetectable by the assay. IgG depleted HS (referred as to IgG(-) HS) was used as a media supplement in the cell culture media in HAV infection studies. Viral production and specific infectivity were compared to infected cells grown in standard IgG(+) HS media.

3.1.5 HAV production from infected cells cultured in either IgG depleted HS or standard HS media

Cells cultured in IgG(-) HS media were infected with cell culture adapted HAV strain, HM175/p16 (or p16) at MOI 1.0. The cells were incubated with inocula overnight at 37°C. The next day, the infected cells were washed five times with DMEM with the last wash collected to determine the background titer. The supernatant was collected every three days until 12 days post-infection. Infection of cells in IgG(+) (standard) HS media was included for comparison. HAV RNA from these samples was extracted and quantified by RT-qPCR as described in Methods and Materials (Sec. 2.9 and 2.10).

HAV infection of Huh7 cells in IgG(-) HS media (Fig. 3.1.3, blue line) shared a similar growth curve with infection of Huh7 cells in IgG(+) HS media (Fig. 3.1.3, red line). The infected cells in both HS media conditions developed a persistent HAV infection without causing any CPE (Fig. 3.1.3). The red dotted line indicates the limit of detection level. The HAV titer of the final wash at day zero is the baseline from these infection studies: 1.2E+04 GE/mL HAV collected from IgG(-) HS cultured Huh7 cells, and 3.9E+03 GE/mL HAV collected from IgG(+) HS cultured Huh7. This difference was not significant ($p > 0.05$).

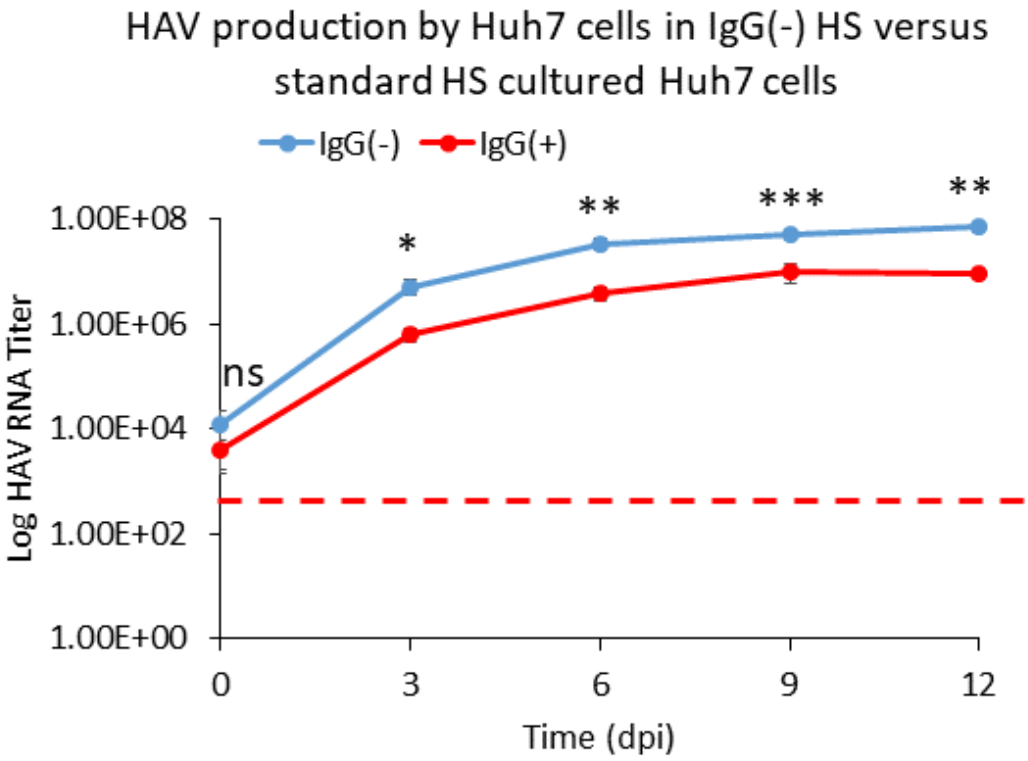

Figure 3.1.3: HAV production by HAV-infected Huh7 cells cultured in either IgG(-) HS or standard HS media.

The cells cultured in either IgG(-) HS or standard HS (IgG(+) HS) media were infected by cell culture adapted HAV strain, HM175/p16 (or p16), at 1.0 GE per cell. The cells were incubated with inocula at 37°C overnight. The next day, the infected cells were washed five times with DMEM. The last wash was collected to determine the background viral titer. Culture supernatants were collected every three days. HAV RNA of each was extracted and quantified. The red dotted line represented the limit of detection level of RT-qPCR assay. The infected cells cultured in both IgG(-) and standard HS media developed a persistent HAV infection without causing CPE. HAV production of the infected cells in both HS media conditions plateaued at day six post-infection. However, HAV-infected Huh7 cells cultured in IgG(-) HS media produced about seven-fold more virus when compared to the HAV-infected Huh7 cells in standard HS media throughout the course of HAV infection studies. These differences were significant. dpi=day post-infection; n=4; ns=not significant; *$p \leq 0.05$; **$p \leq 0.01$; ***$p \leq 0.001$

Compared to the baseline, there was a 430-fold increase in HAV production of the infected Huh7 cells in IgG(-) HS media at day three post-infection (approximately 5.2E+06 GE/mL) (Fig. 3.1.3, blue line), and a 166-fold increase in HAV production by cells grown in IgG(+) HS media (6.5E+05 GE/mL) (Fig. 3.1.3, red line). HAV production of the infected Huh7 cells in both HS media conditions plateaued at day six post-infection: 3.4E+07 GE/mL HAV by Huh7 cells infected in IgG(-) HS media (Fig. 3.1.3, blue line) and 3.8E+06 GE/mL HAV by cells cultured in IgG(-) HS media (Fig. 3.1.3, red line).

HAV production by the infected Huh7 cells in IgG(-) HS media (Fig. 3.1.3, blue line) was always seven-fold higher than the infected Huh7 cells in IgG(+) HS media (Fig. 3.1.3, red line). These differences were statistically significant for each day post-infection ($p \leq 0.05$). This demonstrated that removal of IgG specific against HAV promoted higher HAV virus production. Next, we tested the specific infectivity of HAV collected from infected Huh7 cells cultured in different HS media conditions.

3.1.6 Specific infectivity of HAV produced by infected cells cultured in FBS, IgG non-depleted and IgG depleted HS media

To study the specific infectivity of HAV produced by infected cells cultured in different media conditions (FBS, IgG(+) HS and IgG(-) HS), we performed assays using the Reed-Muench method (68) to determine the 50% endpoint titer of the viral samples (TCID50/mL). The specific infectivity of the samples is reported as the ratio of an infectious particle per total viral genomes of the different HAV samples.

The specific infectivity of HAV samples collected from the infected cells cultured in FBS media was determined to be 92.7, only one in 93 viral particles was infectious (Fig. 3.1.4, green bar). The specific infectivity of HAV samples collected from the infected cells cultured in IgG(-) HS media was very similar, that was 119 (Fig.

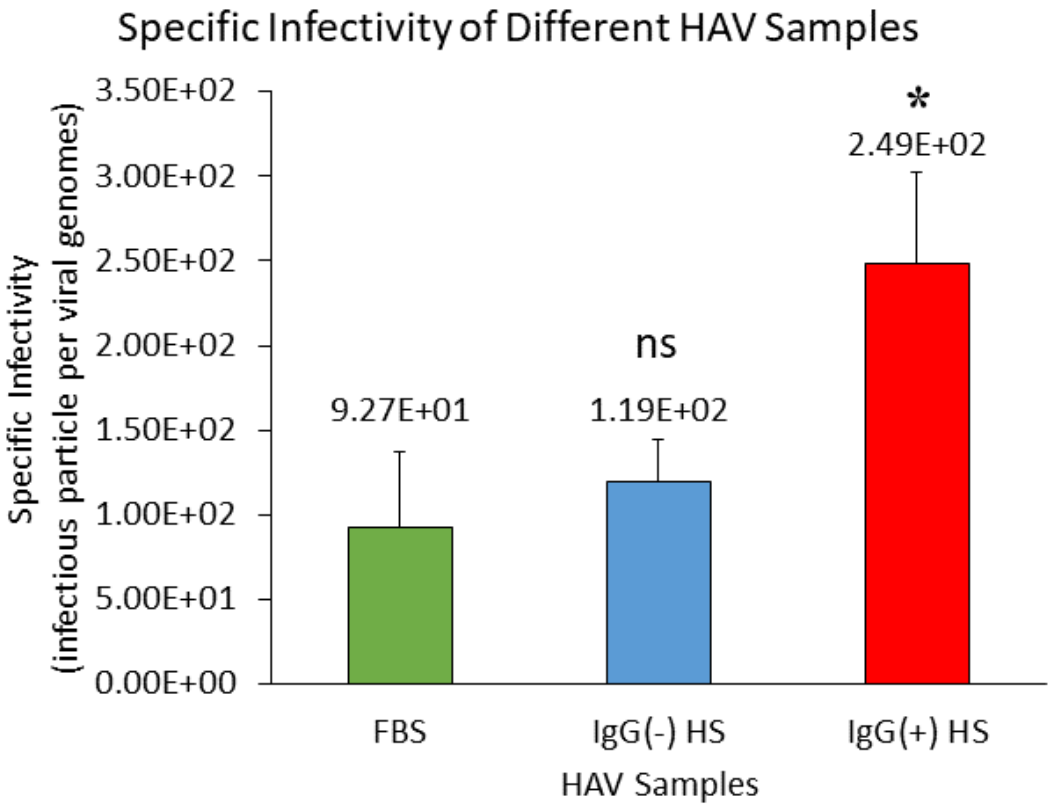

Figure 3.1.4: Specific infectivity of HAV samples produced in different media conditions.

Samples were collected from infected cells cultured in different media conditions, FBS, IgG(-) HS or IgG(+) HS media to study the specific infectivity of the HAV produced. The Reed-Muench method was used to calculate the value of TCID50 per mL (68). The results are reported as the ratio of an infectious particle per total viral genomes. HAV collected from infected cells in FBS media (green bar) had a specific infectivity of 93, that produced in IgG(-) medium was 119 (blue bar), that produced by IgG(+) HS medium was 249 (red bar). FBS HAV and IgG(-) HS HAV shared similar specific infectivity. IgG(+) HS HAV had the significantly lower specific infectivity than FBS HAV and IgG(-) HS HAV. n=4. ns= not significant; *$p \leq 0.05$.

3.1.4, blue bar). HAV samples collected from the infected cells cultured in IgG(+) HS media had a specific infectivity of 249 (Fig. 3.1.4, red bar), a statistically significant difference ($p \leq 0.05$).

In conclusion, the presence of anti-HAV IgG in HS media was shown to reduce viral titer and the specific infectivity of HAV collected from the infected Huh7 cells. Next, we examined the density profile of viruses collected from HAV-infected Huh7 cells cultured in IgG(-) HS media and compared it to the density profile of viruses from infected Huh7 cells cultured in IgG(+) HS media.

3.1.7 The density profile of HAV from infected cells cultured in IgG depleted HS and standard HS media

To examine HAV populations produced by infected IgG(-) HS cells, we collected supernatant from the infected cells and performed isopycnic gradient ultracentrifugation. Twenty fractions were collected, the refractive index of the fractions was used to determine the density of the fractions, and HAV RNA was assayed in all fractions.

Only one peak of HAV, comprising 85% of the population, was identified in the samples collected from cells cultured in IgG depleted HS media (Fig. 3.1.5A). The density range of this HAV population was between 1.06 g/cm^3 to 1.11 g/cm^3, with a density peak at 1.09 g/cm^3. This low density peak has the similar to that identified in the sample collected from the infected cells cultured in FBS media (Fig. 3.1.2A) and matched the density range of quasi-eHAV (32). HAV produced in standard HS medium (Fig. 3.1.5B) was similar to that seen in Fig. 3.1.2 with a low density population centered at 1.08 g/cm^3 (64%) and a high density peak at 1.18 g/cm^3 (23%). The absence of the high density population when cells were grown in IgG depleted HS medium suggested a potential role of IgG in generating the high density viral population.

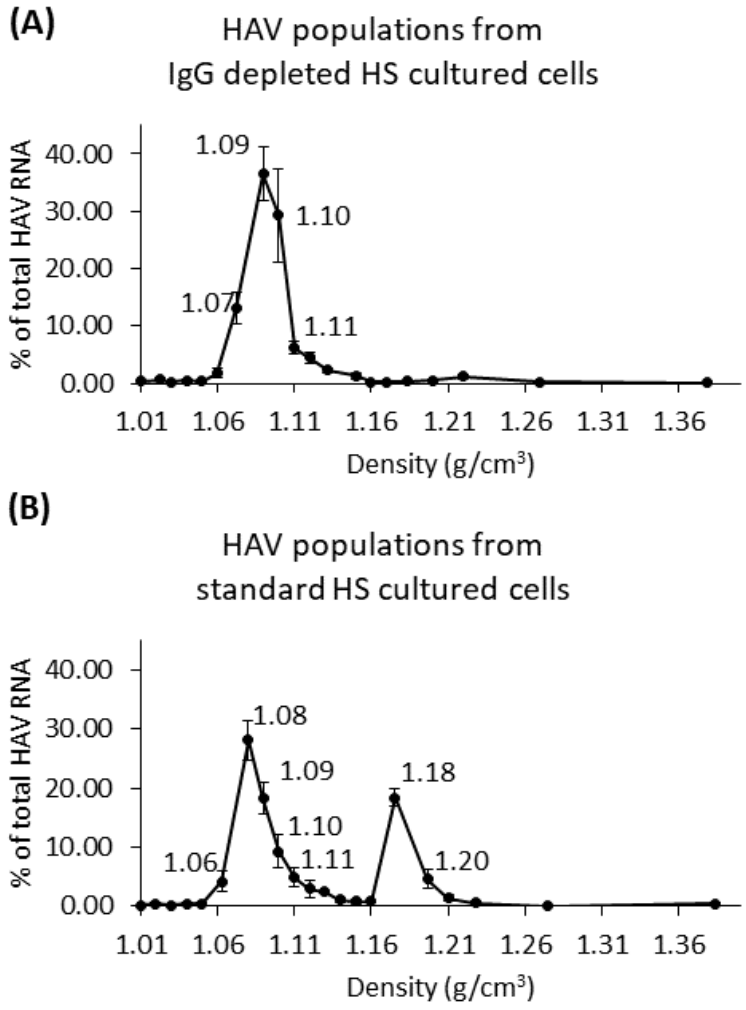

Figure 3.1.5: The density profile of HAV produced by cells cultured in either IgG(-) HS or standard HS media.

Supernatant collected from infected cells cultured in either (A) IgG depleted HS media or (B) standard HS media were loaded onto iodixanol (8%, 20%, 30%, 40%) gradients (141,000 x g, 42 hrs, 4°C). Twenty fractions were collected from the bottom of the tubes. The refractive index of the fractions was read to determine their viral density. Viral RNA of the fractions was extracted and quantified using RT-qPCR. The samples from the infected cells cultured in IgG depleted HS media had a different density profile when compared to the samples collected from the infected cells cultured in standard HS media. (A) There was only one peak (1.06-1.11 g/cm^3) seen in HAV collected from the cells cultured in IgG depleted HS media. n=5 (B) There were two HAV populations, one between 1.06 g/cm^3 and 1.11 g/cm^3 and the other between 1.17 g/cm^3 and 1.20 g/cm^3, identified in HAV produced by cells grown in standard HS medium. n=5.

3.1.8 Studies on the high density HAV produced in the presence of IgG specific against HAV

The presence of IgG specific against HAV in HS media supplement yielded a high density peak of 1.18 g/cm^3. We hypothesized that an immunocomplex formed between IgG and HAV was responsible for this high density HAV population. To characterize this HAV population produced by infected Huh7 cells in IgG containing HS media, several approaches were used. First, gradient fractions were precipitated in the presence of Protein G Sepharose beads to test for the presence of IgG in the high density population. Second, media was supplemented with volunteer sera that was negative for anti-HAV IgG to test the possible role of non-specific IgG in generating this high density HAV population. Third, gradient fractions of the lower density population were incubated with IgG to test whether they could be complexed with IgG to produce this high density HAV population.

3.1.8.1 Immunoprecipitation

To determine whether high density HAV population produced in IgG(+) HS HAV is an immunocomplex of HAV and IgG, we incubated gradient fractions from either low density or high density HS HAV populations with Protein G Sepharose beads, an affinity resin for IgG at 4°C overnight. These two HAV populations that were not exposed to Protein G Sepharose beads were included as controls. HAV RNA was quantified in both supernatant (before washing steps) and pellet (after washing steps). The sum of the viral titers detected in both pellet and supernatant was determined to be the total virus. The amount fraction of total HAV from either low density and high density HAV bound to Protein G Sepharose beads is shown in Fig. 3.1.6.

In the absence of Protein G Sepharose beads, there was virtually no viral

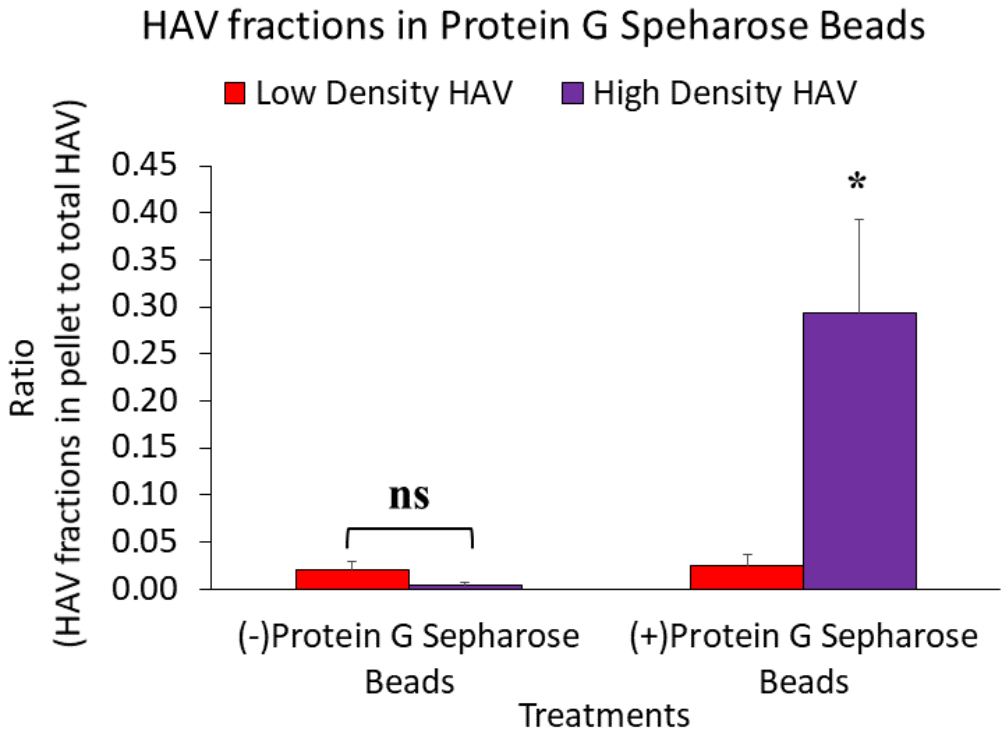

Figure 3.1.6: Immunoprecipitation studies using Protein G Sepharose Beads
The gradient fractions representing low density (red bar) and high density (purple bar) HAV populations were incubated with Protein G Sepharose beads at 4°C overnight. The two HAV populations not exposed to Protein G Sepharose beads were included as a control. The supernatant was collected after pelleting the beads, followed by the washing steps of the beads. Both supernatant and beads were assayed for HAV RNA (GE/mL). The sum of viral titer detected in both pellet and supernatant fractions was determined as total virus. The results are displayed as the ratio of the HAV fraction in the pellet to total virus. (Left) In the absence of Protein G Sepharose beads, there was virtually no HAV RNA detected in the tubes for both HAV populations. (Right) In the presence of Protein G Sepharose beads, no viral RNA of low density population was detected in Protein G Sepharose beads, but 30% of high density HAV did bind to the Protein G Sepharose beads. This difference was significant ($p = 0.0363$). n=4; ns= not significant; *$p \leq 0.05$.

RNA (GE/mL) detected in the tube for either low density HAV (Fig. 3.1.6, right red bar) or high density HS HAV (Fig. 3.1.6, right purple bar). In the presence of Protein G Sepharose beads, there was no viral RNA of low density HAV bound to the Protein G Sepharose beads (Fig. 3.1.6, left red bar), but 30% of high density HS HAV population did bind to the Protein G Sepharose beads (Fig. 3.1.6, left purple bar). This difference was significant ($p \leq 0.05$). This showed at least some of the high density HS HAV from infected Huh7 cells cultured in standard HS media was an immunocomplex of IgG and HAV.

3.1.8.2 Treatment with volunteer sera free of anti-HAV IgG

To address whether HAV complexes with non-specific IgG to generate high density HAV, supernatant was collected from the infected cells cultured in 2% volunteer sera negative for anti-HAV IgG. The clarified samples were analyzed by isopycnic gradient ultracentrifugation, as described in earlier experiments.

A single low density peak of HAV (about 88% of the HAV population) was present in the supernatant of these cultures (Fig. 3.1.7). This density profile is similar that of samples collected from HAV-infected Huh7 cells cultured in FBS media (Fig. 3.1.2A) and IgG(-) HS media (Fig. 3.1.5A). High density HAV detected in the samples collected from HAV-infected Huh7 cells grown in IgG(+) HS media (Fig. 3.1.2B) was not found. The difference between the volunteer sera and IgG(+) HS was the lack of IgG specific against HAV, but both still had the general IgG. This result indicates that non-specific IgG binding does not generate the high density HAV population produced by cells grown in IgG(+) HS medium.

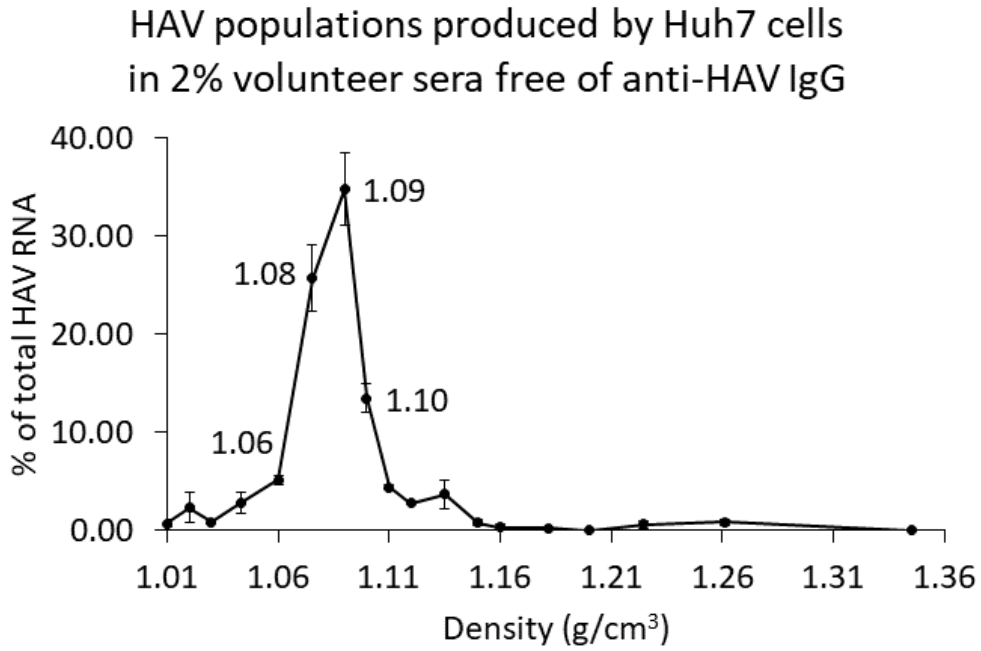

Figure 3.1.7: The density profile of HAV from the infected cells cultured in 2% volunteer sera negative for IgG specific against HAV.

The supernatant from infected cells cultured in media containing 2% volunteer sera negative for anti-HAV IgG was collected and clarified. The supernatant was loaded onto an iodixanol steps gradient (141,000 x g, 42 hrs, 4°C). Twenty fractions were collected from the bottom of the tubes. The refractive index of the fractions was determined to measure fraction density. Viral RNA of all the fractions was extracted and quantified using RT-qPCR. A single peak of HAV with a density range between 1.06 g/cm^3 and 1.11 g/cm^3 is found in supernatant collected from the infected cells cultured in the media supplemented with 2% volunteer sera free of anti-HAV IgG. n=3.

3.1.8.3 Treatment of low density HAV with anti-HAV IgG

To address the question of whether the high density HAV population is derived from low density HAV through formation of an IgG immunocomplex, we divided a sample of low density HAV in two: one was treated with anti-HAV IgG [10.0 mg/mL] and one was an untreated control. Both samples had the final volume of 2.5 mL and were incubated at 37°C for 1.5 hrs. The IgG used was bound to the Protein A column in the process of depleting IgG from HS, then eluted at low pH. It was positive for anti-HAV IgG. The samples were applied to an iodixanol gradient.

As expected, the untreated sample had only one peak of low density (1.06 g/cm^3 and 1.11 g/cm^3) (Fig. 3.1.8 A). The IgG-treated samples had the same density profile as the untreated samples (Fig. 3.1.8 B). This result showed that binding of IgG antibodies specific against HAV could not convert the low density HAV form to the high density form.

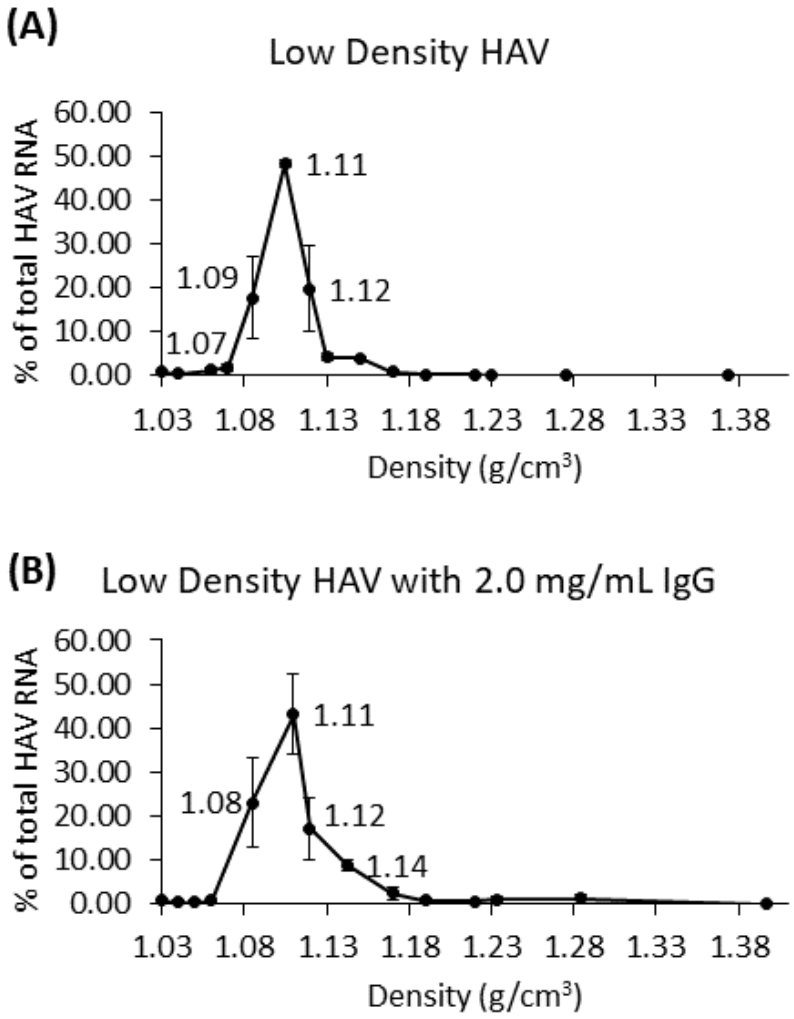

Figure 3.1.8: The treatment of low density HAV with anti-HAV IgG

A low density HAV population produced in IgG(-) HS medium was divided into two portions. One of the samples was mixed with IgG containing anti-HAV antibodies [2.0 mg/mL] while the other was not. After incubation at 37°C for 1.5 hrs, the samples were loaded onto an iodixanol step gradient (141,000 x g, 42 hrs, 4°C). Twenty fractions were collected from the bottom of the tubes. The refractive index of the fractions was used to determine the viral density and HAV RNA were extracted and quantified using RT-qPCR from all fractions. There was a single peak at low HAV in both samples, regardless of the treatment with IgG antibodies specific for HAV. n=2.

CHAPTER THREE: RESULTS

Part 2: The behaviour of two HAV populations produced by Huh7 cells in HS media when grown in a dual-chamber system

3.2.1 Tight junction formation of Huh7 cells cultured in a dual-chamber system with HS media

To determine whether HS cells cultured in a dual-chamber system formed the tight junctions typical of hepatocytes, we used dextran diffusion studies to assess formation of such a barrier. In these studies, fluorescently labelled 70 kDa Oregon Green dextran was added to the upper compartment of the dual-chamber system. Huh7 cells were plated on a permeable membrane forming the floor of this compartment. Samples were collected from the lower compartment of the dual-chamber system and their fluorescence was measured to assess diffusion between the compartments.

Huh7 cells grown in FBS media do not form a diffusion barrier and do not hinder the movement of dextran across the membrane of the dual-chamber system. The extent of dextran diffusion through confluent FBS cells grown on the dual-chamber membrane for two hours was set to 100%. This value was used to normalize the relative dextran diffusion through cultures of HS cells and through the empty wells of the system. The confluency of Huh7 cells cultured in FBS media was determined as described in Methods and Materials (Sec. 2.9).

Empty wells resulted in the highest level of dextran diffusion through the insert of the dual-chamber system with a value of 118%, the maximum relative dextran diffusion level (red dashed line, Fig. 3.2.1). This value was not significantly different from the value for diffusion through Huh7 cells in FBS media ($p > 0.05$).

The ability of dextran to diffuse through Huh7 cells in HS media on the dual chamber membrane was measured at several times of their exposure to human serum,

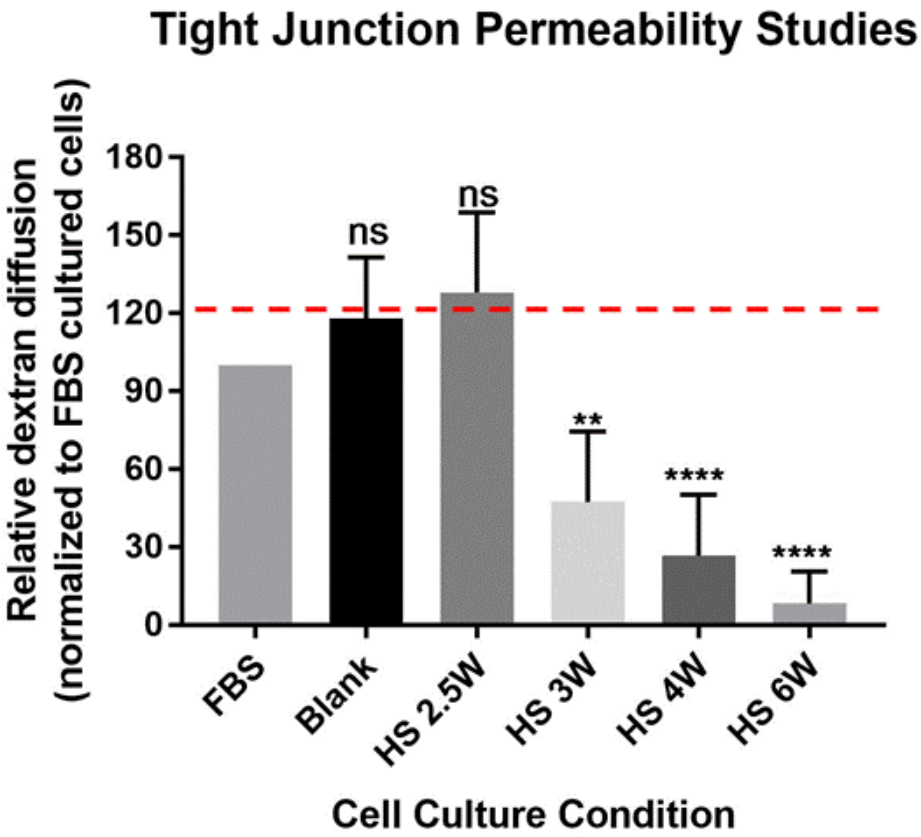

Figure 3.2.1: Tight junction formation of Huh7 cells cultured in the dual-chamber system with HS media

Huh7 cells were transferred onto the dual-chamber system ten days after being cultured in HS media. Dextran diffusion studies were performed to study tight junction formation by Huh7 cells grown in HS media. Fluorescently labelled 70 kDa Oregon Green dextran [1.0 µg/mL] was added to the upper compartment of the dual-chamber system. Samples were collected from the lower compartment for fluorescent readings as described in Sec.2.8. Diffusion was normalized to that of Huh7 cells in FBS media. The time course experiments of dextran diffusion studies were performed after different length of times of culture in HS media (t= 2.5, 3, 4, 6 weeks (W)). Blank insert was used to determine the maximum extent of dextran diffusion. There was no significant difference in dextran diffusion between the blank insert and FBS cultured cells grown in the dual-chamber system. Huh7 cells in HS media formed tight junctions gradually over the course of six weeks. n=4; ** $p \leq 0.01$; **** $p \leq 0.0001$; ns= not significant.

shown in weeks (W), in Fig. 3.2.1. The dextran diffusion studies were first performed a week after Huh7 cells in HS media were plated in the dual-chamber system (Week 2.5). At that time, the value of the relative dextran diffusion was determined to be 130% (Fig. 3.2.1), a value comparable to that of empty wells or Huh7 cells in FBS media grown in the dual-chamber system ($p > 0.05$). It is likely the cells were not yet confluent and that tight junctions had not yet been made at this early time point. There was a significant drop in relative dextran diffusion to 47% by Week 3 ($p \leq 0.01$) (Fig. 3.2.1), suggesting that Huh7 cells in the dual-chamber system with HS media were increasingly confluent and were forming tight junctions. The relative dextran diffusion through Huh7 cells cultured in the dual-chamber system with HS media decreased even more significantly on Week 4 (27%) and Week 6 (8%) ($p \leq 0.0001$) (Fig. 3.2.1). This study showed that Huh7 cells in HS media form tight junctions gradually once they were grown to confluency in the dual-chamber system.

3.2.2 HAV infection on Huh7 cells cultured in the dual-chamber system with IgG(-) HS media

Huh7 cells in HS media cultured in the dual-chamber system were used to perform HAV infection studies. The HS supplemented media used in these HAV infection studies was confirmed to be negative for anti-HAV IgG (IgG(-) HS media). To study time course of HAV infection on HS cells cultured in the dual-chamber system, we infected cultures at 1.0 GE per cell from the basolateral site (lower compartment). After overnight incubation, the inocula were aspirated and the cells were washed five times with DMEM. The last wash was collected to determine the background viral titer. The supernatant was collected every three days from the top and the bottom compartments and these samples were assayed for HAV RNA.

Huh7 cells in IgG(-) HS media cultured in the dual-chamber system developed

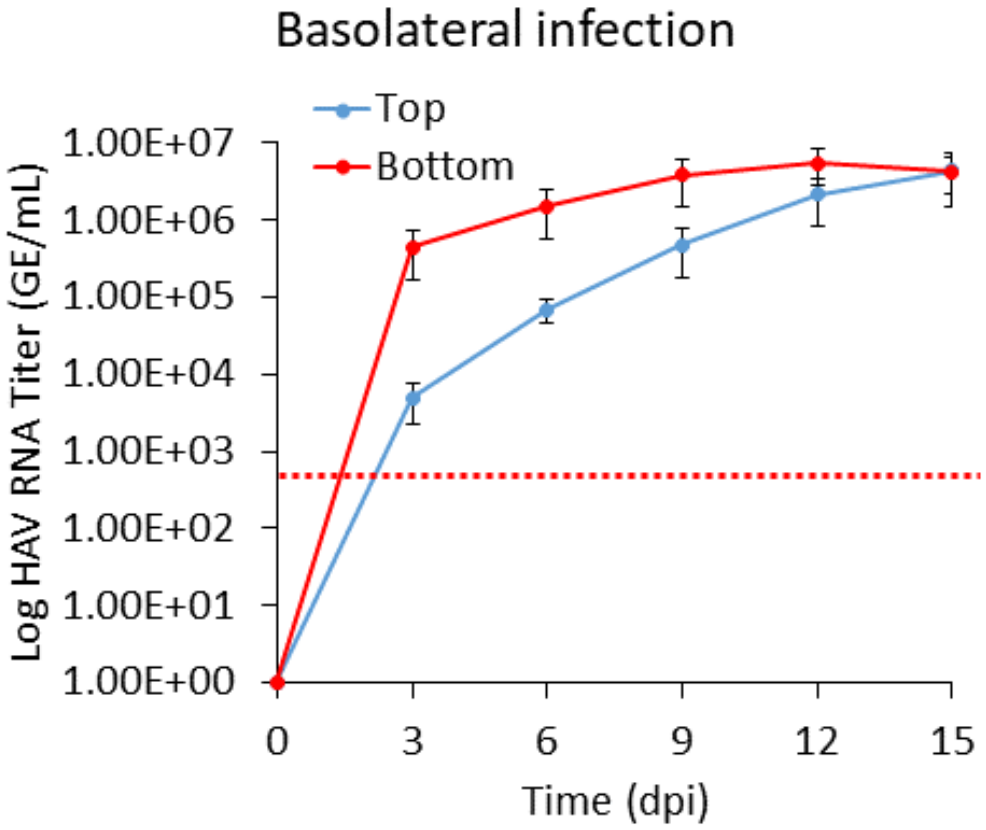

Figure 3.2.2: HAV infection of Huh7 cells cultured in the dual-chamber system with IgG(-) HS supplemented media

Huh7 cells in IgG(-) HS media were infected by the cell culture adapted HAV strain, HM175/p16 (or p16) from the basolateral site (bottom compartment) at 1.0 GE per cell. The cells were incubated with the inocula at 37°C overnight. The next day, the infected cells were washed five times with DMEM. The last wash was collected to determine the background viral titer. The supernatant was collected every three days. The samples collected from the top (blue line) and the bottom (red line) compartments were assayed for HAV RNA. The red dotted line was the limit of detection of the assay. HAV was secreted by the infected cells into both compartments by day 3 post-infection. (Blue) HAV collected from the top compartment increased gradually and plateaued by day 12 post-infection. HAV collected from the top compartment had the similar HAV production range to the samples collected from the bottom compartment at day 12 of post-infection. (Red) HAV collected from the bottom compartment plateaued more quickly, at six days post-infection. n=4.

persistent HAV infection without CPE. HAV RNA at day zero post-infection was below the limit of detection (red dotted line), indicating that the washing steps to remove inocula (background titer) was sufficient. HAV RNA was detected in both top (apical) (blue) and bottom (basolateral) (red) compartments at days three post-infection (Fig. 3.2.2). HAV secreted into the top compartment (5.0E+03 GE/mL) was about 100-fold less than HAV secreted into the lower compartment (4.5E+05 GE/mL). HAV collected from the top compartment increased gradually and plateaued at day 12 post-infection (Fig. 3.2.2, blue line). This was also the time point when HAV collected from the top compartment (2.2E+06 GE/mL) reached a similar range to HAV collected from the bottom compartment (5.5E+06 GE/mL). HAV secreted into the lower compartment, unlike HAV in the upper compartment, plateaued more quickly, at day six post-infection (about 1.5E+06 GE/mL) (Fig. 3.2.2, red line).

The results showed that HAV was secreted into both top and bottom chambers of the dual-chamber system by Huh7 cells maintained in HS media. However, secretion through the apical surface was less efficient than through the basolateral surface of the cells. Therefore, the interpretation of these results assumes HAV infection does not affect the permeability barrier between the two compartments, which was further confirmed using dextran diffusion studies.

3.2.3 The effect of HAV infection on tight junction permeability of Huh7 cells in the dual-chamber system containing HS media

The objective of this study was to determine whether HAV infection affected tight junction permeability of HS cells cultured in the dual-chamber system. We performed dextran diffusion studies as described in Methods and Materials (Sec. 2.7) on cells infected with HAV for 15 days. Dextran diffusion through uninfected cells was measured as a comparison.

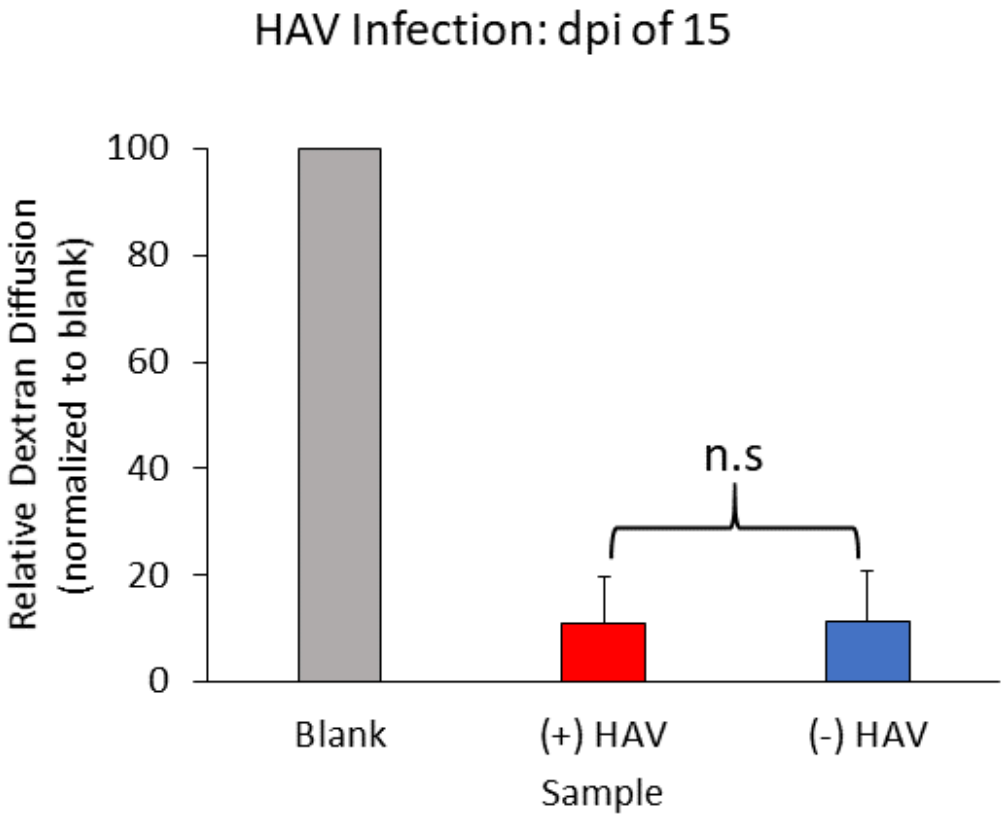

Figure 3.2.3: The effect of HAV infection in tight junction permeability of Huh7 cells in HS media grown in the dual-chamber system.

The tight junction permeability was studied using dextran diffusion on infected Huh7 cells in IgG(-) HS media at day 15 post-infection. Fluorescently labelled 70kDa Oregon Green dextran was added to the top compartment of the dual-chamber system. The samples were collected from the bottom compartment for fluorescent readings at different time points (t (min)= 0, 30, 60, 90, 120). The readings were normalized to that of a dual-chamber system without the cells (blanks) (gray bar). The relative dextran diffusion of the infected Huh7 cells in IgG(-) HS media (red bar) was 11.3%. Uninfected Huh7 cells in IgG(-) HS media (blue bar) had the value of 11.3%. This difference was insignificant. dpi= day of post-infection; n=4; ns=not significant.

Maximum dextran diffusion in the dual-chamber system without cells (blank) was used to normalize the relative dextran diffusion level of the samples and it was set to 100% (Fig. 3.2.3, gray bar). Huh7 cells in HS media were found to maintain tight junction, regardless of whether the cells were infected with HAV or not. The relative dextran diffusion level of both HAV-infected and uninfected Huh7 cells in HS media at 15 days post-infection was 11% (Fig. 3.2.3). This indicated that HAV infection did not affect tight junction permeability of Huh7 cells in HS media. Next, we examined the density profile of HAV populations secreted by infected Huh7 into the upper and lower compartments of the dual-chamber system.

3.2.4 HAV populations from HAV-infected cells in IgG(-) HS media that were grown either in the dual-chamber system or on plastic.

Huh7 cells in HS media grown in the dual-chamber system were well-differentiated (Fig. 3.2.1). To test whether this cell culture model secreted the two density classes of HAV *in vitro*, Huh7 cells grown on the dual-chamber system containing IgG(-) HS media were infected with the p16 HAV strain at 1.0 GE per cell from the basolateral site (bottom compartment). The supernatants from both the upper and lower compartments of the dual-chamber system were collected and clarified and the density classes were analyzed by isopycnic gradient ultracentrifugation.

HAV-infected Huh7 cells in the dual-chamber system with HS media secreted two viral RNA peaks into both the upper and lower compartments (Fig. 3.2.4, A & B), a low density peak between 1.06 g/cm^3 and 1.11 g/cm^3 and a high density between 1.21 g/cm^3 and 1.28 g/cm^3. These populations matched the density profiles reported by Feng et al. (2013) in HAV-infected human and chimpanzee, low density HAV (1.06-1.10 g/cm^3) in the sera samples and high density HAV (1.22-1.28 g/cm^3) in the feces samples. Because of this match, we refer to the low density HAV secreted by infected

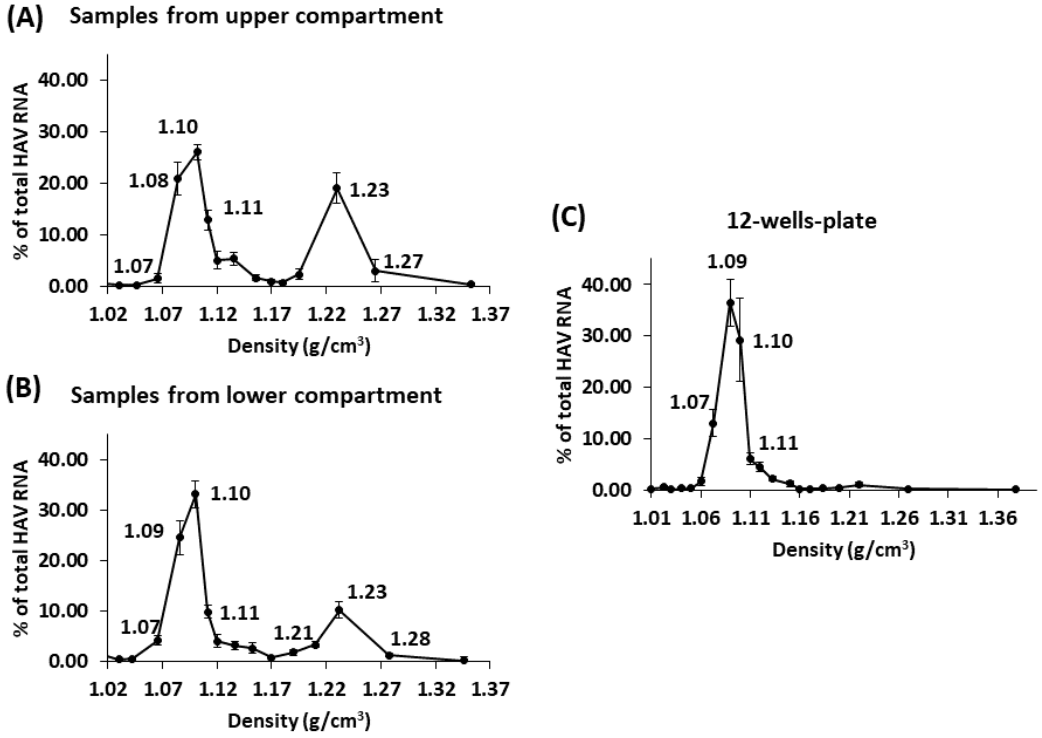

Figure 3.2.4: HAV populations from infected Huh7 cells in IgG(-) HS media grown either in the dual-chamber system or on plastic (12-wells-plate).

The supernatant of infected cells cultured in the dual-chamber system with IgG(-) HS supplemented media were collected from either (A) upper or (B) lower compartment. The samples were loaded onto a iodixanol step gradient (141,000 x g, 42 hrs, 4°C). Twenty fractions were collected from the bottom of the tubes. The index of refraction of each was read to determine viral density. The viral RNA of each was extracted and quantified using RT-qPCR. HAV populations with different density ranges were identified in the samples collected from both (A) upper and (B) lower compartments. One peak had a density range of 1.06-1.11 g/cm^3 (quasi-eHAV) and the second peak had a density range of 1.21-1.28 g/cm^3 (non-enveloped HAV). n=6 (C) HAV density profile of samples collected from HAV-infected Huh7 cells cultured on the 12-wells-plates with IgG(-) HS was included for comparison. Theses samples were found to have a single peak of HAV in the density ranges 1.06-1.11 g/cm^3. n=5

HS cells as quasi-eHAV while high density HAV secreted by infected HS cells is referred to as non-enveloped HAV.

The density profile of HAV collected from infected cells cultured in IgG(-) HS media was compared between the cells cultured in the dual-chamber system and the cells cultured on plastic (Fig. 3.2.4C). In contrast to the two density populations produced by cells cultured in the dual chamber system, Huh7 cells cultured on plastic secreted only low density HAV with a density range between 1.06 g/cm^3 and 1.11 g/cm^3 (Fig. 3.2.4C). Thus, HS cells grown in the dual-chamber system with IgG(-) HS media is a better *in vitro* model with which to study production of the two HAV density populations seen *in vivo*.

3.2.5 The proportion of quasi-eHAV and non-enveloped HAV in apical and basolateral chambers of the dual-chamber system

To determine whether quasi-eHAV and non-enveloped secreted by HAV-infected Huh7 cells on dual-chamber system showed preferential secretion in either the apical or the basolateral direction, we compared the proportions of these two HAV populations in the two compartments of the dual chamber system. Somewhat more quasi-eHAV were detected in the lower chambers (73%) (Fig. 3.2.5A, red) than in the upper chambers (61%) (Fig. 3.2.5B, black). The difference was significant ($p = 0.0131$). In contrast, more non-enveloped HAV were detected in the apical chambers (23%) (Fig. 3.2.5B, black) than in the basolateral chambers (14%). This difference was also significant ($p = 0.0286$). This suggested that the two HAV populations showed a modest preference in their secretion from the two surfaces of polarized cells *in vitro*.

3.2.6 Specific infectivity of quasi-eHAV and non-enveloped HAV secreted *in vitro*

Two HAV populations, as defined by the density, were identified in the samples

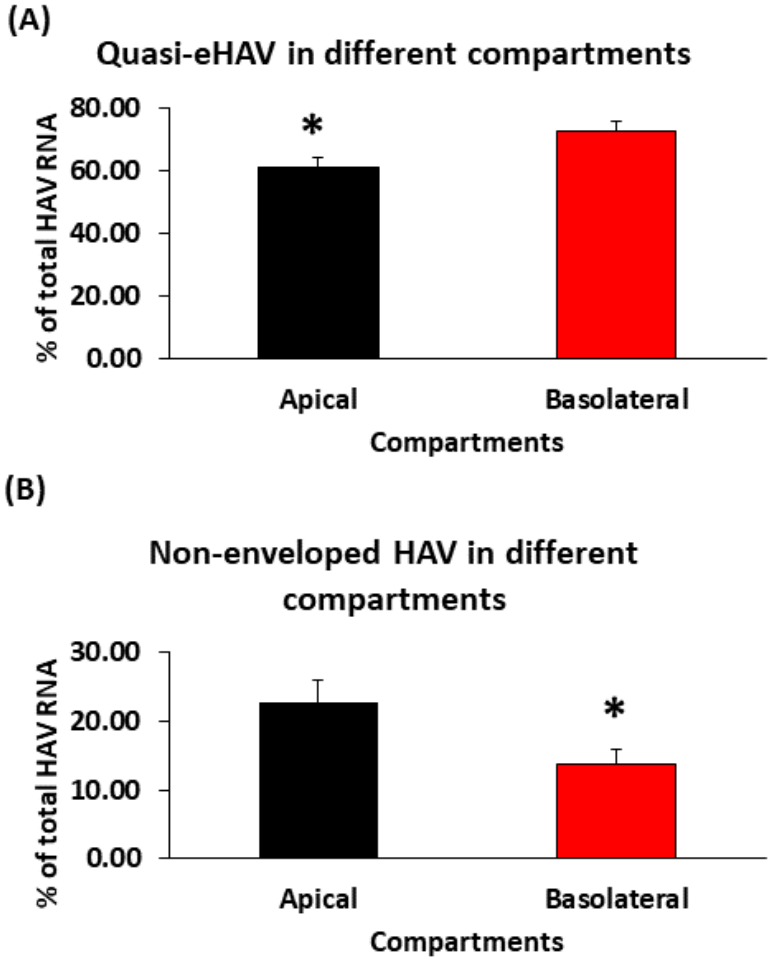

Figure 3.2.5: The proportions of quasi-eHAV and non-enveloped HAV in upper (apical) and lower (basolateral) compartments.

The fraction of non-enveloped HAV and quasi-eHAV secreted into the upper compartment (apical) and lower compartment (basolateral) of the dual-chamber system was measured. This was used to determine whether the HAV populations were secreted in preferential manner from the infected Huh7 cells in HS media. (A) More quasi-eHAV were detected in the basolateral chambers (73%) (red) than in the apical chambers (61%) (black). The difference was significant ($p = 0.0113$). (B) More non-enveloped HAV were detected in the apical chambers (23%) (black) than in the basolateral chambers (14%) (red). This difference was significant ($p = 0.0291$). n=6; * $p \leq 0.05$.

collected from infected Huh7 cells cultured in the dual-chamber system with IgG(-) HS media. The objective of this study was to determine the specific infectivity of these two HAV populations. We performed TCID50 assays using the Reed-Muench method (68) to determine the 50% endpoint titer of the viral samples. The specific infectivity of the samples is defined as the ratio of an infectious particle per total viral genomes of the two HAV populations.

The specific infectivity of quasi-eHAV was determined to be 52 viral genomes per infectious unit (Fig. 3.2.6). Non-enveloped HAV was more infectious with a specific infectivity of 11 genomes per infectious unit (Fig. 3.2.6). The specific infectivity of these two HAV populations was significantly different ($p = 0.0012$). In summary, both quasi-eHAV and non-enveloped HAV secreted by HAV-infected Huh7 cells cultured in IgG(-) HS media were infectious. The results showed that non-enveloped HAV had higher specific infectivity than quasi-eHAV. Next, we studied the ability of these two HAV populations to be neutralized by IgG antibodies specific against HAV.

3.2.7 Neutralization studies of quasi-eHAV and non-enveloped HAV secreted *in vitro*

Neutralization studies were performed on the two HAV populations. Huh7 cells in FBS media were seeded at 17% and incubated overnight in the preparation for the neutralization studies. We pre-treated the two HAV populations with human sera that were either positive (+) or negative (-) for IgG antibodies specific against HAV (volume ratio of one to ten) at 37°C for 1.5 hrs as previously described (71). Untreated samples of either quasi-eHAV or non-enveloped HAV were included as controls. The inocula were applied to the sub-confluent cells overnight with uninfected cells as negative controls. The cells were washed once and incubated at 37°C for five days. At

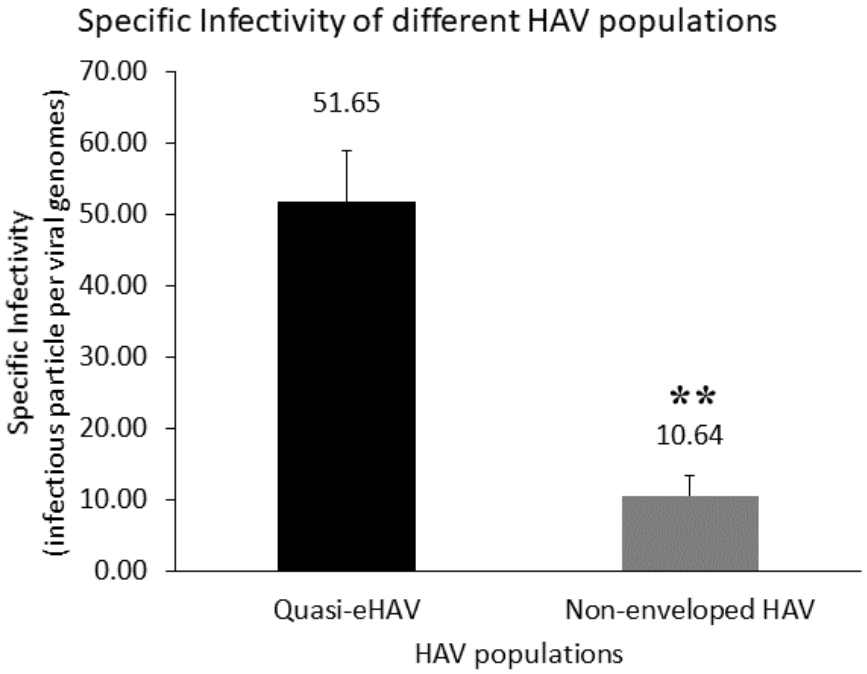

Figure 3.2.6: Specific infectivity of quasi-eHAV and non-enveloped HAV secreted *in vitro*.

Two HAV populations were identified in samples collected from HAV-infected Huh7 cells cultured in the dual-chamber system containing IgG(-) HS media. TCID50 assays were performed to study the specific infectivity of these two HAV populations. The Reed-Muench method was used to calculate the value of TCID50 per mL (68). The result is shown as the ratio of one infectious particle per total viral genomes. Quasi-eHAV had a specific infectivity of 52 genomes per infectious unit. Non-enveloped HAV had a specific infectivity of 11 genomes per infectious unit. This difference was significant ($p = 0.0012$). n=5; $^{**}p \leq 0.01$.

day five post-infection, we collected supernatants and cell lysates to assay for extracellular and intracellular HAV RNA by RT-qPCR. The intracellular titers were normalized to mRNA levels of the housekeeping gene huHPRT.

As expected, HAV RNA was undetectable in uninfected cells intracellularly or extracellularly (Fig. 3.2.7, #1 in all panels). Untreated inocula (positive control) resulted in robust infection of both populations with HAV RNA detected both intracellularly and extracellularly (Fig.3.2.7, #2 in all panels). The result of treatment of both HAV populations with HS containing anti-HAV IgG (+) is shown in #3 of all panels of Fig. 3.2.7. When quasi-eHAV samples were pre-treated with anti-HAV IgG (+) HS, the serum failed to neutralize quasi-eHAV (Fig. 3.2.7 A and C, #3) and infection ensued. When non-enveloped HAV samples were treated with anti-HAV IgG(+) HS, the serum neutralized it (Fig. 3.2.7 B and D, #3) and no infection of the target cells was detected at five days of post-infection either within the cells (Fig. 3.2.7D, #3) or in the supernatants (Fig. 3.2.7D, #3). The result of treatment of the two HAV populations with anti-HAV IgG(-) HS is shown in #4 of all panels of Fig. 3.2.7 (A-D). This serum treatment failed to neutralize either enveloped or non-enveloped HAV (Fig. 3.2.7 A-D, #4). At five days post-infection, both treated HAV populations resulted in robust infection detected both intracellularly (Fig. 3.2.7 A & C, #4) and extracellularly (Fig. 3.2.7 B & D, #4).

Quasi-eHAV, but not non-enveloped HAV, was protected from neutralization by IgG specific against anti-HAV when pre-treated with anti-HAV IgG (+) HS.

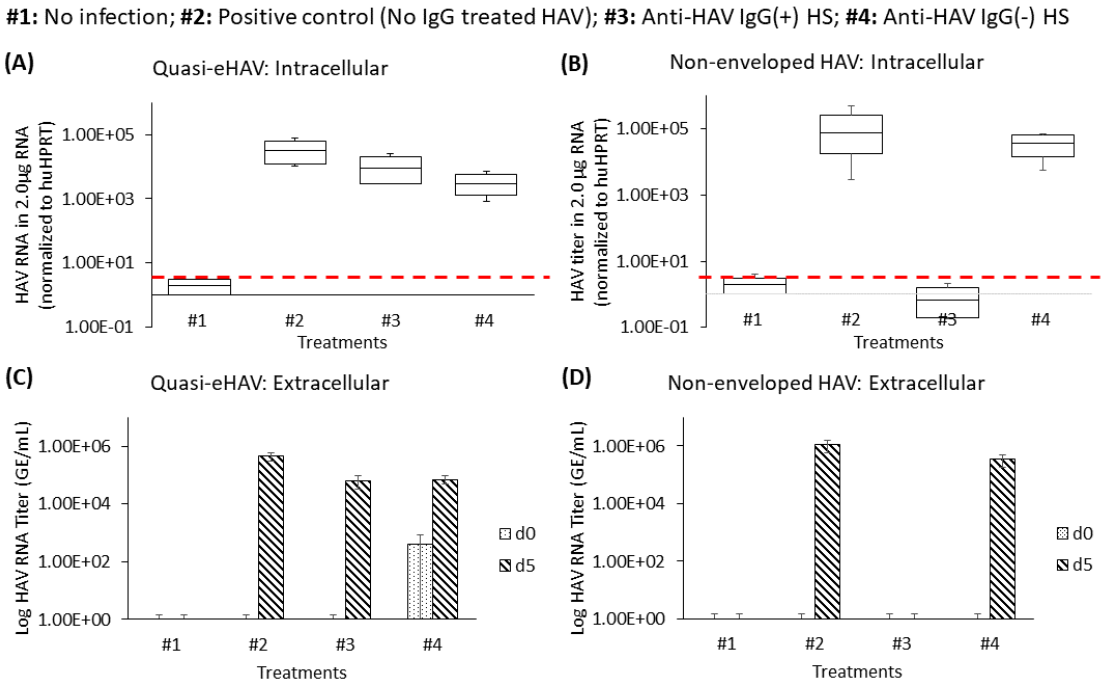

Figure 3.2.7: Neutralization studies of quasi-eHAV and non-enveloped HAV secreted *in vitro*.

The conditions of the treatments are numbered and stated in the legend at the top of the figure. (#1) Uninfected cells were used as the negative control. (#2) Positive control were infected with untreated HAV with serum but incubated to show that this did not reduce infectivity. To perform neutralization studies, we pre-treated both HAV populations with human sera that was either (#3) positive or (#4) negative for IgG specific against HAV (anti-HAV IgG) (1:10, 37°C, 1.5 hrs). Huh7 cells (17%) in FBS media were seeded and incubated overnight (37°C, 5% CO_2). Inocula were incubated with the sub-confluent cells overnight. The next day, the cells were washed once with PBS. The wash was collected and clarified (21,100 x g, 10 min, 4°C). The cells were replaced with FBS media. At five days post-infection, supernatants were collected and clarified (21,100 x g, 10 min, 4°C). A volume of 200.0 µL sample of the supernatant was assayed for extracellular HAV RNA. Meanwhile, cell lysates in 0.1 mL QIAzol Lysis Buffer were processed for relative HAV RNA quantification normalized to an endogenous control, huHPRT in 2.0 µg RNA. Uninfected cells (#1 in all panels) remained uninfected. The red dotted line indicates the limit of detection of HAV RNA. At five days of post-infection, HAV RNA was detected intracellularly (A & C, #2) and extracellularly (B & D, #2) for positive controls of both HAV populations. Anti-HAV IgG(+) HS had no effect on quasi-eHAV (A and C, #3) but this serum neutralized non-enveloped HAV (B and D,#3) . Anti-HAV IgG(-) HS did not have effect on either quasi-eHAV (A and C, #4) or non-enveloped HAV (B and D, #4). At five days of post-infection, HAV titer was detected intracellularly (A & C, #4) and extracellularly (B & D, #4). n=4.

CHAPTER FOUR: DISCUSSION

Part 1: HAV infection studies on monolayer-infected cells cultured in different media conditions

HAV is a non-enveloped, single-stranded positive RNA virus, thus belonging to the family of *Picornaviridae*. However, the identification of both quasi-eHAV and standard non-enveloped HAV in samples collected from HAV-infected chimpanzees or humans has challenged this conventional classification method (32-34). Quasi-eHAV is enclosed within a membrane, has a lower buoyant density range (1.06-1.10 g/cm^3) and is found only in blood (32). Standard non-enveloped HAV has a higher density (1.22-1.28 g/cm^3) and is detected only in feces (32).

A cell culture model secreting the two HAV populations was not available until Hirai-Yuki et al. (2016) showed that these two HAV populations are secreted by a hepatoma-derived cell line, HepG2-N6, grown in dual-chamber system (53). We wanted to test whether different media conditions promoted a better hepatoma cell culture to study the behaviours of the two HAV populations *in vitro*. Human sera (HS) used as media supplement promotes changes in properties of the hepatoma cell lines that render them more hepatocyte-like (120). Because of this, we studied HAV infection in Huh7 cells grown in HS media. In these studies, we compared the HAV populations secreted by more differentiated infected cells grown in HS media to those secreted by less differentiated cells grown in FBS media. We hope that HAV-infected Huh7 cells grown in human sera (HS) media would secrete both quasi-eHAV and non-enveloped HAV *in vitro*.

The density profiles of HAV samples collected from HAV-infected Huh7 cells cultured under four different media conditions. The samples collected from HAV-infected cells cultured in media supplemented with FBS (Fig. 3.1.2A), IgG depleted

HS (Fig. 3.1.5A), and volunteer sera free of antibodies specific against HAV (Fig. 3.1.7) produced a single peak of low density HAV (1.06-1.11 g/cm^3), a density characteristic of quasi-eHAV (32). However, the samples collected from HAV-infected cells cultured in the media supplemented with standard HS not depleted of IgG (Fig. 3.1.2B & Fig. 3.1.5B) yielded two peaks, a low density peak and a high density peak (1.17-1.20 g/cm^3). The high density peak did not match with previously reported ranges (32).

IgG antibodies specific against HAV (referred as anti-HAV IgG) were present in the HS media used in the HAV infection studies. HS is a commercial product that was pooled samples from 80 to 120 donors. Thus, some of these donors were likely exposed to HAV infection or were vaccinated against HAV and would contribute antibodies specific against HAV to the pooled serum.

By using Protein A column, IgG was removed from HS. HS with IgG removed tested negative for antibodies specific against HAV. The samples collected from the infected cells cultured under this HS condition (referred as IgG(-) HS HAV) had only one major virion peak in the low density range (1.06-1.11 g/cm^3) (Fig. 3.1.5A). IgG(-) HS HAV shared a similar density profile to HAV produced by cells cultured in FBS medium (Fig. 3.1.2A), but differed from the density profile of HAV produced in standard HS medium containing anti-HAV antibodies (Fig. 3.1.2B & Fig. 3.1.5B).The absence of anti-HAV IgG was the main difference between these two HS conditions that were used for cell culture. Thus, we proposed that IgG specific against HAV was possibly responsible for the high density peak centred at 1.18 g/cm^3.

A role of IgG specific against HAV in generating this high density HAV population (the peak at 1.18 g/cm^3) was supported by the further studies. In immunoprecipitation studies using Protein G Sepharose beads, high density population was the only HAV type detected in the pellet, the low density HAV population was

barely detected in the pellet (Fig. 3.1.6). This suggested that 1.18 g/cm^3 HS HAV was possibly an immunocomplex of HAV with IgG.

By using volunteer sera free of anti-HAV IgG in HAV infection studies, we showed that general immunoglobulin (IgG that was not specific against HAV) did not generate the high density peak of HS HAV (Fig. 3.1.7). The viral density profile seen was similar to that of IgG(-) HS HAV (Fig. 3.1.5) and differed from the two peak profile seen in IgG(+) HS HAV (Fig. 3.1.2B). The main difference between volunteer sera and IgG non-depleted HS is the absence of IgG specific against HAV. This shows binding of IgG not specific against HAV to virions was not responsible for the peak of high density HS HAV.

Treatment of low density HAV population with IgG containing anti-HAV antibodies did not generate the high density HAV populations (Fig. 3.1.8). Thus, this study eliminated the possibility that an immunocomplex between low density HAV and anti-HAV antibodies produced the high density peak, at least extracellularly. However, our immunoprecipitation experiment showed that the high density population of HAV does contain IgG. The contradictory results of our experiments are puzzling.

The proportion of HAV population(s) detected in all media conditions is always not 100%. Perhaps, other HAV popualtions are secreted by Huh7 cells. The virion population with peak at 1.167 g/cm^3 is detected in bile samples collected from *Mavs*$^{-/-}$ mice and sera of HAV-infected chimpanzee (53). Compared to non-enevloped HAV, this population is still less dense and thus, it is likely associated with membranes. However, the treatment of 1% NP40 failed to shift this population to denser peak, and thus, its identity remains unknown (53). Besides, Feng et al. (2014) showed that the treatment of quasi-eHAV with 1% NP40 partially shifts its density to the intermediate range and renders its capsid to be detectable by ELISA (32). Thus, we proposed that

the intermediate density HAV population is secreted by Huh7 cells and immunocomplexed with IgG in standard HS media to form high density peak. When intermediate density virions are secreted by cells in standard HS media, anti-HAV antibodies bind to viral capsids to form immunocomplex and accumulate in media over three days, resulting in the generation of high density peak in iodixanol gradient (Fig. 3.1.2B & Fig. 3.1.5B). This was consistent with our preliminary data that more HAV were found in the denser peak when the samples with the intermediate density range (1.15-1.17 g/cm^3) were treated with IgG than the untreated sample (Supplementary Fig. 1). Further studies, for example higher IgG concentration or longer incubation period, could be done to explain why only partial proportion of HAV shifted right.

The formation of this intermediate density virion population is yet to be elucidated. First, it is possibly derived from quasi-enveloped and partially loss envelope due to the shearing force of centrifuge. However, our studies showed no density shift in quasi-eHAV treated with 2.0 mg/mL IgG (Fig. 3.1.8). Thus, this is unlikely the hypothesis to explain the formation of high density populatin centered at 1.18g/cm^3. Second, it is likely another HAV population as proposed by Hirai-Yuki et al (2016). Futher studies are required to characterize this population.

Huh7 cells cultured in HS media could be infected, even though HS used for the media supplement contained anti-HAV IgG antibodies capable of neutralizing HAV (Fig. 3.1.1). Quasi-eHAV in the infectious materials derived from infected Huh7 cells in FBS media (Fig. 3.1.2A) were used in these experiments (Fig.3.1.2B). Quasi-eHAV, cloaked within the membrane, could be protected from being neutralized by anti-HAV IgG and be the source of infectious virus (32). Thus, samples collected from HAV-infected Huh7 cells in IgG non-depleted HS remain infectious (Fig 3.1.1). However, compared to the cells in IgG(-) HS media, there was lesser viral production

by the cells cultured in standard HS media (Fig. 3.1.3), consistent with the previous report (32). By infecting cells with gradient-purified quasi-eHAV, Feng et al. (2013) showed that lesser HAV RNA were detected both intracellularly and extracellularly in cells either pre-treated or post-treated with anti-HAV antibodies than in untreated cells. The authors proposed quasi-eHAV is neutralized after binding to or entering cells (post-endocytosis neutralization (Fig. 4.1.2) (32,33). Anti-HAV antibodies are likely endocytosed together with some quasi-eHAV into the lysosome (Fig. 4.1.2.1a). This gives access to anti-HAV antibodies to bind to HAV for neutralization when the membranes of quasi-eHAV are degraded in the lysosomes (Fig. 4.1.2.1, b & c) (32,33). Quasi-eHAV escaped from the post-endocytosis neutralization are uncoated to release viral RNA genomes to continue the enterohepatic cycle of HAV (Fig. 4.1.2.2, a-c). Neutralized quasi-eHAV reduces the availability of infectious materials and possibly explains lower infectivity level of the samples from standard HS media (Fig. 3.1.4). Besides, high density HAV population, proposed to be an immunocomplex HAV and IgG (Fig. 3.1.6), might also affect the viral infectivity of inocula.

In summary, removing anti-HAV antibodies in HS used for media supplement resulted in production of HAV with a different density profile, higher titer and greater infectivity. Although the identity of high density HAV population remains puzzling, it is important to further study HAV infection using Huh7 cells cultured in the dual-chamber system with IgG(-) HS (see Chapter 3.2, Result: Part 2).

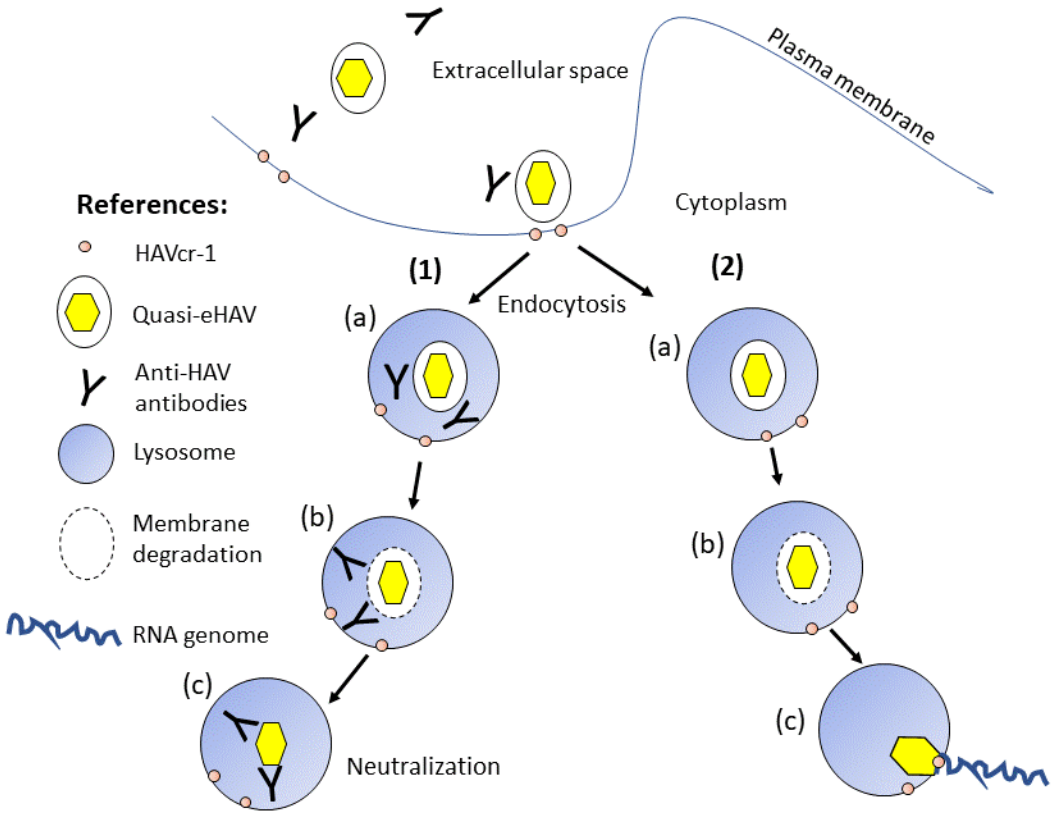

Figure 4.1.2: Post-endocytosis neutralization mechanism of quasi-eHAV (adapted from Feng et al., 2014)

This diagram depicts the post-endocytosis mechanism of quasi-eHAV, as proposed by Feng et al, 2014 (33). After quasi-eHAV are taken up by the cells via endocytosis process, they move to the late endosome and lysosome. The membrane of quasi-eHAV are degraded slowly in the lysosome. (1, a-c) If quasi-eHAV are endocytosed together with anti-HAV antibodies, the antibodies will bind to HAV capsid once the membrane of quasi-eHAV are fully degraded, resulting in neutralization. (2, a-c) If membranes of quasi-eHAV are degraded in the lysosome without the presence of anti-HAV antibodies, the viral capsid will interact with the entry receptor, HAVcr-1. This is followed by the subsequent uncoating process to release of HAV RNA genome into the cytoplasm to continue the enterohepatic cycle of HAV.

CHAPTER FOUR: DISCUSSION

Part 2: The behaviour of two HAV populations produced by Huh7 cells in HS media when grown in a dual-chamber system

Two HAV populations have been identified in samples collected from HAV-infected humans and chimpanzees (32) or from HAV infection of the mouse model developed in our lab (90). Feng et al. (2013) showed that quasi-eHAV is found only in sera while non-enveloped HAV is found only in feces. Our studies of HAV-infected chimeric SCID-beige/Alb-uPA mice also identified two HAV populations in samples collected from different sites: sera, feces and bile (90). Quasi-eHAV is found only in mouse sera while non-enveloped HAV is found only in mouse bile and feces.

The report of two HAV populations in different sites (sera versus feces) suggests that HAV may be secreted by the hepatocytes through two routes or that only quasi-eHAV is produced by hepatocytes and the envelope is subsequently stripped off by bile to form HAV (32,34). For the first mechanism, the authors proposed that quasi-eHAV could leave the infected hepatocytes through the basolateral surface of the hepatocytes and enter the bloodstream whereas non-enveloped HAV would exit liver to the bile canaliculus through the apical surface of the hepatocytes. For the second mechanism, quasi-eHAV would be modified after secretion. Quasi-eHAV retains its envelope if secreted from the basolateral surface and then circulates in blood. Alternatively, if quasi-eHAV is secreted from the apical aspect of hepatocytes into the bile canaliculus, its envelope membranes would be stripped off by the bile and become non-enveloped HAV in the feces. However, concentrated porcine bile fails to strip off the membrane of quasi-eHAV (32). Studies show that bile acid components vary among species (43,54). Perhaps, the bile acid component required to strip off the membrane of quasi-eHAV is species-specific and is not present in procine bile (53).

We were interested to develop a cell culture system capable of secreting two HAV populations, so such a system can be used to study aspects of HAV biology inaccessible by standard tissue culture methods. The hepatoma cell lines Huh7.5 cultured in media supplemented with human serum had been shown to develop hepatocyte-like characteristics (120). In comparison to the cells cultured in FBS media, Huh7.5 cells in HS media are growth-arrested, shows increased levels of mRNAs of tight junction components, increased secretion of albumin serum and VLDL secretion is restored (120). We tested whether the parental hepatoma cell line, Huh7 cells cultured in HS media would have similar characteristics. When we cultured Huh7 cells in HS media on plastic, the cells were growth arrested after three weeks. In HAV infection studies, only one viral population was produced (Fig. 3.2.4C). This population had the density range (1.06-1.11 g/cm^3) matching that of quasi-eHAV (32).

Hepatocytes are highly polarized cells that have two distinct surfaces: the apical surface facing the bile canaliculus and the basolateral surface facing the Space of Disse, part of the circulatory system (11). This suggested that the possibility that the two surfaces of hepatocyte, each secrete one of the HAV populations. We examined this possibility by culturing Huh7 cells in HS media in the dual-chamber system to simulate polarized hepatocytes. This culture system was used to test whether the polarized hepatoma cells secreted both quasi-eHAV and non-enveloped HAV and from which surface.

Prior to HAV infection studies, we performed dextran diffusion studies to confirm cell contact inhibition and tight junction formation, a barrier essential to our studies. After culturing in HS media for three weeks, Huh7 cells grew to confluency and were growth arrested in the dual-chamber system (Fig. 3.2.1). Our studies also showed that cell became more differentiated (Fig. 3.2.1) and could be maintained for a

long period (more than 1.5 months), consistent with the previous report (120). Huh7 cells cultured in regular FBS media required constant splitting as the cells did not show contact inhibition. Dextran diffusion studies in such cells showed that dextran diffusion was not inhibited, indicating that tight junctions were not formed by Huh7 cells grown in FBS media (Fig. 3.2.1).

Next, we tested whether HAV-infected Huh7 cells in HS media cultured in the dual-chamber system secreted both quasi-eHAV and HAV *in vitro*. After enteric exposure, HAV is proposed to be taken up from the bloodstream via the basolateral surfaces of the hepatocytes (117). Snook et al. (2008) used a polarized HepG2-N6 to show that HAV entered cells through the basolateral surface. Similarly, we infected Huh7 cells cultured in the dual-chamber system after four weeks in HS media from the basolateral side with cell culture adapted HAV strain, p16, at 1.0 GE per cell. HAV infection studies were performed in cells cultured in IgG depleted HS media (negative for anti-HAV IgG). HAV RNA was detected in the samples collected from both upper and lower compartments of the dual-chamber system every three days over 15 days post-infection (Fig. 3.2.2). Dextran diffusion studies showed that the tight junctions were maintained during such HAV infection experiments (Fig. 3.2.3). These studies showed that the HAV infection of cells in HS media developed a persistent HAV infection that did not cause CPE and did not affect the tight junction permeability. This was consistent with previous studies that showed that infection of cell culture adapted HAV strain *in vitro* is not cytopathic (34,59).

Unlike the samples collected from infected cells grown on plastic which only produced low density HAV (Fig. 3.2.4C), samples collected from HAV-infected HS cells grown on the collagen-coated membrane of the dual-chamber system had two virion populations in both upper and lower compartments (Fig. 3.2.4 A & B). One

population had a density range of 1.06-1.11 g/cm^3 (low density) and the other of 1.21-1.28 g/cm^3 (high density). The low density HAV population matched the density of quasi-eHAV and the high density HAV population matched the density of non-enveloped HAV (32). In fact, collagen is shown to enhance polarization of different epithelial cell lines (1,96,123,138). Thus, the difference in the density profiles between infected HS cells grown on plastic and infected HS cells grown in the dual-chamber system further supported the hypothesis that cell polarization was crucial to secretion of both quasi-eHAV and the non-enveloped HAV *in vitro*.

HAV populations secreted by infected cells in HS media cultured in the dual-chamber system showed some preferential secretion (Fig. 3.2.5). More quasi-eHAV was secreted in the basolateral direction (Fig. 3.2.5B) and more non-enveloped HAV was secreted more in the apical direction (Fig. 3.2.5C). This suggested the possibility that HAV uses two routes to exit the infected hepatocytes. However, Hirai-Yuki et al. (2016) used HAV-infected HepG2-N6 cells in the dual-chamber system to show that both compartments had a similar ratio of non-enveloped HAV to quasi-eHAV (53). Thus, they rejected the hypothesis that the two HAV density populations use two routes to exit the hepatocytes. Furthermore, they showed that treatment of quasi-eHAV with a high concentration of human bile acid (930 mM TCA) shifted quasi-eHAV from the low density range to the high density range of non-enveloped HAV (53).

Our cell culture data does not rule out the possibility that bile acids strip the membrane from quasi-eHAV after it exits the cells. Cell polarity plays a crucial role in maintaining hepatic function (85,129,138). Cells grown in HS media are highly polarized with distinct apical and basolateral surfaces on opposite surfaces (paper in preparation). This is similar to HepG2-N6 cells polarized by 1% DMSO supplemented media (117). Bile production of the cells in HS media is upregulated when compared

to the cells grown in FBS media (paper in preparation). We propose that better cell polarization of Huh7 cells in HS media in the dual-chamber system promotes a higher level of bile production when compared to Huh7 cells in HS media plated on plastic. This might explain the fact that infected Huh7 cells in the dual-chamber system with HS media secrete two HAV populations with some preferential direction of secretion while HAV populations on plastic produce only quasi-eHAV.

With the cell culture system capable of secreting the two HAV populations, we wanted to test the hypothesis that bile salts stripped the membrane from quasi-eHAV to produce non-enveloped HAV *in vivo*. We performed pilot studies to suppress CYP7A1, the rate limiting enzyme in bile acid synthesis from cholesterol, using the FXR agonist GW4064 (80). FXR is the key regulator of the bile acid synthesis pathway and one of its primary functions is to suppress CYP7A1 (11,13,47,79,116).

The treatment of 1.0 μM GW4064 is known to suppress CYP7A1 mRNA expression in primary hepatocytes (47,55,119). We treated Huh7 cells in HS media with 1.0 μM GW4046 to increase FXR activity, suppress CYP7A1 and reduce bile acid synthesis. We hoped this would reduce the ability of secretion of bile salts to strip quasi-eHAV of its membrane. We used only samples collected from the apical chambers for isopynic gradient ultracentrifugation in this pilot study because more non-enveloped HAV are found in the apical chamber. No significant difference in HAV to quasi-eHAV populations was seen between GW4064 treated cells and cells treated with the vehicle control (0.01% DMSO) ($p \geq 0.05$) (Supplementary Table 1). Hirai-Yuki et al. (2016) showed that the treatment of quasi-eHAV with high concentration of bile salt converts it to HAV through it detergent action (11,17). Based on our preliminary data, we suggest that it is unlikely that the bile salts play a role in stripping quasi-eHAV of the membrane even though there is upregulation of bile salt production in HS cultured

cells (paper in preparation). In fact, bile salt concentration in the cell culture system would become toxic before reaching that found in the bile duct.

Specific infectivity studies were done to characterize the two HAV populations produced *in vitro*. Both HAV populations secreted by HAV-infected Huh7 cells in HS media were infectious (Fig. 3.2.6), consistent with a previous report (32). However, these authors reported that both quasi-eHAV and non-enveloped have equivalent specific infectivity (32). Surprisingly, our results show that non-enveloped HAV is five times more infectious than quasi-eHAV (Fig. 3.2.6). This is perhaps due to differences in capsid structure: quasi-eHAV has the immature VP1-pX domain but non-enveloped HAV has the mature VP1 domain (32). pX domain (also known as 2A) is a carboxyl terminal extension of VP1 that is cleaved by an unknown protease to form the mature HAV capsid (82). Using vΔ2A-11 (the deletion of C-terminal in 2A sequence) that retains pX sequence on the viral particles by impairing VP1/pX cleavage event, Cohen et al. (2002) showed that compared to the wild-type virus, v18f, there is a reduction in the HAV particles' infectivity and a delay in the production of infectious particles, even though this mutation does not abolish the viral replication (21).

In neutralization studies, both HAV populations were pre-treated with anti-HAV IgG(+) HS before infection. Anti-HAV IgG(+) HS neutralized non-enveloped HAV (Fig. 3.2.7 B & D, #3) but it had no effect on quasi-eHAV (Fig. 3.2.7 A & C, #3). This is consistent with previous studies (32,71). Quasi-eHAV is enclosed within membrane sacs and protected from neutralization by IgG antibodies specific against HAV (32,71). Non-enveloped HAV displaying capsid antigens recognized by IgG antibodies specific against HAV is neutralized.

In conclusion, Huh7 cells in HS media grown in the dual-chamber system were shown to be growth arrested, differentiated, and provide a culture system representative

of the hepatocyte. In our cell culture system, bile salts are unlikely achieve concentrations capable of stripping quasi-eHAV of its membrane. We showed that by growing Huh7 cells in HS media in dual-chamber systems, HAV-infected cells secreted these two HAV populations in modest evidence of directionality, suggesting the possibility of HAV using two routes to exit infected hepatocytes. However, we cannot discount the possibility of other potential factors to strip off the membrane. Further studies are required to test the difference of HS cultured cells grown between on the plastics or in the dual-chamber system. We have shown that Huh7 cells in HS media in the dual-chamber system is a better *in vitro* model to study egress mechanism of HAV than the one grown on plastic.

SUPPLEMENTARY:

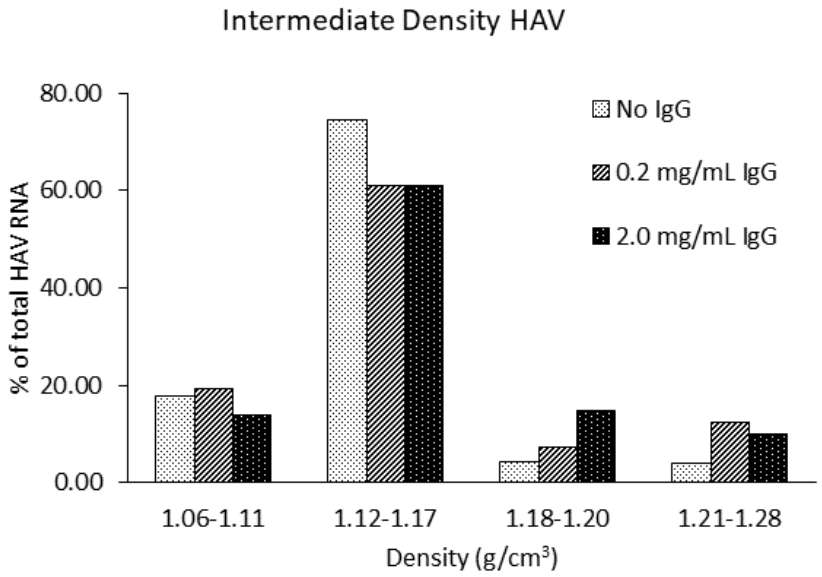

Supplementary Figure 1: Treatment of interemdiate density HAV population with anti-HAV IgG.

The intermediate density HAV population (1.15-1.17 g/cm^3) from IgG(-) HS HAV was divided into three tubes: one without IgG, second with 0.2 g/mL IgG, and third with 2.0 g/mL IgG. IgG contains anti-HAV antibodies. All samples were incubated at 37°C for 1.5hrs and loaded onto iodixanol step gradient (141,000 x g, 42 hrs, 4°C). Twenty fractions were collected from the bottom of the tubes. The refractive index was used to determine the density of the fractions and HAV RNA was assayed for all fractions. The fractions were divided into four density ranges: 1.06-1.10 g/cm^3, 1.12-1.17 g/cm^3, 1.18-1.20 g/cm^3, and 1.21-1.28 g/cm^3. The virion population that had the density range between 1.12-1.17 g/cm^3 comprised of 74% of the total virus in untreated samples (light gray) and 61% in the samples treated with 0.2 mg/mL IgG (dark gray) and 2.0 mg/mL IgG (black). Compared to 4% HAV with the density range of 1.18-1.20 g/cm^3 and 1.21-1.28 g/cm^3 each in untreated samples (light gray), there was 7% and 12% each in the samples treated with 0.2 mg/mL (dark gray) and 15% and 10% each in the samples treated 2.0 mg/mL IgG (black). Duplicates for each experiment; n=2 for untreated and treatment with 2.0 g/mL IgG; n=1 for treatment with 0.2 mg/mL.

Treatments	Quasi-eHAV(%)	Non-enveloped HAV (%)
GW4064	58.7 (58-66)	21.0 (17-23)
DMSO	63.4 (56-63)	19.4 (18-27)

Supplementary Table 1: Treatment of GW4064 (FXR agonist)

HS cells cultured in the dual-chamber system were infected with cell culture adapted HAV strain, p16 for six days. At day six post-infection, infected cells were treated with either GW4964 (1.0 μM) or 0.01% DMSO (vehicle control). After 72 hrs of post-treatment, supernatants from the upper chambers of the dual-chamber system were collected, clarified (12,100 x g, 4°C, 10 min) and loaded onto iodixanol step gradient (141,000 x g force, 4°C, 42 hrs). Twenty fractions were collected from the bottom of the tubes. The refraction index of the fractions was used to determine the viral density. The viral RNA of the fractions was extracted and quantified using real-time qPCR. The bracketed value was the range of HAV proportions of the experiments. There was about 59% of quasi-eHAV in infected cells treated with GW4064 and 63 % of quasi-eHAV in infected cells treated with DMSO. The difference was insignificant ($p \geq 0.05$). There was about 21% of non-enveloped HAV in the infected cells treated with GW4064 and 19% of non-enveloped HAV in the infected cells treated with 0.01% DMSO. This was an insignificant difference ($p \geq 0.05$). n=3.

CHAPTER FIVE: BIBLIOGRPAHY

1. **Ahmadzadeh, H., M. R. Webster, R. Behera, A. M. Jimenez Valencia, D. Wirtz, A. T. Weeraratna, and V. B. Shenoy**. 2017. Modeling the two-way feedback between contractility and matrix realignment reveals a nonlinear mode of cancer cell invasion. Proc.Natl.Acad.Sci.U.S.A **114**:E1617-E1626. doi:1617037114 [pii];10.1073/pnas.1617037114 [doi].

2. **Anderson, D. A. and B. C. Ross**. 1990. Morphogenesis of hepatitis A virus: isolation and characterization of subviral particles. J.Virol. **64**:5284-5289.

3. Applied Biosystems. TaqMan Universal PCR Master Mix. 9-10. 2010. USA, Applied Biosystems.

Ref Type: Online Source

4. **Ashwell, G. and J. Harford**. 1982. Carbohydrate-specific receptors of the liver. Annu.Rev.Biochem. **51**:531-554. doi:10.1146/annurev.bi.51.070182.002531 [doi].

5. **Ashwell, G. and A. Morrell**. 1974. The role of surface carbohydrates in the hepatic recognition and transport of circulating glycoproteins, p. 99-128. *In*: Advances in Enzymology and Realted Areas of Molecular Biology. 41 ed.

6. **Bishop, N. E. and D. A. Anderson**. 2000. Uncoating kinetics of hepatitis A virus virions and provirions. J.Virol. **74**:3423-3426.

7. **Blank, C. A., D. A. Anderson, M. Beard, and S. M. Lemon**. 2000. Infection of polarized cultures of human intestinal epithelial cells with hepatitis A virus: vectorial release of progeny virions through apical cellular membranes. J.Virol. **74**:6476-6484.

8. **Bosch, A., S. Guix, D. Sano, and R. M. Pinto**. 2008. New tools for the study and direct surveillance of viral pathogens in water. Curr.Opin.Biotechnol. **19**:295-301. doi:S0958-1669(08)00051-7 [pii];10.1016/j.copbio.2008.04.006 [doi].

9. **Bosch, A. and RM. Pinto**. 2013. Hepatitis A virus, p. 61-77. *In*: F. J. M. Smulders, B. Norrung, and H. Budka (eds.), Foodborne viruses and prions and their significance for public health., vol. 6. Wageningen Acadamie Publishers.

10. **Bower, W. A., O. V. Nainan, X. Han, and H. S. Margolis**. 2000. Duration of viremia in hepatitis A virus infection. J.Infect.Dis. **182**:12-17. doi:JID991591 [pii];10.1086/315701 [doi].

11. **Boyer, J. L.** 2013. Bile formation and secretion. Compr.Physiol **3**:1035-1078. doi:10.1002/cphy.c120027 [doi].

12. **Brack, K., I. Berk, T. Magulski, J. Lederer, A. Dotzauer, and A. Vallbracht**. 2002. Hepatitis A virus inhibits cellular antiviral defense mechanisms induced by double-stranded RNA. J.Virol. **76**:11920-11930.

13. **Bramlett, KS., S. Yao, and TP. Burris**. 2000. Correlation of Farnesoid X Receptor Coactivator Recruitment and Cholesterol 7a-Hydroxylase Gene Repression by Bile Acids. Molecular Genetics and Metabolism **71**:609-615.

14. **Brown, E. A., A. J. Zajac, and S. M. Lemon**. 1994. In vitro characterization of an internal ribosomal entry site (IRES) present within the 5' nontranslated region of hepatitis A virus RNA: comparison with the IRES of encephalomyocarditis virus. J.Virol. **68**:1066-1074.

15. **Carvalho, C., H. Thomas, K. Balogun, R. Tedder, R. Pebody, M. Ramsay, and S. Ngui**. 2012. A possible outbreak of hepatitis A associated with semi-dried tomatoes, England, July-November 2011. Euro.Surveill **17**.

16. **Chestovich, P. J., Y. Uchida, W. Chang, M. Ajalat, C. Lassman, R. Sabat, R. W. Busuttil, and J. W. Kupiec-Weglinski**. 2012. Interleukin-22: implications for liver ischemia-reperfusion injury. Transplantation **93**:485-492. doi:10.1097/TP.0b013e3182449136 [doi].

17. **Chiang, J. Y.** 2009. Bile acids: regulation of synthesis. J Lipid Res. **50**:1955-1966. doi:R900010-JLR200 [pii];10.1194/jlr.R900010-JLR200 [doi].

18. **Chigor, V. N. and A. I. Okoh**. 2012. Quantitative RT-PCR detection of hepatitis A virus, rotaviruses and enteroviruses in the Buffalo River and source water dams in the Eastern Cape Province of South Africa. Int.J Environ.Res.Public Health **9**:4017-4032. doi:ijerph9114017 [pii];10.3390/ijerph9114017 [doi].

19. **Choi, Y. S., J. Lee, H. W. Lee, D. Y. Chang, P. S. Sung, M. K. Jung, J. Y. Park, J. K. Kim, J. I. Lee, H. Park, J. Y. Cheong, K. S. Suh, H. J. Kim, J. S. Lee, K. A. Kim, and E. C. Shin**. 2015. Liver injury in acute hepatitis A is associated with decreased frequency of regulatory T cells caused by Fas-mediated apoptosis. Gut **64**:1303-1313. doi:gutjnl-2013-306213 [pii];10.1136/gutjnl-2013-306213 [doi].

20. **Ciocca, M.** 2000. Clinical course and consequences of hepatitis A infection. Vaccine **18 Suppl 1**:S71-S74. doi:S0264410X99004703 [pii].

21. **Cohen, L., D. Benichou, and A. Martin**. 2002. Analysis of deletion mutants indicates that the 2A polypeptide of hepatitis A virus participates in virion morphogenesis. J.Virol. **76**:7495-7505.

22. **Collier, M. G., Y. E. Khudyakov, D. Selvage, M. Adams-Cameron, E. Epson, A. Cronquist, R. H. Jervis, K. Lamba, A. C. Kimura, R. Sowadsky, R. Hassan, S. Y. Park, E. Garza, A. J. Elliott, D. S. Rotstein, J. Beal, T. Kuntz, S. E. Lance, R. Dreisch, M. E. Wise, N. P. Nelson, A. Suryaprasad, J. Drobeniuc, S. D. Holmberg, and F. Xu**. 2014. Outbreak of hepatitis A in the USA associated with frozen pomegranate arils imported from Turkey: an epidemiological case study. Lancet Infect.Dis. **14**:976-981. doi:S1473-3099(14)70883-7 [pii];10.1016/S1473-3099(14)70883-7 [doi].

23. **Conaty, S., P. Bird, G. Bell, E. Kraa, G. Grohmann, and J. M. McAnulty**. 2000. Hepatitis A in New South Wales, Australia from consumption of oysters: the first reported outbreak. Epidemiol.Infect. **124**:121-130.

24. **Counihan, N. A. and D. A. Anderson**. 2016. Specific IgA Enhances the Transcytosis and Excretion of Hepatitis A Virus. Sci.Rep. **6**:21855. doi:srep21855 [pii];10.1038/srep21855 [doi].

25. **de Souza, A. J., T. B. Oriss, K. J. O'malley, A. Ray, and L. P. Kane**. 2005. T cell Ig and mucin 1 (TIM-1) is expressed on in vivo-activated T cells and provides a costimulatory signal for T cell activation. Proc.Natl.Acad.Sci.U.S.A **102**:17113-17118. doi:0508643102 [pii];10.1073/pnas.0508643102 [doi].

26. **Debing, Y., J. Neyts, and H. J. Thibaut**. 2014. Molecular biology and inhibitors of hepatitis A virus. Med.Res.Rev. **34**:895-917. doi:10.1002/med.21292 [doi].

27. **Desenclos, J. C., K. C. Klontz, M. H. Wilder, O. V. Nainan, H. S. Margolis, and R. A. Gunn**. 1991. A multistate outbreak of hepatitis A caused by the consumption of raw oysters. Am.J.Public Health **81**:1268-1272.

28. **Donnan, E. J., J. E. Fielding, J. E. Gregory, K. Lalor, S. Rowe, P. Goldsmith, M. Antoniou, K. E. Fullerton, K. Knope, J. G. Copland, D. S. Bowden, S. L. Tracy, G. G. Hogg, A. Tan, J. Adamopoulos, J. Gaston, and H. Vally**. 2012. A multistate outbreak of hepatitis A associated with semidried tomatoes in Australia, 2009. Clin.Infect.Dis. **54**:775-781. doi:cir949 [pii];10.1093/cid/cir949 [doi].

29. **Dotzauer, A., U. Gebhardt, K. Bieback, U. Gottke, A. Kracke, J. Mages, S. M. Lemon, and A. Vallbracht**. 2000. Hepatitis A virus-specific immunoglobulin A mediates infection of hepatocytes with hepatitis A virus via the asialoglycoprotein receptor. J.Virol. **74**:10950-10957.

30. **Feigelstock, D., P. Thompson, P. Mattoo, Y. Zhang, and G. G. Kaplan**. 1998. The human homolog of HAVcr-1 codes for a hepatitis A virus cellular receptor. J.Virol. **72**:6621-6628.

31. **Feinstone, S. M., A. Z. Kapikian, and R. H. Purceli**. 1973. Hepatitis A: detection by immune electron microscopy of a viruslike antigen associated with acute illness. Science **182**:1026-1028.

32. **Feng, Z., L. Hensley, K. L. McKnight, F. Hu, V. Madden, L. Ping, S. H. Jeong, C. Walker, R. E. Lanford, and S. M. Lemon**. 2013. A pathogenic picornavirus acquires an envelope by hijacking cellular membranes. Nature **496**:367-371. doi:nature12029 [pii];10.1038/nature12029 [doi].

33. **Feng, Z., A. Hirai-Yuki, K. L. McKnight, and S. M. Lemon**. 2014. Naked Viruses That Aren't Always Naked: Quasi-Enveloped Agents of Acute Hepatitis. Annu.Rev.Virol. **1**:539-560. doi:10.1146/annurev-virology-031413-085359 [doi].

34. **Feng, Z. and S. M. Lemon**. 2014. Peek-a-boo: membrane hijacking and the pathogenesis of viral hepatitis. Trends Microbiol. **22**:59-64. doi:S0966-842X(13)00203-5 [pii];10.1016/j.tim.2013.10.005 [doi].

35. **Fensterl, V., D. Grotheer, I. Berk, S. Schlemminger, A. Vallbracht, and A. Dotzauer**. 2005. Hepatitis A virus suppresses RIG-I-mediated IRF-3 activation to block induction of beta interferon. J.Virol. **79**:10968-10977. doi:79/17/10968 [pii];10.1128/JVI.79.17.10968-10977.2005 [doi].

36. **Fiore, A. E.** 2004. Hepatitis A transmitted by food. Clin.Infect.Dis. **38**:705-715. doi:10.1086/381671 [doi];CID31695 [pii].

37. **Fitzgerald, M., L. Thornton, J. O'Gorman, L. O'Connor, P. Garvey, M. Boland, A. M. Part, J. Rogalska, H. Coughlan, J. MacDiarmada, J. Heslin, M. Canny, P. Finnegan, J. Moran, and D. O'Flanagan**. 2014. Outbreak of hepatitis A infection associated with the consumption of frozen berries, Ireland, 2013--linked to an international outbreak. Euro.Surveill **19**.

38. **Flehmig, B.** 1980. Hepatitis A-virus in cell culture: I. propagation of different hepatitis A-virus isolates in a fetal rhesus monkey kidney cell line (Frhk-4). Med.Microbiol.Immunol. **168**:239-248.

39. **Flehmig, B.** 1981. Hepatitis A virus in cell culture. II. Growth characteristics of hepatitis A virus in Frhk-4/R cells. Med.Microbiol.Immunol. **170**:73-81.

40. **Fleischer, B., S. Fleischer, K. Maier, K. H. Wiedmann, M. Sacher, H. Thaler, and A. Vallbracht**. 1990. Clonal analysis of infiltrating T lymphocytes in liver tissue in viral hepatitis A. Immunology **69**:14-19.

41. **Franco, E., C. Meleleo, L. Serino, D. Sorbara, and L. Zaratti**. 2012. Hepatitis A: Epidemiology and prevention in developing countries. World J.Hepatol. **4**:68-73. doi:10.4254/wjh.v4.i3.68 [doi].

42. **Gallot, C., L. Grout, A. M. Roque-Afonso, E. Couturier, P. Carrillo-Santisteve, J. Pouey, M. J. Letort, S. Hoppe, P. Capdepon, S. Saint-Martin, V. H. De, and V. Vaillant**. 2011. Hepatitis A associated with semidried tomatoes, France, 2010. Emerg.Infect.Dis. **17**:566-567. doi:10.3201/eid1703.101479 [doi].

43. **Garcia-Canaveras, J. C., M. T. Donato, J. V. Castell, and A. Lahoz**. 2012. Targeted profiling of circulating and hepatic bile acids in human, mouse, and rat using a UPLC-MRM-MS-validated method. J.Lipid Res. **53**:2231-2241. doi:jlr.D028803 [pii];10.1194/jlr.D028803 [doi].

44. **Gauss-Muller, V., G. G. Frosner, and F. Deinhardt**. 1981. Propagation of hepatitis A virus in human embryo fibroblasts. J.Med.Virol. **7**:233-239.

45. **Gauss-Muller, V., D. Jurgensen, and R. Deutzmann**. 1991. Autoproteolytic cleavage of recombinant 3C proteinase of hepatitis A virus. Virology **182**:861-864.

46. **Gerard, G. F., D. K. Fox, M. Nathan, and J. M. D'Alessio**. 1997. Reverse transcriptase. The use of cloned Moloney murine leukemia virus reverse transcriptase to synthesize DNA from RNA. Mol Biotechnol. **8**:61-77. doi:10.1007/BF02762340 [doi].

47. **Goodwin, B., SA. Jones, RR. Price, MA. Watson, DD. McKee, LB. Moore, C. Galardi, JG. Wilson, MC. Lewis, ME. Roth, PR. Maloney, TM. Willson, and SA. Kliewer**. 2000. A Regulatory Cascade of the Nuclear Receptors FXR, SHP-1, and LRH-1 Represses Bile Acid Biosynthesis. Cell Press **6**:517-526.

48. **Govindarajan, S., T. Uchida, and R. L. Peters**. 1983. Identification of T lymphocytes and subsets in liver biopsy cores of acute viral hepatitis. Liver **3**:13-18.

49. **Graff, J., O. C. Richards, K. M. Swiderek, M. T. Davis, F. Rusnak, S. A. Harmon, X. Y. Jia, D. F. Summers, and E. Ehrenfeld**. 1999. Hepatitis A virus capsid protein VP1 has a heterogeneous C terminus. J Virol. **73**:6015-6023.

50. **Guillois-Becel, Y., E. Couturier, J. C. Le Saux, A. M. Roque-Afonso, F. S. Le Guyader, G. A. Le, J. Pernes, B. S. Le, A. Briand, C. Robert, E. Dussaix, M. Pommepuy, and V. Vaillant**. 2009. An oyster-associated hepatitis A outbreak in France in 2007. Euro.Surveill **14**.

51. **Hilleman, M. R.** 1993. Hepatitis and hepatitis A vaccine: a glimpse of history. J Hepatol **18**:S5-10. doi:0168-8278/93/S06.00.

52. **Hilz, H., U. Wiegers, and P. Adamietz**. 1975. Stimulation of proteinase K action by denaturing agents: application to the isolation of nucleic acids and the degradation of 'masked' proteins. Eur.J Biochem. **56**:103-108.

53. **Hirai-Yuki, A., L. Hensley, J. K. Whitmire, and S. M. Lemon**. 2016. Biliary Secretion of Quasi-Enveloped Human Hepatitis A Virus. MBio. **7**. doi:mBio.01998-16 [pii];10.1128/mBio.01998-16 [doi].

54. **Hofmann, A. F., L. R. Hagey, and M. D. Krasowski**. 2010. Bile salts of vertebrates: structural variation and possible evolutionary significance. J.Lipid Res. **51**:226-246. doi:jlr.R000042 [pii];10.1194/jlr.R000042 [doi].

55. **Holt, J. A., G. Luo, A. N. Billin, J. Bisi, Y. Y. McNeill, K. F. Kozarsky, M. Donahee, D. Y. Wang, T. A. Mansfield, S. A. Kliewer, B. Goodwin, and S. A. Jones**. 2003. Definition of a novel growth factor-dependent signal cascade for the suppression of bile acid biosynthesis. Genes Dev. **17**:1581-1591. doi:10.1101/gad.1083503 [doi];1083503 [pii].

56. **Hu, Y. and I. Arsov**. 2009. Nested real-time PCR for hepatitis A detection. Lett.Appl.Microbiol. **49**:615-619. doi:LAM2713 [pii];10.1111/j.1472-765X.2009.02713.x [doi].

57. **Innis, B. L., R. Snitbhan, P. Kunasol, T. Laorakpongse, W. Poopatanakool, C. A. Kozik, S. Suntayakorn, T. Suknuntapong, A. Safary, D. B. Tang, and .** 1994. Protection against hepatitis A by an inactivated vaccine. JAMA **271**:1328-1334.

58. **Jacobsen, K. H. and S. T. Wiersma**. 2010. Hepatitis A virus seroprevalence by age and world region, 1990 and 2005. Vaccine **28**:6653-6657. doi:S0264-410X(10)01182-5 [pii];10.1016/j.vaccine.2010.08.037 [doi].

59. **Jansen, R. W., J. E. Newbold, and S. M. Lemon**. 1988. Complete nucleotide sequence of a cell culture-adapted variant of hepatitis A virus: comparison with wild-type virus with restricted capacity for in vitro replication. Virology **163**:299-307.

60. **Jeong, S. H. and H. S. Lee**. 2010. Hepatitis A: clinical manifestations and management. Intervirology **53**:15-19. doi:000252779 [pii];10.1159/000252779 [doi].

61. **Jothikumar, N., T. L. Cromeans, M. D. Sobsey, and B. H. Robertson**. 2005. Development and evaluation of a broadly reactive TaqMan assay for rapid detection of hepatitis A virus. Appl.Environ.Microbiol. **71**:3359-3363. doi:71/6/3359 [pii];10.1128/AEM.71.6.3359-3363.2005 [doi].

62. **Kaplan, G., A. Totsuka, P. Thompson, T. Akatsuka, Y. Moritsugu, and S. M. Feinstone**. 1996. Identification of a surface glycoprotein on African green monkey kidney cells as a receptor for hepatitis A virus. EMBO J. **15**:4282-4296.

63. **Kaplan, G. G., K. Konduru, M. Manangeeswaran, J. Jacques, N. Amharref, and S. Nakamura**. 2013. Structure, Molecular Virology, Natural History, and Experimental Models, p. 27-42. *In*: Viral Hepatitis. John Wiley & Sons, Ltd.

64. **Keeffe, E. B., S. Iwarson, B. J. McMahon, K. L. Lindsay, R. S. Koff, M. Manns, R. Baumgarten, M. Wiese, M. Fourneau, A. Safary, R. Clemens, and D. S. Krause**. 1998. Safety and immunogenicity of hepatitis A vaccine in patients with chronic liver disease. Hepatology **27**:881-886. doi:S027091399800130X [pii];10.1002/hep.510270336 [doi].

65. **Koff, R. S.** 1992. Clinical manifestations and diagnosis of hepatitis A virus infection. Vaccine **10 Suppl 1**:S15-S17.

66. **Konduru, K. and G. G. Kaplan**. 2006. Stable growth of wild-type hepatitis A virus in cell culture. J.Virol. **80**:1352-1360. doi:80/3/1352 [pii];10.1128/JVI.80.3.1352-1360.2006 [doi].

67. **Kotewicz, M. L., C. M. Sampson, J. M. D'Alessio, and G. F. Gerard**. 1988. Isolation of cloned Moloney murine leukemia virus reverse transcriptase lacking ribonuclease H activity. Nucleic Acids Res. **16**:265-277.

68. **L.J.Reed and H.Muench**. 1938. A Simple Method of Estimating Fifty Per Cent Endpoints. Am.J.Epidemiol. **27**:493-497.

69. **Lanford, R. E., Z. Feng, D. Chavez, B. Guerra, K. M. Brasky, Y. Zhou, D. Yamane, A. S. Perelson, C. M. Walker, and S. M. Lemon**. 2011. Acute hepatitis A virus infection is associated with a limited type I interferon response and persistence of intrahepatic viral RNA. Proc.Natl.Acad.Sci.U.S.A **108**:11223-11228. doi:1101939108 [pii];10.1073/pnas.1101939108 [doi].

70. **Lednar, W. M., S. M. Lemon, J. W. Kirkpatrick, R. R. Redfield, M. L. Fields, and P. W. Kelley**. 1985. Frequency of illness associated with epidemic hepatitis A virus infections in adults. Am.J.Epidemiol. **122**:226-233.

71. **Lemon, S. M. and L. N. Binn**. 1985. Incomplete Neutralization of Hepatits A Virus *in vitro* due to Lipid-associated Virions. J.Gen.Virol. **66**:2501-2505.

72. **Lemon, S. M., P. C. Murphy, P. J. Provost, I. Chalikonda, J. P. Davide, T. L. Schofield, D. R. Nalin, and J. A. Lewis**. 1997. Immunoprecipitation and virus neutralization assays demonstrate qualitative differences between protective antibody responses to inactivated hepatitis A vaccine and passive immunization with immune globulin. J.Infect.Dis. **176**:9-19.

73. **Leoni, E., C. Bevini, E. S. Degli, and A. Graziano**. 1998. An outbreak of intrafamiliar hepatitis A associated with clam consumption: epidemic transmission to a school community. Eur.J.Epidemiol. **14**:187-192.

74. **Lindenbach, B. D., M. J. Evans, A. J. Syder, B. Wolk, T. L. Tellinghuisen, C. C. Liu, T. Maruyama, R. O. Hynes, D. R. Burton, J. A. McKeating, and C. M. Rice**. 2005. Complete replication of hepatitis C virus in cell culture. Science **309**:623-626. doi:1114016 [pii];10.1126/science.1114016 [doi].

75. **Lundell, K. and K. Wikvall**. 2008. Species-specific and age-dependent bile acid composition: aspects on CYP8B and CYP4A subfamilies in bile acid biosynthesis. Curr.Drug Metab **9**:323-331.

76. **Luyten, J. and P. Beutels**. 2009. Costing infectious disease outbreaks for economic evaluation: a review for hepatitis A. Pharmacoeconomics. **27**:379-389. doi:3 [pii].

77. **Mackinney-Novelo, I., J. Barahona-Garrido, F. Castillo-Albarran, J. J. Santiago-Hernandez, N. Mendez-Sanchez, M. Uribe, and N. Chavez-Tapia**. 2012. Clinical course and management of acute hepatitis A infection in adults. Ann.Hepatol. **11**:652-657. doi:1008953 [pii].

78. **Mackowiak, P. A., C. T. Caraway, and B. L. Portnoy**. 1976. Oyster-associated hepatitis: lessons from the Louisiana experience. Am.J.Epidemiol. **103**:181-191.

79. **Makishima, M., AY. Okamoto, JJ. Repa, H. Tu, M. Learned, A. Luk, MV. Hull, KD. Lusting, DJ. Mangelsdorf, and B. Shan**. 1999. Identification of a Nuclear Receptor for Bile Acids. Science **284**.

80. **Maloney, P. R., D. J. Parks, C. D. Haffner, A. M. Fivush, G. Chandra, K. D. Plunket, K. L. Creech, L. B. Moore, J. G. Wilson, M. C. Lewis, S. A. Jones, and T. M. Willson**. 2000. Identification of a chemical tool for the orphan nuclear receptor FXR. J.Med.Chem. **43**:2971-2974.

81. **Manangeeswaran, M., J. Jacques, C. Tami, K. Konduru, N. Amharref, O. Perrella, J. M. Casasnovas, D. T. Umetsu, R. H. Dekruyff, G. J. Freeman, A. Perrella, and G. G. Kaplan**. 2012. Binding of hepatitis A virus to its cellular receptor 1 inhibits T-regulatory cell functions in humans. Gastroenterology **142**:1516-1525. doi:S0016-5085(12)00253-3 [pii];10.1053/j.gastro.2012.02.039 [doi].

82. **Martin, A., D. Benichou, S. F. Chao, L. M. Cohen, and S. M. Lemon**. 1999. Maturation of the hepatitis A virus capsid protein VP1 is not dependent on processing by the 3Cpro proteinase. J.Virol. **73**:6220-6227.

83. **Martin, A. and S. M. Lemon**. 2006. Hepatitis A virus: from discovery to vaccines. Hepatology **43**:S164-S172. doi:10.1002/hep.21052 [doi].

84. **Mathiesen, L. R., J. Drucker, D. Lorenz, J. A. Wagner, R. J. Gerety, and R. H. Purcell**. 1978. Localization of hepatitis A antigen in marmoset organs during acute infection with hepatitis A virus. J.Infect.Dis. **138**:369-377.

85. **McNiven, M. A., A. W. Wolkoff, and A. Hubbard**. 2009. A stimulus needed for the study of membrane traffic in hepatocytes. Hepatology **50**:345-348. doi:10.1002/hep.23004 [doi].

86. **Mee, C. J., J. Grove, H. J. Harris, K. Hu, P. Balfe, and J. A. McKeating**. 2008. Effect of cell polarization on hepatitis C virus entry. J Virol. **82**:461-470. doi:JVI.01894-07 [pii];10.1128/JVI.01894-07 [doi].

87. **Melnick, J. L.** 1992. Properties and classification of hepatitis A virus. Vaccine **10 Suppl 1**:S24-S26.

88. **Mitro, N., C. Godio, F. E. De, E. Scotti, A. Galmozzi, F. Gilardi, D. Caruso, A. B. Vigil Chacon, and M. Crestani**. 2007. Insights in the

regulation of cholesterol 7alpha-hydroxylase gene reveal a target for modulating bile acid synthesis. Hepatology **46**:885-897. doi:10.1002/hep.21819 [doi].

89. **Pan, C. X., J. Tang, X. Y. Wang, F. R. Wu, J. F. Ge, and F. H. Chen**. 2014. Role of interleukin-22 in liver diseases. Inflamm.Res. **63**:519-525. doi:10.1007/s00011-014-0727-3 [doi].

90. **Pang, D.** 2013.

91. **Paulmann, D., T. Magulski, R. Schwarz, L. Heitmann, B. Flehmig, A. Vallbracht, and A. Dotzauer**. 2008. Hepatitis A virus protein 2B suppresses beta interferon (IFN) gene transcription by interfering with IFN regulatory factor 3 activation. J Gen.Virol. **89**:1593-1604. doi:89/7/1593 [pii];10.1099/vir.0.83521-0 [doi].

92. **Paulmann, D., T. Magulski, R. Schwarz, L. Heitmann, B. Flehmig, A. Vallbracht, and A. Dotzauer**. 2008. Hepatitis A virus protein 2B suppresses beta interferon (IFN) gene transcription by interfering with IFN regulatory factor 3 activation. J.Gen.Virol. **89**:1593-1604. doi:89/7/1593 [pii];10.1099/vir.0.83521-0 [doi].

93. **Pavlovec, A., D. P. Evenson, and M. G. Hamilton**. 1978. The use of guanidine-HCl for the isolation of both RNA and protein from RNA tumour viruses. J Gen.Virol. **40**:239-243. doi:10.1099/0022-1317-40-1-239 [doi].

94. **Perrella, A., L. Vitiello, L. Atripaldi, C. Sbreglia, S. Grattacaso, P. Bellopede, T. Patarino, G. Morelli, S. Altamura, L. Racioppi, and O. Perrella**. 2008. Impaired function of CD4+/CD25+ T regulatory lymphocytes characterizes the self-limited hepatitis A virus infection. J.Gastroenterol.Hepatol. **23**:e105-e110. doi:JGH5008 [pii];10.1111/j.1440-1746.2007.05008.x [doi].

95. **Petrignani, M., L. Verhoef, H. R. van, C. Swaan, S. J. van, I. Boxman, H. J. Ober, H. Vennema, and M. Koopmans**. 2010. A possible foodborne outbreak of hepatitis A in the Netherlands, January-February 2010. Euro.Surveill **15**.

96. **Petrov, Y., L. V. Kukhareva, and T. A. Krylova**. 2013. The effect of type I collagen and fibronectin on the morphology of human mesenchymal stromal cells in culture. Cell and Tissue Biology **7**:545-555.

97. PHAC. Canadian Immunization Guide: Part 4- Active Vaccines (Hepatitis A Vaccine). 2016. Government of Canada.

Ref Type: Online Source

98. **Pinto, R. M., A. Bosch, and G. Kaplan**. 2014. Hepaitis A: Immune Response and Virus Evolution, p. 173-189. *In*: Gershwin ME, Vierling JM, and Manns MP (eds.), Liver Immunology: Priniciples and Practice. Springer Science, New York.

99. **Probst, C., M. Jecht, and V. Gauss-Muller**. 1999. Intrinsic signals for the assembly of hepatitis A virus particles. Role of structural proteins VP4 and 2A. J.Biol.Chem. **274**:4527-4531.

100. **Provost, P. J. and M. R. Hilleman**. 1978. An inactivated hepatitis A virus vaccine prepared from infected marmoset liver. Proc.Soc.Exp.Biol.Med. **159**:201-203.

101. **Provost, P. J. and M. R. Hilleman**. 1979. Propagation of human hepatitis A virus in cell culture in vitro. Proc.Soc.Exp.Biol.Med. **160**:213-221.

102. **Provost, P. J., J. V. Hughes, W. J. Miller, P. A. Giesa, F. S. Banker, and E. A. Emini**. 1986. An inactivated hepatitis A viral vaccine of cell culture origin. J.Med.Virol. **19**:23-31.

103. **Qu, L., Z. Feng, D. Yamane, Y. Liang, R. E. Lanford, K. Li, and S. M. Lemon**. 2011. Disruption of TLR3 signaling due to cleavage of TRIF by the hepatitis A virus protease-polymerase processing intermediate, 3CD. PLoS.Pathog. **7**:e1002169. doi:10.1371/journal.ppat.1002169 [doi];PPATHOGENS-D-11-00567 [pii].

104. **Read, S. J.** 2001. Recovery efficiencies of nucleic acid extraction kits as measured by quantitative LightCycler™ PCR. Mol Pathol **54**:86-90.

105. **Rio, D. C., M. Ares, Jr., G. J. Hannon, and T. W. Nilsen**. 2010. Purification of RNA using TRIzol (TRI reagent). Cold Spring Harb.Protoc. **2010**:db. doi:2010/6/pdb.prot5439 [pii];10.1101/pdb.prot5439 [doi].

106. **Rowe, S. L., K. Tanner, and J. E. Gregory**. 2009. Hepatitis a outbreak epidemiologically linked to a food handler in Melbourne, Victoria. Commun.Dis.Intell.Q.Rep. **33**:46-48.

107. **Sabat, R., W. Ouyang, and K. Wolk**. 2014. Therapeutic opportunities of the IL-22-IL-22R1 system. Nat.Rev.Drug Discov. **13**:21-38. doi:nrd4176 [pii];10.1038/nrd4176 [doi].

108. **Sanchez, G., R. M. Pinto, H. Vanaclocha, and A. Bosch**. 2002. Molecular characterization of hepatitis a virus isolates from a transcontinental shellfish-borne outbreak. J.Clin.Microbiol. **40**:4148-4155.

109. **Schmid, D., R. Fretz, G. Buchner, C. Konig, H. Perner, R. Sollak, A. Tratter, M. Hell, M. Maass, M. Strasser, and F. Allerberger**. 2009. Foodborne outbreak of hepatitis A, November 2007-January 2008, Austria. Eur.J.Clin.Microbiol.Infect.Dis. **28**:385-391. doi:10.1007/s10096-008-0633-0 [doi].

110. **Schulman, A. N., J. L. Dienstag, D. R. Jackson, J. H. Hoofnagle, R. J. Gerety, R. H. Purcell, and L. F. Barker**. 1976. Hepatitis A antigen particles in liver, bile, and stool of chimpanzees. J.Infect.Dis. **134**:80-84.

111. **Schulte, I., T. Hitziger, S. Giugliano, J. Timm, H. Gold, F. M. Heinemann, Y. Khudyakov, M. Strasser, C. Konig, E. Castermans, J. Y. Mok, W. J. van Esch, A. Bertoletti, T. N. Schumacher, and M. Roggendorf**. 2011. Characterization of CD8+ T-cell response in acute and resolved hepatitis A virus infection. J.Hepatol. **54**:201-208. doi:S0168-8278(10)00782-8 [pii];10.1016/j.jhep.2010.07.010 [doi].

112. **Sciot, R., J. J. Van den Oord, C. de Wolf-Peeters, and V. J. Desmet**. 1986. In situ characterisation of the (peri)portal inflammatory infiltrate in acute hepatitis A. Liver **6**:331-336.

113. **Severi, E., L. Verhoef, L. Thornton, B. R. Guzman-Herrador, M. Faber, L. Sundqvist, R. Rimhanen-Finne, A. M. Roque-Afonso, S. L. Ngui, F. Allerberger, A. Baumann-Popczyk, L. Muller, K. Parmakova, V. Alfonsi, L. Tavoschi, H. Vennema, M. Fitzgerald, M. Myrmel, M. Gertler, J. Ederth, M. Kontio, C. Vanbockstael, S. Mandal, M. Sadkowska-Todys, M. E. Tosti, B. Schimmer, O. Gorman, K. Stene-Johansen, J. J. Wenzel, G. Jones, K. Balogun, A. R. Ciccaglione, L. O' Connor, L. Vold, J. Takkinen, and C. Rizzo**. 2015. Large and prolonged food-borne multistate hepatitis A outbreak in Europe associated with consumption of frozen berries, 2013 to 2014. Euro.Surveill **20**:21192.

114. Shin, E. C. Liver injury mechanism by antigen-nonspecifically activated bystander T cells in acute hepatitis A. The 62nd annual meeting of the American Association for the study of liver disease . 2011.
Ref Type: Conference Proceeding

115. **Simms, D., P. E. Cizdziel, P. Chomczynski, and .** 1993. TRIZOL™: A New Reagent for Optimal Single-Step Isolation of RNA. FOCUS **4**:99-102.

116. **Sinal, CJ., M. Tohkin, M. Miyata, JM. Ward, G. Lambert, and FJ. Gonzalez**. 2000. Targeted Disruption of the Nuclear Receptor FXR/BAR imparis Bile Acid and Lipid Homeostasis. Cell Press **102**:731-744.

117. **Snooks, M. J., P. Bhat, J. Mackenzie, N. A. Counihan, N. Vaughan, and D. A. Anderson**. 2008. Vectorial entry and release of hepatitis A virus in polarized human hepatocytes. J.Virol. **82**:8733-8742. doi:JVI.00219-08 [pii];10.1128/JVI.00219-08 [doi].

118. **Song, K. H., T. Li, E. Owsley, S. Strom, and J. Y. Chiang**. 2009. Bile acids activate fibroblast growth factor 19 signaling in human hepatocytes to inhibit cholesterol 7alpha-hydroxylase gene expression. Hepatology **49**:297-305. doi:10.1002/hep.22627 [doi].

119. **Song, K. H., T. Li, E. Owsley, S. Strom, and J. Y. Chiang**. 2009. Bile acids activate fibroblast growth factor 19 signaling in human hepatocytes to inhibit cholesterol 7alpha-hydroxylase gene expression. Hepatology **49**:297-305. doi:10.1002/hep.22627 [doi].

120. **Steenbergen, R. H., M. A. Joyce, B. S. Thomas, D. Jones, J. Law, R. Russell, M. Houghton, and D. L. Tyrrell**. 2013. Human serum leads to differentiation of human hepatoma cells, restoration of very-low-density lipoprotein secretion, and a 1000-fold increase in HCV Japanese fulminant hepatitis type 1 titers. Hepatology **58**:1907-1917. doi:10.1002/hep.26566 [doi].

121. **Stoop, J. W., B. J. Zegers, P. C. Sander, and R. E. Ballieux**. 1969. Serum immunoglobulin levels in healthy children and adults. Clin.Exp.Immunol. **4**:101-112.

122. **Strobel, B., F. D. Miller, W. Rist, and T. Lamla**. 2015. Comparative Analysis of Cesium Chloride- and Iodixanol-Based Purification of Recombinant Adeno-Associated Viral Vectors for Preclinical Applications. Hum.Gene Ther.Methods **26**:147-157. doi:10.1089/hgtb.2015.051 [doi].

123. **Tuschl, G. and S. O. Mueller**. 2006. Effects of cell culture conditions on primary rat hepatocytes-cell morphology and differential gene expression. Toxicology **218**:205-215. doi:S0300-483X(05)00529-9 [pii];10.1016/j.tox.2005.10.017 [doi].

124. **Umetsu, S. E., W. L. Lee, J. J. McIntire, L. Downey, B. Sanjanwala, O. Akbari, G. J. Berry, H. Nagumo, G. J. Freeman, D. T. Umetsu, and R. H. Dekruyff**. 2005. TIM-1 induces T cell activation and inhibits the development of peripheral tolerance. Nat.Immunol. **6**:447-454. doi:ni1186 [pii];10.1038/ni1186 [doi].

125. **Vallbracht, A., P. Gabriel, K. Maier, F. Hartmann, H. J. Steinhardt, C. Muller, A. Wolf, K. H. Manncke, and B. Flehmig**. 1986. Cell-mediated

cytotoxicity in hepatitis A virus infection. Hepatology **6**:1308-1314. doi:S0270913986001428 [pii].

126. **Vallbracht, A., L. Hofmann, K. G. Wurster, and B. Flehmig**. 1984. Persistent infection of human fibroblasts by hepatitis A virus. J.Gen.Virol. **65 (Pt 3)**:609-615. doi:10.1099/0022-1317-65-3-609 [doi].

127. **Vallbracht, A., K. Maier, Y. D. Stierhof, K. H. Wiedmann, B. Flehmig, and B. Fleischer**. 1989. Liver-derived cytotoxic T cells in hepatitis A virus infection. J.Infect.Dis. **160**:209-217.

128. **Wan, Y. Y. and R. A. Flavell**. 2007. 'Yin-Yang' functions of transforming growth factor-beta and T regulatory cells in immune regulation. Immunol.Rev. **220**:199-213. doi:IMR565 [pii];10.1111/j.1600-065X.2007.00565.x [doi].

129. **Wang, L. and J. L. Boyer**. 2004. The maintenance and generation of membrane polarity in hepatocytes. Hepatology **39**:892-899. doi:10.1002/hep.20039 [doi].

130. **Werzberger, A., B. Mensch, B. Kuter, L. Brown, J. Lewis, R. Sitrin, W. Miller, D. Shouval, B. Wiens, G. Calandra, J. Ryan, P. Provost, and D. Nalin**. 1992. A controlled trial of a formalin-inactivated Hepatitis A vaccine in healthy children. N Engl J Med **327**:453-457. doi:10.1056/NEJM199208133270702.

131. **Werzberger, A., B. Mensch, D. R. Nalin, and B. J. Kuter**. 2002. Effectiveness of hepatitis A vaccine in a former frequently affected community: 9 years' followup after the Monroe field trial of VAQTA. Vaccine **20**:1699-1701. doi:S0264410X02000427 [pii].

132. WHO. The Global Prevalence of Hepatitis A Virus Infection and Susceptibility: A Systemic Review. 2009.

Ref Type: Online Source

133. **Wiegers, U. and H. Hilz**. 1971. A new method using 'proteinase K' to prevent mRNA degradation during isolation from HeLa cells. Biochem.Biophys.Res.Commun. **44**:513-519. doi:0006-291X(71)90632-2 [pii].

134. **Wiegers, U. and H. Hilz**. 1972. Rapid isolation of undegraded polysomal RNA without phenol. FEBS Lett. **23**:77-82. doi:0014-5793(72)80289-8 [pii].

135. **Wolk, K., S. Kunz, E. Witte, M. Friedrich, K. Asadullah, and R. Sabat**. 2004. IL-22 increases the innate immunity of tissues. Immunity. **21**:241-254. doi:10.1016/j.immuni.2004.07.007 [doi];S1074-7613(04)00194-3 [pii].

136. **Yang, Y., Y. Liang, L. Qu, Z. Chen, M. Yi, K. Li, and S. M. Lemon**. 2007. Disruption of innate immunity due to mitochondrial targeting of a picornaviral protease precursor. Proc.Natl.Acad.Sci.U.S.A **104**:7253-7258. doi:0611506104 [pii];10.1073/pnas.0611506104 [doi].

137. **Zegers, B. J., J. W. Stoop, E. E. Reerink-Brongers, P. C. Sander, R. C. Aalberse, and R. E. Ballieux**. 1975. Serum immunoglobulins in healthy children and adults. Levels of the five classes, expressed in international units per millilitre. Clin.Chim.Acta **65**:319-329. doi:0009-8981(75)90257-0 [pii].

138. **Zeigerer, A., A. Wuttke, G. Marsico, S. Seifert, Y. Kalaidzidis, and M. Zerial**. 2017. Functional properties of hepatocytes in vitro are correlated with cell polarity maintenance. Exp.Cell Res. **350**:242-252. doi:S0014-4827(16)30400-1 [pii];10.1016/j.yexcr.2016.11.027 [doi].

139. **Zhou, Y., B. Callendret, D. Xu, K. M. Brasky, Z. Feng, L. L. Hensley, J. Guedj, A. S. Perelson, S. M. Lemon, R. E. Lanford, and C. M. Walker**. 2012. Dominance of the CD4(+) T helper cell response during acute resolving hepatitis A virus infection. J Exp.Med **209**:1481-1492. doi:jem.20111906 [pii];10.1084/jem.20111906 [doi].